

Washington University in St. Louis
Washington University Open Scholarship

All Theses and Dissertations (ETDs)

January 2009

In vivo function of Otopetrin 1 in the Vestibular Sensory Epithelium

Euysoo Kim

Washington University in St. Louis

Follow this and additional works at: <https://openscholarship.wustl.edu/etd>

Recommended Citation

Kim, Euysoo, "In vivo function of Otopetrin 1 in the Vestibular Sensory Epithelium" (2009). *All Theses and Dissertations (ETDs)*. 412.
<https://openscholarship.wustl.edu/etd/412>

This Dissertation is brought to you for free and open access by Washington University Open Scholarship. It has been accepted for inclusion in All Theses and Dissertations (ETDs) by an authorized administrator of Washington University Open Scholarship. For more information, please contact digital@wumail.wustl.edu.

WASHINGTON UNIVERSITY
Division of Biology and Biomedical Sciences
Program in Molecular Cell Biology

Dissertation Examination Committee:

David M. Ornitz, Chair
Thomas J. Baranski
J. David Dickman
Paul Schlesinger
Thomas H. Steinberg
Mark E. Warchol

IN VIVO FUNCTION OF OTOPETRIN 1
IN THE VESTIBULAR SENSORY EPITHELIUM

by

Euysoo Kim

A dissertation presented to the
Graduate School of Arts and Sciences
of Washington University in
partial fulfillment of the
requirements for the degree
of Doctor of Philosophy

August, 2009

Saint Louis, Missouri

ABSTRACT OF THE DISSERTATION

In vivo function of Otopetrin 1 in the vestibular sensory epithelium

by

Euysoo Kim

Doctor of Philosophy in Biology and Biomedical Sciences
(Molecular and Cell Biology)

Washington University in St. Louis, 2009

Professor David M. Ornitz, Chairperson

Otopetrin family genes encode multi-transmembrane domain proteins with three highly conserved domains. In mice, three Otopetrin paralogues are found. One of its members, Otopetrin 1 (*Otop1*) has been previously shown to be essential for the formation of otoconia in the vestibular system of the inner ear. Otoconia are calcium carbonate biominerals that are required for normal balance and the sensation of linear acceleration with respect to gravity. The mechanism by which OTOP1 mediates otoconia biosynthesis is not known, but the ability of OTOP1 to modulate $[Ca^{2+}]_i$ in response to purinergic signals in heterologous systems suggest that OTOP1 may be involved in concentrating $[Ca^{2+}]$ within the sensory epithelium and/or the globular substance vesicles, which are secreted from the epithelium. In this study, we generated null alleles of *Otop1* (*Otop1* ^{β gal/ β gal}) and *Otop2* (*Otop2* ^{$n\beta$ gal/ $n\beta$ gal}) in mice to investigate the *in vivo* functions of these genes. The otoconial agenesis phenotype in *Otop1* ^{β gal/ β gal} mice suggests that the most sensitive and important role for OTOP1 during development is mediating otoconia formation. X-gal staining and immunohistochemical analysis reveal that *Otop1* is expressed in the developing and adult supporting cells in the non-striola region of the maculae. Within these sensory epithelia, OTOP1 localizes near the apical end. In primary

utricle cultures, endogenous OTO1 is necessary to inhibit P2Y function and the influx of extracellular Ca^{2+} in a Ca^{2+} - and ATP-dependent manner. The two different recessive missense mutations of *Otop1*, *tilted (tlt)* and *mergulhador (mlh)*, result in the same phenotype as in *Otop1*^{*βgal/βgal*}, suggesting that they have inactivated essential OTO1 activity. Localization studies and ratiometric Ca^{2+} imaging in COS7 cells and primary utricle cultures show that both *tlt* and *mlh* alter normal localization of OTO1 and that the *mlh* mutation has a greater effect on modulating $[Ca^{2+}]_i$ compared to *tlt*. When examined in heterologous systems, OTO2 and 3 can modulate $[Ca^{2+}]_i$ in a similar manner to OTO1, suggesting possible functional redundancy between Otopetrins. However, the double knockout allele for *Otop1* and *Otop2* does not exhibit additional phenotypes, suggesting that these genes may have more prominent functional redundancy with OTO3. Alternatively, a subtler phenotype may exist but will require a more careful analysis to be revealed. Because otoconia formation is affected by altered gravity it is possible that the genes important for otoconia biosynthesis, such as *Otoconin90* and *Otop1*, may also be affected. However, a quantitative RT-PCR analysis of quail embryo development under constant hypergravity conditions shows that expression of these genes is not significantly affected by altered gravity treatment. This result indicates that gravity is unlikely to serve as an epigenetic factor for these two genes during development of otoconia.

ACKNOWLEDGMENTS

I would like to thank my thesis committee members, Drs. David Ornitz, Thomas Baranski, David Dickman, Paul Schlesinger, Thomas Steinberg, and Mark Warchol for sharing their expertise and providing helpful advice.

I would also like to thank the Program in Molecular Cell Biology for providing the opportunity to participate in excellent research and their support throughout my study. In addition, I would like to thank the Department of Developmental Biology and Department of Otolaryngology for creating an intellectually stimulating and collaborative environment. I am particularly indebted to Dr. David Ornitz and the members of the Ornitz lab for their helpful discussions and support.

This project was aided by collaboration with laboratories within Washington University as well as Boys Town National Research Hospital and National Institute of Deafness and Other Communication Disorders. I am particularly grateful for the generous funding provided for this project through grants from National Institute of Health.

TABLE OF CONTENTS

Abstract	ii-iii
Acknowledgments	iv
Table of Contents	v-vii
List of Figures	viii-ix
Introduction	1
<i>Structure and development of otoconia and otolithic membrane</i>	2
<i>Tilted/Mergulhador and Otopetrin 1</i>	3
<i>Otopetrin gene family</i>	4
<i>Biochemical function of OTOPI in vitro</i>	5
<i>Summary</i>	7
References.....	8
Legends and Figures.....	11
Table.....	18
Chapter I: Otopetrin 1 regulates purinergic signaling in vivo in vestibular supporting cells	19
Abstract.....	20
Introduction.....	21
Materials and Methods.....	24
Results.....	31
Conclusion.....	40
References.....	45
Legends and Figures.....	51

Chapter II: <i>Tlt</i> and <i>mlh</i> differentially disrupt OTOP1 function	66
Introduction.....	67
Materials and Methods.....	69
Results.....	73
Conclusion.....	77
References.....	78
Legends and Figures.....	80
Chapter III: Generation and characterization of <i>Otop2</i>^{n^{βgal}} mice	88
Introduction.....	89
Materials and Methods.....	91
Results.....	96
Future Directions.....	99
References.....	101
Legends and Figures.....	102
Chapter IV: Comparison of otoconia weight and expression of <i>Otopetrin 1</i> and <i>Otoconin 90</i> at normal and hypergravity in developing quail	106
Introduction.....	107
Materials and Methods.....	110
Results.....	113
Conclusion.....	115
References.....	117
Legends and Figures.....	121

Conclusion and Future Directions	137
Conclusion.....	138
Future Directions.....	141
References.....	148
Appendix	150
Technique for dissecting adult inner ear.....	151
Curriculum Vitae	152

LIST OF FIGURES

Introduction

Figure 1. Structure of the inner ear and the otoconial organs.

Figure 2. Predicted secondary structure and topologic model for Otopetrin 1 insertion into the lipid bilayer and expression of *Otop1* mRNA.

Figure 3. Purinergic receptor signaling cascade.

Chapter I: Otopetrin 1 regulates purinergic signaling in vivo in vestibular Supporting cells

Figure 1. Targeting the *Otopetrin 1* (*Otop1*) gene.

Figure 2. Spatial and temporal expression of OTOP1^{βGAL}.

Figure 3. OTOP1 is localized at the apex of supporting cells.

Figure 4. OTOP1 regulation of the purinergic response in primary chick utricular macular cultures.

Figure 5. Purinergic response of organotypic macular cultures from the utricles of P0-P3 mice.

Figure 6. Purinergic response of dissociated macular cultures from the utricles of P0-P3 mice.

Figure 7. Semi-quantitative RT-PCR analysis of P2X and P2Y receptors in *Otop1*^{+/+} mouse dissociated culture cells.

Chapter II: *Tlt* and *mlh* differentially disrupt OTOP1 function

Figure 1. Localization of EGFP^{Otop1}^{tl} and EGFP^{Otop1}^{mlh} in COS7 cells.

Figure 2. Overexpression of EGFP^{Otop1}, EGFP^{Otop1}^{tl}, and EGFP^{Otop1}^{mlh} in COS7 cells alters the purinergic response.

Figure 3. Apical trafficking of endogenous OTOP1 is affected in *Otop1*^{tl} and *Otop1*^{mlh} utricular maculae.

Figure 4. *Otop1*^{tl} macular culture cells respond to ATP in a similar manner to *Otop1*^{+/+}.

Chapter III: Generation and characterization of *Otop2^{nβgal}* mice

Figure 1. Targeting scheme of *Otop2^{nβgal}* allele.

Figure 2. Response of GFP*Otop2* and GFP*Otop3*-expressing COS7 cells to different purinergic agonists.

Chapter IV: Comparison of otoconia size and expression of *Otopetrin 1* and *Otoconin 90* at normal and hypergravity in developing quail

Figure 1. Development of otoconia in the embryonic quail.

Figure 2. The equipment used to induce hypergravity during quail egg development.

Figure 3. *Oc90 in-situ* hybridization and OC90 immunohistochemistry in quail inner ear tissues.

Figure 4. Comparison of body weight of embryos developed at normal (1G) and hypergravity (2G).

Figure 5. Relative quantification of *Otogelin* expression using qRT-PCR.

Figure 6. Relative quantification of *Oc90* gene expression at 1G vs 2G.

Figure 7. Relative quantification of *Otop1* expression at 1G vs 2G.

Figure 8. Comparison of otoconial calcium weight in 1G and 2G animal.

Introduction

The ability to sense movement with respect to gravity is a phylogenetically ancient system shared by organisms from plants to humans. Orientation in a gravitational field not only affects balance but can also affect the heart and respiratory rates (Yates and Miller, 1998), blood pressure (Miller et al., 1995), and emotional states (Douglas et al., 1979). The sensory systems responsible for maintenance of equilibrium and balance in vertebrates are located in the vestibular portion of the inner ear. The gravity receptor lies within small fluid-filled sacs called the utricle and saccule (Figure 1A). The spatial adaptation to sense gravity is an extracellular superstructure, the otoconial complex, which contains high-density calcium carbonate particles called otoconia (otolith in teleost fish) embedded in a gelatinous (otolithic) membrane (Figure 1B). This structure couples forces of gravity to cilia of the sensory cells. Bending of the cilia in response to linear accelerations initiates the neuronal response. Human otoconia are subject to demineralization and to alterations in structure and composition (Figure 1D) because of aging, disease and exposure to commonly used medications, including diuretics, antibiotics, and psychiatric medicines (Hughes et al., 2006). These different forms of damage to the otoconial membrane lead to vertigo, a leading cause of falls in the elderly resulting in injury and death (Oghalai et al., 2000). Moreover, mammals cannot regenerate otoconia once they are damaged or lost. Despite such clinical significance, little information has been compiled about the development and maintenance of otoconia in humans.

Structure and development of otoconia and otolithic membrane

The otoconial complex is divided into 3 layers (Figure 1B). Beginning in the endolymphatic space, (a) the otoconial layer contains thousands of otoconia, 0.1 to 25 μm biominerals consisting of a glycoprotein/proteoglycan core surrounded by minute crystallites (Figure 1C), and the fibrous proteins that attach them to the underlying matrix, (b) the gelatinous layer is glutinous and amorphous, and (c) the subcupular meshwork (also called the veils) is a dense reticular network of fibrillar proteins that surround the processes of sensory hair cells. This complex extracellular structure is established in mid embryonic development within the aqueous environment of the endolymph (Hughes et al., 2006).

Otoconial formation begins over the sensory epithelia of the utricle and saccule when the core proteins (Otoconin 90 (Oc90)) and other “minor” otoconial proteins (Thalmann et al., 2006) coalesce into distinct structures, with faint rhombohedral shapes at approximately embryonic day 14 (E14) in the mouse (Ballarino and Howland, 1982; Thalmann et al., 2006; Wang et al., 1998). Calcification of this proteinaceous otoconial precursor is rapid, with maximal mineralization occurring between E15-E16.5 (Anniko, 1980; Anniko et al., 1987). Otoconial growth is most likely mediated through accretion of new calcium carbonate crystals at the pointed tips of the calcifying otoconia; this is supported by the localization of the calcium binding protein calbindin d28k to these sites in developing avian otoconia (Balsamo et al., 2000). The crystal polymorph of calcium carbonate in mammalian otoconia is calcite, which is the thermodynamically most stable form (Mann et al., 1983). Otoconia achieve essentially full size by postnatal day 7 (Erway et al., 1986; James et al., 1969; Lim, 1973), and in mammals, it is thought that no

new otoconia are added after this point, although turnover of otoconial calcium has been observed at a low rate in the adult rodent (Lim, 1973; Preston et al., 1975).

The essential requirement to form calcium carbonate, the inorganic phase of otoconia, is the availability of Ca^{2+} and CO_3^{2-} ions. The presence of carbonate ions depend on the activity of carbonic anhydrase, which is abundant in the inner ear (Lim et al., 1983; Shiao et al., 2005). However, little is currently known about the source of Ca^{2+} in otoconial formation.

Tilted/Mergulhador and Otopetrin 1

Several mouse strains with vestibular system pathology have missing or defective otoconia (Hughes et al., 2006), including *tilted* (*tlt*) and *mergulhador* (*mlh*). The *tilted* mouse arose spontaneously in a $\text{p}^{6\text{H}}/\text{p}^{\text{d}}$ stock and has subsequently been bred onto a C57BL/6J background and cryopreserved at the Jackson Laboratory (Lane, 1986). The *tlt* locus was previously mapped to mouse chromosome 5 (Lane, 1986; Lane, 1987). The homozygous *tilted* mouse often holds its head in a slightly tilted position. Under normal laboratory conditions, the animal shows no other behavioral abnormalities (e.g., circling, head-tossing). However, when dropped into water, the mouse cannot find the surface and would drown if not rescued. *Tlt* mice lack otoconia despite normal development of the inner ear and other structures. The penetrance of this defect is 100 percent (Hurle et al., 2003).

A second mutant allele, *mergulhador* (*mlh*), or “diver” in Portuguese, arose in an ENU (N-ethyl-N-nitrosourea) mutagenesis screen (Massironi et al., 1994) and exhibits non-swimming behavior and lack of otoconia, similar to the *tlt* mutant mice.

Homozygous *mlh* mice are viable and fertile. They hold their head tilted to one side, shake when suspended by the tail, and exhibit non-swimming behavior indicative of vestibular dysfunction. *Mlh* and *tlt* phenotypes are indistinguishable (Hurle et al., 2003).

Through positional cloning, *tlt* and *mlh* were found to be mutant alleles of a novel gene (*Otopetrin 1*, *Otop1*), encoding a multi-transmembrane domain protein (Hurle et al., 2003). Both mutants carry single missense mutations leading to non-conservative amino acid substitutions that affect two putative transmembrane (TM) domains (*tlt*, Ala₁₅₁->Glu in TM3; *mlh*, Leu₄₀₈->Gln in TM9) (Figure 2A).

Otopetrin gene family

Homologous genes for murine *Otop1* have been identified in all vertebrate groups examined, including rat, human, *G. gallus* (chicken), *F. rubripes* (fugu), and *D. rerio* (zebrafish). Additionally, two *Otop1*-like genes (*Otop2* and *Otop3*) were found. Mouse OTO2 and OTO3 show 34% and 30% amino acid identity with OTO1, respectively (Hurle et al., 2003). Comparison of the cDNA assemblies and genomic sequence indicated that all *Otopetrin* family members share a common gene structure with conserved splice-site positions. Otopetrins have homology to the invertebrate Domain of Unknown Function 270 genes (DUF 270; pfam03189). Multi-species comparison of the predicted primary sequences and predicted secondary structures of 62 vertebrate Otopetrins, and arthropod and nematode DUF270 proteins, has found highly conserved domains (Otopetrin Domain I, II, and III) (Figure 2A) (Hughes et al., 2008).

Preliminary data on *in situ* hybridization, RT-PCR, microarray analysis and presence in EST libraries indicate that *Otopetrins* are expressed in many of the major

organs (Table 1). Considerable overlap in expression between *Otop1* and *Otop1* homologues suggest possible functional redundancy. *Otop1* expression was detected in the macular epithelia of the utricle and saccule in the inner ear, using radioactive *in situ* hybridization (Figure 2B).

Biochemical function of Otop1 in vitro

The source of calcium to form otoconia is predicted to come from the endolymph, which is the extracellular fluid bathing hair cells and supporting cells of the macula. However, the calcium concentration in the endolymph is too low (10-100 μ M) (Anniko, 1980; Salt et al., 1989) to drive nucleation of calcium crystals on its own. Therefore, a system to concentrate these calcium ions in a closed environment is required. Several previous studies have observed membrane vesicles called “globular substance” in embryonic inner ears, which are thought to be precursors of otoconia formation that are extruded or budded from the apical surface of the cells of the developing utricular and saccular sensory epithelium (Erway et al., 1986; Preston et al., 1975; Ross, 1979; Suzuki et al., 1995; Tateda et al., 1998). The predicted secondary structure (integral membrane protein) (Figure 2A) suggests that Otop1 may be associated with the globular substance. Suzuki et al. showed that globular substance vesicles in isolated otoconial membranes had a dose-dependent response to ATP characterized by a 5-6 fold increase in intravesicular Ca²⁺ as assessed by fluo-3 fluorescence (Suzuki et al., 1997). This finding suggested that increasing the concentration of Ca²⁺ ion in globular substance vesicles could permit nucleation of CaCO₃ crystals in a protected environment.

The kinetics and concentration dependence of ATP-dependent intravesicular Ca^{2+} accumulation suggested that the ATP-mediated Ca^{2+} increase in globular substance had some similarities to known purinergic P2 receptors, which mediate intracellular Ca^{2+} increases in response to ATP (Hughes et al., 2007). Typically, ATP-dependent Ca^{2+} increases involved the activity of the P2Y or P2X receptors (Figure 4) (North, 2002; Ralevic and Burnstock, 1998). P2Y receptors have 7 transmembrane domains and their activation is coupled to the activation of G proteins. Several P2Y receptors interact with $\text{G}\alpha_q$ subunits of the G protein. Nucleotide binding to the P2Y receptor leads to the activation of $\text{G}\alpha_q$, subsequent activation of phospholipase C and IP3 kinase and the generation of inositol 1, 4, 5-triphosphate (IP3). IP3 binds the IP3 receptor on the endoplasmic reticulum (ER) membrane, releasing ER Ca^{2+} stores and rapidly increasing intracellular cytoplasmic Ca^{2+} concentrations ($[\text{Ca}^{2+}]_i$). This change in $[\text{Ca}^{2+}]_i$ is represented as a sharp spike, which is followed by a rapid return to an elevated base line as Ca^{2+} is extruded from the cytoplasm through a Plasma Membrane Ca^{2+} -ATPase (PMCA) or returned to the ER through the Sarcoplasmic/Endoplasmic Reticulum Ca^{2+} -ATPase (SERCA). The P2X family of purinergic receptors has only 2 transmembrane domains. Binding of nucleotides to the extracellular domain of the P2X receptor family leads to opening of a non-selective cation channel formed by homo- or hetero-trimers of the 7 P2X family members. P2X channel opening results in an influx of extracellular Ca^{2+} into the cytoplasm, raising $[\text{Ca}^{2+}]_i$. The different P2 family members are distinguished by the source of Ca^{2+} (intracellular versus extracellular), nucleotide or nucleotide-analogue sensitivity, the use or absence of second messengers, and sensitivity to a variety of pharmacologic agents (North, 2002; Ralevic and Burnstock, 1998).

Considering the previous genetic studies (mouse and zebrafish mutants), which suggests a prominent role for OTOPI in the initiation of calcium mineralization (Hughes et al., 2004; Hurle et al., 2003; Ornitz et al., 1998; Sollner et al., 2004), we hypothesized that OTOPI may have a role in modulating Ca^{2+} flux in globular substance vesicles. We performed single cell ratiometric Ca^{2+} imaging techniques to investigate changes in intracellular calcium regulation due to expression of *Otop1* in immortalized cell lines (COS7, ROS cells) and primary chick utricular cultures (Hughes et al., 2007).

Overexpression of *Otop1* lead to a nonspecific depletion of endoplasmic reticulum (ER) Ca^{2+} stores, specific inhibition of the purinergic receptor P2Y2, and initiation of a novel P2X-like purinoceptor influx of extracellular Ca^{2+} in response to certain purinergic nucleotides (ATP=ADP>>UDP, with αBMeATP , BzATP, ATP γ S, UTP, and 2-MeSATP not effective). All of these activities were shown to be pharmacologically and reversibly blocked by prolonged exposure to the polyanion suramin. This combination of activities is unique to OTOPI, and one or all of these activities may be required for otoconial development.

Summary

Previous studies showed that OTOPI activity is vital for Otoconial formation (Hughes et al., 2004; Hurle et al., 2003; Sollner et al., 2004), and that expression of *Otop1* modulates intracellular calcium regulation (Hughes et al., 2007). However, it is still not clear how this activity can be correlated to the developmental function of *Otop1* during otoconial formation. Besides this role, OTOPI could have additional functions in other organs that express *Otop1*, but they are not revealed in any of the mutant mice. To

decipher the *in vivo* role of *Otop1*, it is necessary to examine the phenotype of a true null allele. In addition, because *Otop1* and *Otop1* homologues, *Otop2* and *3*, are expressed in overlapping patterns, we should not overlook possible functional redundancy between Otopetrins. Therefore, it is also vital to generate null alleles of *Otopetrin* genes and make double knockouts for further analysis. Moreover, to strengthen the hypothesis of functional redundancy, biochemical studies on other Otopetrins (OTOP2 and OTOP3) needs to be done to determine if other paralogues have similar biochemical activities as OTOP1. Additionally, the mutations associated with otoconial agenesis (*tlr*, *mlh*) should have some changes in biochemical properties.

References

- Anniko, M. (1980). Development of otoconia. *Am J Otolaryngol* *1*, 400-410.
- Anniko, M., Wikstrom, S. O., and Wroblewski, R. (1987). X-ray microanalytic studies on developing otoconia. *Acta Otolaryngol* *104*, 285-289.
- Ballarino, J., and Howland, H. C. (1982). Otoconial morphology of the developing chick. *Anat Rec* *204*, 83-87.
- Balsamo, G., Avallone, B., Del Genio, F., Trapani, S., and Marmo, F. (2000). Calcification processes in the chick otoconia and calcium binding proteins: patterns of tetracycline incorporation and calbindin-D28K distribution. *Hear Res* *148*, 1-8.
- Douglas, R. J., Clark, G. M., Erway, L. C., Hubbard, D. G., and Wright, C. G. (1979). Effects of genetic vestibular defects on behavior related to spatial orientation and emotionality. *J Compar Physiol Psychol* *93*, 467-480.
- Erway, L. C., Purichia, N. A., Netzler, E. R., D'Amore, M. A., Esses, D., and Levine, M. (1986). Genes, manganese, and zinc in formation of otoconia: labeling, recovery, and maternal effects. *Scanning Electron Microscopy*, 1681-1694.
- Hughes, I., Binkley, J., Hurle, B., Green, E. D., NISC Comparative Sequencing Program, Sidow, A., and Ornitz, D. M. (2008). Identification of the Otopetrin Domain, a conserved domain in vertebrate otopetrins and invertebrate otopetrin-like family members. *BMC Evolutionary Biology* *8*:41.

- Hughes, I., Blasiolo, B., Huss, D., Warchol, M. E., Rath, N. P., Hurle, B., Ignatova, E., Dickman, J. D., Thalmann, R., Levenson, R., and Ornitz, D. M. (2004). Otopetrin 1 is required for otolith formation in the zebrafish *Danio rerio*. *Dev Biol* 276, 391-402.
- Hughes, I., Saito, M., Schlesinger, P. H., and Ornitz, D. M. (2007). Otopetrin1 activation by purinergic nucleotides regulates intracellular calcium. *Proc Natl Acad Sci U S A* 104, 12023-12028.
- Hughes, I., Thalmann, I., Thalmann, R., and Ornitz, D. M. (2006). Mixing model systems: Using zebrafish and mouse inner ear mutants and other organ systems to unravel the mystery of otoconial development. *Brain Res* 1091, 58-74.
- Hurle, B., Ignatova, E., Massironi, S. M., Mashimo, T., Rios, X., Thalmann, I., Thalmann, R., and Ornitz, D. M. (2003). Non-syndromic vestibular disorder with otoconial agenesis in tilted/mergulhador mice caused by mutations in otopetrin 1. *Hum Mol Genet* 12, 777-789.
- James, J., Schellens, J. P., and Veenhof, V. B. (1969). Electron microscopy of formation of statoconia. *Experientia* 25, 1173-1174.
- Lane, P. (1986). *Tilted* (tl). *Mouse News Lett* 75, 28.
- Lane, P. W. (1987). New mutants and linkages: *Tilted*. *Mouse News Lett* 77, 129.
- Lim, D. J. (1973). Formation and fate of the otoconia. Scanning and transmission electron microscopy. *Ann Otol Rhinol Laryngol* 82, 23-35.
- Lim, D. J., Karabinas, C., and Trune, D. R. (1983). Histochemical localization of carbonic anhydrase in the inner ear. *Am J Otolaryngol* 4, 33-42.
- Mann, S., Parker, S. B., Ross, M. D., Skarnulis, A. J., and Williams, R. J. (1983). The ultrastructure of the calcium carbonate balance organs of the inner ear: an ultra-high resolution electron microscopy study. *Proc R Soc Lond B Biol Sci* 218, 415-424.
- Massironi, S. M., Dagi, M. L., Lima, M. R., Alvarez, J. M., and Kipnis, T. L. (1994). A new mutant hairless mouse with lymph node hyperplasia and late onset of autoimmune pathology. *Braz J Med Biol Res* 27, 2401-2405.
- Miller, A. D., Yamaguchi, T., Siniiaia, M. S., and Yates, B. J. (1995). Ventral respiratory group bulbospinal inspiratory neurons participate in vestibular-respiratory reflexes. *J Neurophysiol* 73, 1303-1307.
- North, R. A. (2002). Molecular physiology of P2X receptors. *Physiol Rev* 82, 1013-1067.
- Oghalai, J. S., Manolidis, S., Barth, J. L., Stewart, M. G., and Jenkins, H. A. (2000). Unrecognized benign paroxysmal positional vertigo in elderly patients. *Otolaryngol Head Neck Surg* 122, 630-634.

- Ornitz, D. M., Bohne, B. A., Thalmann, I., Harding, G. W., and Thalmann, R. (1998). Otoconial agenesis in *tilted* mutant mice. *Hearing Res* 122, 60-70.
- Preston, R. E., Johnsson, L. G., Hill, J. H., and Schacht, J. (1975). Incorporation of radioactive calcium into otolithic membranes and middle ear ossicles of the gerbil. *Acta Otolaryngol* 80, 269-275.
- Ralevic, V., and Burnstock, G. (1998). Receptors for purines and pyrimidines. *Pharmacol Rev* 50, 413-492.
- Ross, M. D. (1979). Calcium ion uptake and exchange in otoconia. *Adv Otorhinolaryngol* 25, 26-33.
- Salt, A. N., Inamura, N., Thalmann, R., and Vora, A. (1989). Calcium gradients in inner ear endolymph. *Am J Otolaryngol* 10, 371-375.
- Shiao, J. C., Lin, L. Y., Horng, J. L., Hwang, P. P., and Kaneko, T. (2005). How can teleostean inner ear hair cells maintain the proper association with the accreting otolith? *J Comp Neurol* 488, 331-341.
- Sollner, C., Schwarz, H., Geisler, R., and Nicolson, T. (2004). Mutated otopetrin 1 affects the genesis of otoliths and the localization of Starmaker in zebrafish. *Dev Genes Evol* 214, 582-590.
- Suzuki, H., Ikeda, K., Furukawa, M., and Takasaka, T. (1997). P2 purinoceptor of the globular substance in the otoconial membrane of the guinea pig inner ear. *Am J Physiol* 273, C1533-1540.
- Suzuki, H., Ikeda, K., and Takasaka, T. (1995). Biological characteristics of the globular substance in the otoconial membrane of the guinea pig. *Hear Res* 90, 212-218.
- Tateda, M., Suzuki, H., Ikeda, K., and Takasaka, T. (1998). pH regulation of the globular substance in the otoconial membrane of the guinea-pig inner ear. *Hear Res* 124, 91-98.
- Thalmann, I., Hughes, I., Tong, B. D., Ornitz, D. M., and Thalmann, R. (2006). Microscale analysis of proteins in inner ear tissues and fluids with emphasis on endolymphatic sac, otoconia, and organ of Corti. *Electrophoresis* 27, 1598-1608.
- Wang, Y., Kowalski, P. E., Thalmann, I., Ornitz, D. M., Mager, D. L., and Thalmann, R. (1998). Otoconin-90, the mammalian otoconial matrix protein contains two domains of homology to secretory phospholipase A2. *Proc Natl Acad Sci, USA* 95, 15345-15350.
- Yates, B. J., and Miller, A. D. (1998). Physiological evidence that the vestibular system participates in autonomic and respiratory control. *J Vestib Res* 8, 17-25.

Figure 1. Structure of the inner ear and the otoconial organs. A) Schematic representation of the mammalian inner ear (Hughes et al., 2006). The cochlea is required for the sensation of sound. The vestibular portion of the inner ear is made up of 5 sensory maculae: the anterior, posterior, and lateral semicircular canal ampullae and the utricle and saccule. The semicircular canals detect angular motion, whereas the utricle and saccule are responsible for sensation of linear motion, including gravity. Otoconia lie within the utricle and saccule. All of the inner ear organs are filled with endolymph fluid, which is low in calcium (Ca^{2+}) and rich in potassium (K^+) (Hughes et al., 2006). B) Schematic representation of the utricular maculae and associated structures. Figure adapted from (Hughes et al., 2008). A thin, nonsensory epithelium lies opposite the sensory macula and contains melanocytes (m), which provide trace elements in melanosomes to the epithelial cells, giving them a dark appearance (dc). The macula is composed of hair cells (hc), supporting cells (sc); transitional cells (tc) border the edges of the maculae. Above the macula lie the otoconia and the otolithic membrane. The otolithic membrane is composed of a gelatinous layer, where otoconia crystals are embedded, and the underlying subcupular meshwork, which surrounds the stereocilia of the hair cells. Otoconia are held in place on the otolithic membrane by strands of non-collagenous extracellular matrix proteins that resemble beads on a string. C) Each otoconium is formed by calcium carbonate biominerals precipitated around a proteinaceous core. The majority of the proteinaceous core contains Otoconin90 (Oc90), and other minor matrix proteins (fetuin, laminin α 3, osteopontin, SC-1, MyI9) have been discovered (Thalmann et al., 2006). D) Otoconia are prone to damage. The affected otoconia appear pitted or hallowed out and subsequently break into fragments, which can

result in displacement of otoconia into other inner ear organs. This causes abnormal sensations of dizziness and loss of balance.

Figure 1

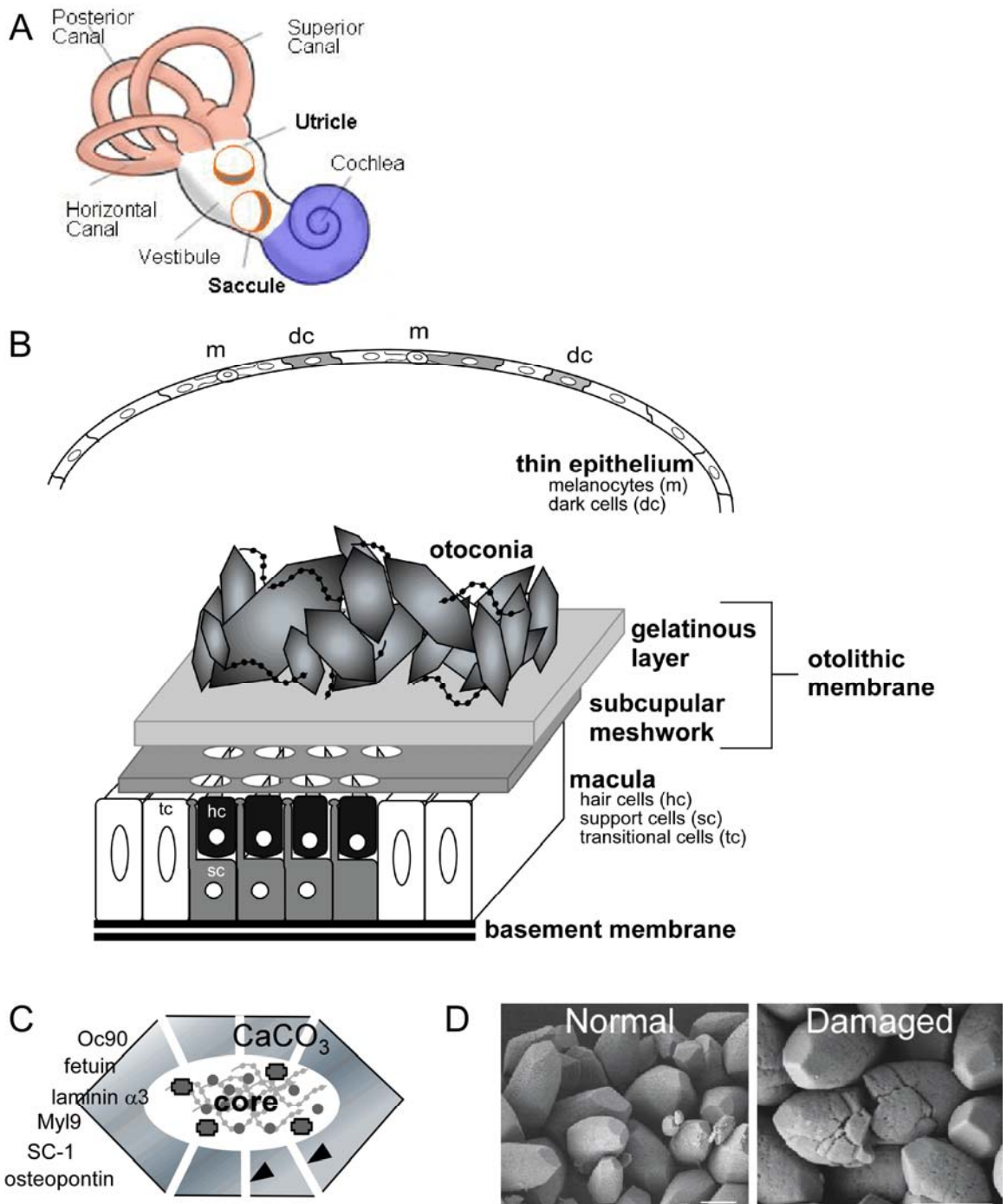


Figure 2. Predicted secondary structure and topologic model for Otopetrin 1

insertion into the lipid bilayer and expression of *Otop1* mRNA.

A) Otopetrin 1 is predicted to encode a 12-transmembrane domain protein with both the N- and C-termini in the cytosol. The locations of the *tlt*, *mlh*, and *bks* mutations are noted by arrows in TM3, TM9, and TM10, respectively. Otopetrin Domain-I, -II, and -III (OD-I, OD-II, and OD-III, respectively) are marked by shaded green, pink, and blue rectangles. Each amino acid is represented as a circle and the chemical properties of amino acids are denoted by color: charged residues (red), polar residues (blue), and non-polar residues (green). Cysteine (yellow) and proline (dark green) are noted. The two consensus N-glycosylation sites (N) are indicated in loop 5. The predicted intracellular and extracellular loops and TM domains are numbered L1 to L11 and TM1 to TM12, respectively. Figure adapted from (Hughes et al., 2008).

B) *In situ* hybridization with an *Otop1* probe marked *Otop1* expression in the sensory epithelium (SE). No signal is present in the non-sensory epithelium (arrowheads). Figure adapted from (Hurle et al., 2003).

Figure 2

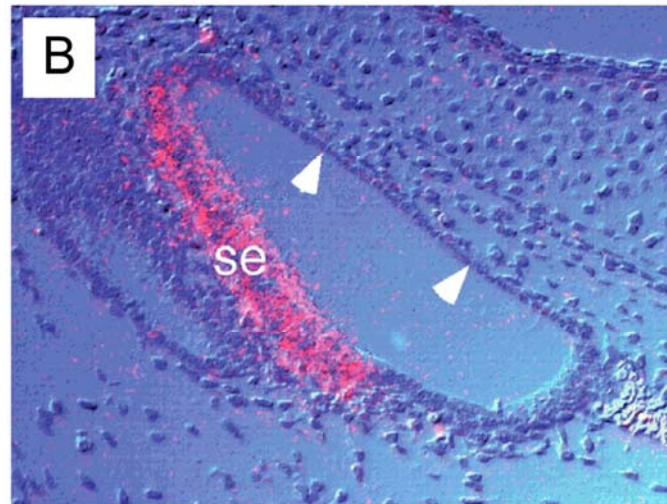
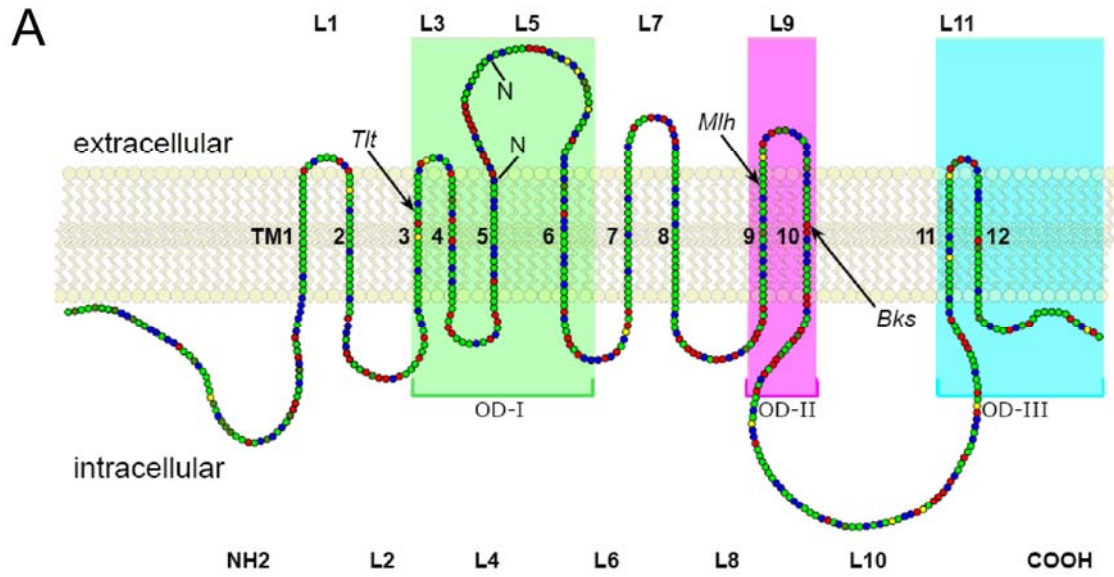


Figure 3. Purinergic receptor signaling cascade. There are two classes of P2 purinergic receptors which modulate Ca^{2+} from different sources. Ionotropic P2X receptors are Ca^{2+} channels which mediate influx of extracellular Ca^{2+} by binding to ATP. Metabotropic P2Y receptors are G-protein coupled receptors, and thus stimulation with ATP activates a trimeric G protein. The alpha subunit then activates phospholipase β ($\text{PLC}\beta$), which acts on membrane phospholipids to cleave off inositol triphosphate (IP3). Remaining in the membrane is the diacylglycerol (DAG). IP3 diffuses to the endoplasmic reticulum (ER), where it binds to the IP3 receptors. This allows intracellular Ca^{2+} to move out into the cytosol.

Figure 3

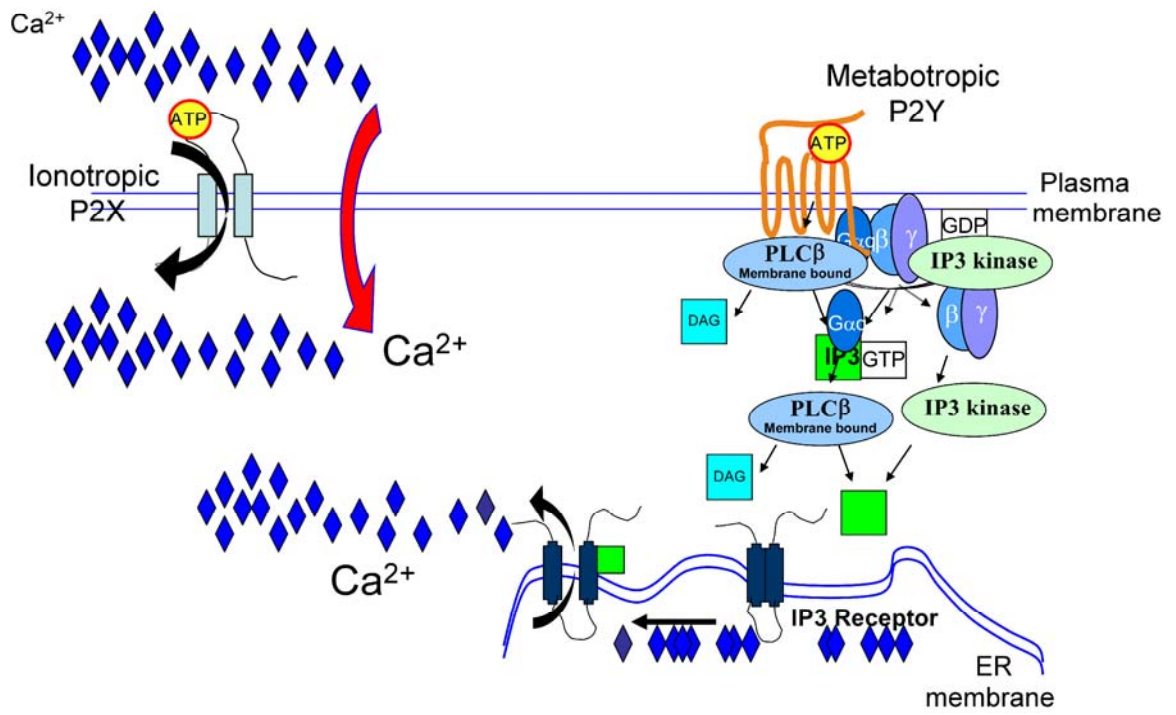


Table 1. Spatial expression pattern of Otopetrin family proteins.

Tissue	Otop1	Otop2	Otop3
Adrenal gland	●		●
Brain	●	●	●
Brown fat	●	●	
Ear	●	?	?
Eye	●		●
Kidney	●	●	
Lactating mammary gland	●		
Lung/Trachea	●	●	●
Pancreas		●	
Salivary gland	●	●	
Skeletal muscle			●
Skin/Hair	●	●	●
Spleen		●	
Stomach/GI	●	●	●
Testis/Prostate	●	●	
Thymus	●		
Tongue		●	●
Uterus	●		
Vascular (heart, aorta, vein)	●		
Vomerol nasal organ	●		

Otopetrin 1 regulates purinergic signaling *in vivo* in vestibular supporting cells

Euysoo Kim¹, Krzysztof L. Hyrc², Judith Speck³, Yunxia W. Lundberg⁴, Inna Hughes¹, Felipe T. Salles⁵, Bechara Kachar⁵, Mark E. Warchol³, David M. Ornitz¹

Departments of Developmental Biology¹, Neurology², Otolaryngology³, Washington University School of Medicine, St. Louis, MO USA

Department of Genetics⁴, Boys Town National Research Hospital, Omaha, NE USA
Laboratory of Cell Structure and Dynamics⁵, National Institute of Deafness and Other Communication Disorders, National Institute of Health, Bethesda MD USA

Running title: OTOPI function in vestibular supporting cells

Key words: utricle, saccule, ATP, calcium, otoconia

This work was supported by NIH DC02236

Corresponding author
David M. Ornitz
Washington University School of Medicine
Department of Developmental Biology
Campus Box 8103
660 S. Euclid Avenue
St. Louis, MO 63110 USA

Email: dornitz@wustl.edu
Phone: 314-362-3908
Fax: 314-362-7058

Abstract

Otoconia are dense calcium carbonate biominerals found in the utricle and saccule of the inner ear that are essential for vestibular function and the normal sensation of gravity. In mice, missense mutations in *Otopetrin 1 (Otop1)* result in otoconial agenesis and severe deficits in balance. By replacing coding regions of *Otop1* with β -*galactosidase* we localized sites of *Otop1* expression in the non-striolar region of the utricle and saccule throughout development and demonstrate that its expression persists in the adult. Localization of the OTOP1 protein in the apical side of supporting cells suggests a direct function in the regulation of apical ion flux, regulation of apical membrane protein activity and/or membrane trafficking. Analysis of the purinergic response in primary macular epithelial cultures showed that *in vivo* OTOP1 inhibits P2Y receptor-mediated release of intracellular Ca^{2+} stores and activates a P2X receptor-like influx of extracellular Ca^{2+} . We also found that the P2Y inhibitory activity of OTOP1 was dependent on the presence of extracellular Ca^{2+} , suggesting a role for OTOP1 in sensing extracellular or intravesicular Ca^{2+} concentrations. These data identify an *in vivo* biochemical activity for OTOP1 and suggest a model for interaction between OTOP1 and apically localized purinergic receptors in the regulation of otoconia formation, maintenance and potentially regeneration.

Introduction

Otoconia are dense calcium carbonate biominerals in the utricle and saccule of the vertebrate inner ear that are required for sensation of linear acceleration and gravity.

Otoconia are composed of a proteinaceous core of calcium (Ca^{2+}) binding and matrix proteins surrounded by a shell composed of calcium carbonate (CaCO_3) microcrystalites in the form of calcite (Lins et al., 2000; Mann et al., 1983; Ross et al., 1985; Suzuki et al., 1995; Thalmann et al., 2006). Otoconia are embedded in a fibrous extracellular matrix (gelatinous membrane) which couples the force of gravity to stereocilia of the underlying sensory hair cells. Otoconial precursors begin to form at embryonic day 14 (E14) in the mouse. Maximal rates of mineralization occur between E15-E16.5 (Anniko, 1980; Anniko et al., 1987). Otoconial growth is most likely mediated through accretion of new calcium carbonate crystals at the pointed tips of the calcifying otoconia (Balsamo et al., 2000). Otoconia achieve essentially full size by postnatal day 7 (Erway et al., 1986; James et al., 1969; Lim, 1973), and in mammals, it is thought that no new otoconia are added after this point. However, turnover of otoconial calcium has been observed at a low rate in the adult rodents (Erway et al., 1986; Preston et al., 1975).

Otoconia are prone to demineralization and displacement with aging, head trauma, and exposure to commonly used medications (Ross et al., 1976). Otoconial damage leading to vertigo is considered a leading cause of falls in the elderly resulting in skeletal fracture and accidental death (Oghalai et al., 2000). In mammals, once damaged or lost, otoconia cannot be regenerated. Despite clinical significance, little is known about the mechanisms that regulate the development and maintenance of otoconia in humans.

Tilted (tlt) mice lack otoconia and present with a non-syndromic vestibular disorder (Ornitz et al., 1998). Homozygous *tlt* mice show a head tilting behavior and an

inability to swim. Positional cloning identified *tlt* as a mutant allele of a novel gene, *Otopetrin 1 (Otop1)* (Hurle et al., 2003). A second mutant allele, *Mergulhador (mlh)* exhibits a similar phenotype to the *tlt* mice. Both *tlt* and *mlh* have missense mutations (*tlt*, Ala151Glu; *mlh*, Leu408Gln) leading to non-conservative amino acid substitutions. In addition to *tlt* and *mlh*, phenotypes observed in *Otop1* morphant zebrafish (Hughes et al., 2004) and *backstroke* zebrafish mutant (Glu->Val) (Sollner et al., 2004) show that OTOPI is essential for otolith mineralization in teleosts. Consistent with its requirement for otoconia formation, *Otop1* is expressed in the sensory epithelium underlying the otoconial layer in the utricle and saccule (Hurle et al., 2003).

Otop1 is predicted to have 12 putative TM domains, which cluster into three evolutionarily conserved protein domains (Hughes et al., 2008). *Tlt* and *mlh* mutations are located in putative TM 3 and TM 9, respectively, which are both within conserved regions of OTOPI.

Otoconia are initially formed in a fibrous extracellular matrix that contains a vesicular structure called “globular substance” which is thought to be extruded or budded from the apical surface of the sensory epithelium of the utricle and saccule in the embryonic inner ear (Hughes et al., 2006; Suzuki et al., 1995; Tateda et al., 1998; Zhao et al., 2007). Suzuki et al (Suzuki et al., 1997a) showed that addition of ATP to isolated guinea pig globular substance vesicles resulted in a 5-6 fold increase in intravesicular Ca^{2+} . This suggested that increasing the concentration of Ca^{2+} in globular substance vesicles could permit nucleation of $CaCO_3$ crystals, and that ATP might serve as the trigger *in vivo*.

The role of ATP in the inner ear has been primarily studied in the cochlea (Housley, 2000; Lee and Marcus, 2008). Extracellular ATP affects depolarization and stiffness of the stereocilia of hair cells, level of Na^+ and Ca^{2+} in the endolymph, and endocochlear potential which ultimately alters hearing sensitivity. In the vestibular system, dark cells in the non-sensory epithelium are thought to be a possible site for ATP release (Lee and Marcus, 2008).

Diverse signaling pathways are activated by ATP in the inner ear (Housley, 2000), but the kinetics and concentration dependence of the ATP-mediated Ca^{2+} increase in globular substance vesicles (Suzuki et al., 1997a) was most similar to that of known purinergic P2 receptors (P2Y and P2X families). P2Y receptors are metabotropic G-protein coupled receptors which mediate release of Ca^{2+} from intracellular stores (Burnstock, 2007; Ralevic and Burnstock, 1998). P2X family receptors contain ionotropic channels which form homo- or hetero-trimers, and binding of nucleotides leads to an influx of extracellular Ca^{2+} into the cytosol (Burnstock, 2007; North, 2002). Each receptor subtype in the P2 families has different sensitivities to nucleotide agonists and pharmacological agents (North, 2002; Ralevic and Burnstock, 1998).

Based on the hypothesis that OTOPI1 may regulate Ca^{2+} flux in inner ear cells, our previous studies demonstrated that *in vitro* OTOPI1 is sufficient to modulate a purinergic response (Hughes et al., 2007). Overexpression of OTOPI1 in immortalized cell lines leads to specific modulation of purinergic signaling mediated increase in intracellular calcium ($[\text{Ca}^{2+}]_i$); a non-specific depletion of endoplasmic reticulum (ER) Ca^{2+} stores, a specific inhibition of P2Y receptor signaling, and initiation of a novel influx of extracellular Ca^{2+} .

Here, we have targeted the *Otop1* gene by insertion of β -galactosidase. Homozygous null mice show a balance defect caused by otoconia agenesis with no major histological abnormalities in the sensory epithelia. High resolution expression studies localize *Otop1* in the extra-striolar region of the utricle and saccule, and at the apex of supporting cells. In addition to the anticipated embryonic expression, we found that *Otop1* expression persisted in the adult, suggesting a role for OTOPI in the maintenance of otoconia. Calcium imaging showed that OTOPI functions *in vivo* in macular supporting cells where it regulates purinergic signaling. These data support a role for OTOPI and purinergic regulation of Ca^{2+} in the formation, growth and maintenance of otoconia.

Materials and methods

Generation of $Otop1^{\beta gal/\beta gal}$ allele

The targeting construct was made using recombineering methods (Liu et al., 2003). First, about 5 kb upstream and downstream of the regions to target was retrieved from BAC clone RP24-286E11 (derived from C57BL/J6 mice) which completely spanned the *Otop1* gene. We designed a deletion of the last 62 bp of exon 2 after the *Otop1c* splice acceptor site and 2.7 kb of intron 2 and inserted the β -galactosidase (*βgal*) gene and *LoxP/pol-2-neo/LoxP* selectable marker (6.1 kb). To achieve this, 500 bp sequences immediately 5' and 3' of the site that we aimed to target was ligated to the βgal coding sequence and the neo cassette, which was excised from the PL452 vector, and cloned into a pBluescript vector. This construct was electroporated into DY380 cells already containing the retrieved BAC plasmid, and heat shock (32°C -> 42°C) was used

to induce homologous recombination to generate the targeting vector. The 5' and 3' regions of homology contained a total of 8.5 kb of genomic DNA. The targeting vector was verified by restriction mapping and sequencing.

Before electroporation, the integrity and function of the OTOP1^{βGAL} fusion protein was tested in tissue culture cells. The Otop1-βgal portion of the targeting vector was transiently expressed using lipofectamine (Invitrogen) in COS7 cells under a CMV promoter and cells were stained for βgal activity. OTOP1^{βGAL} positive cells showed X-gal staining consistent with either cytoplasmic or ER localization of the chimeric protein. The first 109 amino acid residues of OTOP1 containing the first two TM domains were also fused to EGFP and tested for known biochemical activities using a ratiometric calcium assay in which full length OTOP1 functions to alter cytoplasmic calcium levels in response to purinergic stimuli (Hughes et al., 2007). This assay (data not shown) demonstrated that the amino terminal two TM domains are by themselves biologically inactive and therefore, that the insertion of *βgal* and the deletion of the remaining OTOP1 protein likely constitutes a null mutation. The targeting construct was linearized and electroporated into SCC-10 ES cells, which were derived from 129X1/SvJ mice. Electroporation was carried out in the Washington University Siteman Cancer Center Muring Embryonic Stem Cell Core facility. G418 resistant clones were screened for homologous recombination by Southern blot using 5' probes. Two positive clones were identified and homologous recombination was verified using a 3' Southern blot probe. ES clones were karyotyped and then microinjected into mouse blastocysts by the Washington University Mouse Genetics Core facility. Chimerism was determined by coat color and high percentage chimeric males were mated with C57BL6/J females. The

subsequent F1 mice were intercrossed, and the litters were examined for the germline transmission of the *Otop1* ^{β gal} allele using Southern blotting with 5' and 3' probes extrinsic to the targeting vector, and by genomic PCR (Figure 1D, E). The LoxP-neo cassette was excised *in vivo* by mating to a mouse that expressed Cre in the germ line, and then the male progenies were bred to C57BL6/J females to transfer the targeted allele onto a C57BL6/J genetic background. Phenotypes that we observed in this study appeared independent of genetic background.

Southern blotting and genotyping

Genomic DNA was extracted with phenol/choloroform and isopropanol precipitation. 10 μ g of each sample was digested with EcoRV at 37°C overnight, and electrophoresed on 1% agarose gel. Southern blots were probed with 5' and 3' probes, which were labeled with ³²P (Stratagene Prime-It II Random Primer Labeling Kit) and purified (Amersham Biosicences MicroSpin S-200 HR columns). 5' and 3' probes were made by amplification from RP24-286E11 BAC DNA with the following primers; 5' probe: primer 1 (5'-CACCACGTCTAAACAAGCCA- 3' (forward)), primer 2 (5' - GCCACACAGGACTTTCTTTT- 3' (reverse)), 3' probe: primer 1 (5' - GATAATTTCACTGTAAAGC- 3' (forward)), primer 2 (5' - GAGATTCAGTACCAATGATT- 3' (reverse)). For genotyping PCR, mouse tail DNA was amplified with the following primers; primer 1 (5'-AGGGTCTCCACAAGCTTCCGGT-3' (forward)), primer 2 (5'-TGACAGCCTACAGCCCAGGATG-3' (wild-type reverse)), primer 3 (5'-CCATTCAGGCTGCGCAACTGT-3' (*Otop1* ^{β gal} reverse)). 30 cycles of denaturation at

94°C for 1 min, annealing at 65°C for 1 min, and extension at 68°C for 3 min were used to amplify either 545 (wild-type) or 369 (*Otop1*^{βgal}) bp fragments.

H&E and X-gal staining

E16.5 temporal bones were dissected in cold PBS, and fixed in 4% paraformaldehyde at 4°C overnight. After washing in PBS, tissues were embedded in paraffin. 8 μm sections were deparaffinized and stained with Hematoxylin and eosin (H&E).

For X-gal staining, temporal bones were fixed at 4°C overnight in 0.2% glutaraldehyde, 5 mM EGTA (pH 7.3), 100 mM MgCl₂ in PBS (3.2 mM Na₂HPO₄, 0.5 mM KH₂PO₄, 1.3 mM KCl, 135 mM NaCl, pH 7.4.). Adult temporal bones were decalcified in 0.35 M EDTA in 0.1 M sodium phosphate buffer (pH 7.2-7.4) before further processing. To make frozen sections, fixed temporal bones were incubated in 30 % sucrose overnight and then frozen in OCT prior to cryosectioning. Whole temporal bones or frozen sections were stained for βgal at room temperature or 4°C in the following solution; 2 mM MgCl₂, 0.01% sodium deoxycholate, 0.02% Nonidet-P40, 5mM potassium ferricyanide, 5mM potassium ferrocyanide, 0.1% X-gal in PBS. After sufficient color development, temporal bones or sections were washed in PBS and imaged.

RNA extraction, cDNA synthesis, semi-quantitative and quantitative RT-PCR

For detection of mouse *Otop1* mRNA, tissues (utricle, saccule, cochlea, lung) from either 4 adult or 8 pups were dissected and pooled. For detection of chicken *Otop1* mRNA, 8 utricular epithelia were pooled for each culture and two cultures were assayed as each time point (1 DIV, 7 DIV). For detection of purinergic receptors, a plate of mouse

utricular dissociated cultures made from 8 P3 mouse pups was used. RNA was extracted with Trizol (Invitrogen) and ethanol precipitation. 0.5-1 µg of RNA was treated with DNase I (Invitrogen) to remove genomic DNA contamination prior to cDNA synthesis (Invitrogen SuperScript III First-Strand Synthesis System for RT-PCR). Mouse *Otop1* mRNA levels were quantified using a TaqMan® gene expression assay (#00554705_m1, ABI inc.). Quantitative RT-PCR using Sybr green (ABI inc.) was used to measure chick *Otop1* levels. Primers to chick *Otop1* (Forward: 5'-TAAATTCTGGACTCCTTTAAAATTGGA-3', Reverse: 5'-GAACACAGAATGGATAACCCCAAAC-3') and *GAPDH* (Forward: 5'-TGATGGGTGTCAACCATGAGA-3', Reverse: 5'-TGGCATGGACAGTGGTCATAA-3') were designed. Taqman and Sybr green assays were run in a 7500 fast real-time PCR machine (ABI inc.). For semiquantitative RT-PCR analysis of P2X and P2Y receptors in mouse dissociated epithelial cultures, previously designed primers and published PCR conditions were used (Hayato et al., 2007).

Production of anti-Otop1 antibody

A rabbit polyclonal antibody was made using a 16-amino acid peptide epitope (ARGSPQASGPRRGASV) derived from the N-terminus of OTOPI (Figure 1C). The synthetic peptide was conjugated to maleimide-activated keyhole limpet hemocyanin prior to injection into the rabbit. The resulting antibody was purified on the peptide affinity column, and validated by Western blotting of extracts from inner ear tissues. Further validation was performed in this study by comparing the immunostaining patterns with those of X-gal staining.

Wholemout immunohistochemistry

Temporal bones were isolated in Leibovitz's medium L15 (Sigma) and fixed in 4% paraformaldehyde for 1-2hr at room temperature. Utricular and saccular maculae were dissected from the temporal bones in cold PBS, incubated in 0.5% Triton X-100 for 30 min at room temperature, and then washed with PBS. Samples were blocked using 4% BSA/PBS overnight at 4°C, and incubated with rabbit anti-OTOP1 (1:800) and/or mouse anti-parvalbumin (Sigma- 1:500) for 90 min at room temperature in a humidified chamber. After washing with PBS, samples were incubated with secondary antibodies, Alexa 488 anti-rabbit IgG (Invitrogen- 1:600) and Alexa 555 anti-mouse IgG (Invitrogen- 1:600), respectively, for 45 min at room temperature. For stereocilia staining, samples were further incubated with rhodamine-phalloidin (1:200, Invitrogen) for 15 min at room temperature. After washing with PBS, samples were transferred to a superfrost slide, mounted with vectashield (Vector labs), and coverslipped before imaging.

Frozen section immunohistochemistry

Frozen sections were recovered in PBS, and blocked with 4% BSA, 0.3% Triton in PBS. Sections were incubated with anti-OTOP1 (1:800) and anti- β -gal (1:1000) antibodies overnight at 4°C. After washing with 0.3% Triton in PBS, sections were incubated with secondary antibodies (Cy3 anti-rabbit IgG – 1:200, Alexa 488 anti-chicken IgG – 1:600) for 2 hr at RT. Samples were mounted with vectashield (Vector labs).

Utricular macular organotypic and dissociated cultures

P0-P3 mouse utricles and 6-14 days post hatch chicken utricles were dissected in medium 199 (Gibco #12350039), and the nonsensory epithelium and otoconial layer were

completely removed. After incubation in thermolysin (25 mg diluted in 50 ml medium 1999 (Gibco #12340030)) (Sigma) at 37°C for 50 min, the underlying stroma was removed and the remaining epithelial sheet was attached to a MatTek dish using ECM gel (Sigma). The tissue was incubated in growth media overnight at 37°C. For dissociated culture, isolated epithelial sheets were treated with Trypsin/EDTA (0.05%, 0.02%) for 15 min at 37 °C. After replacing Trypsin/EDTA with Medium 199 (Gibco #12340030) cells were triturated 5 to 10 times and plated on laminin coated MatTek dishes and incubated overnight at 37°C. The next day Medium 199 (Gibco #12340030) containing 10% fetal bovine serum (Gibco) (growth media) was added. For transfection of chicken utricular macular cells, cultures were treated with Lipofectamine 2000 (Invitrogen) and approximately 1 µg plasmid DNA (EGFP, FLAG-Otop1 (Hughes et al., 2007)) in OptiMEM (Invitrogen) for 4-5 hours following manufacturer's instructions. Cultures were allowed to recover overnight in growth media.

Ratiometric calcium imaging and data analysis

All imaging experiments were carried out at room temperature in a HEPES-buffered salt solution (HCSS) containing, in mM: 140 NaCl, 5.4 KCl, 1 NaH₂PO₄, 1.8 CaCl₂, 1 MgSO₄, 12 HEPES, and 5.5 D-glucose, pH 7.4±0.1. Nominally calcium-free media was HCSS solution without CaCl₂. Organotypic or dissociated utricular macular cultures were loaded with fura-2 by incubation for 60 min with 5-10 µM acetoxymethyl (AM) ester (Invitrogen, Eugene, OR) and 0.1% Pluronic F-127 (Invitrogen, Eugene, OR) in HCSS (pH=7.2) at room temperature, washed with HCSS and incubated for another 60 min to allow for ester hydrolysis. After loading, cells were imaged on an inverted microscope (Nikon Eclipse TE300, Nikon Inc., Melville, NY) equipped with a cooled

CCD camera (Cooke Corp., Auburn Hill, MI) using a 20x/0.45 Plan Fluor objective (Nikon). The fluorescence excitation (75 W xenon arc lamp) was provided by band-specific filters (340 and 380 nm; Semrock, Rochester, NY) in combination with a XF73 dichroic beam splitter (Omega Optical, Brattleboro, VA). Pairs of images were collected constantly at alternate excitation wavelengths. After subtracting the matching background, the images were divided by one another to yield ratio values for individual cells. For studies done with mouse macular dissociated cultures, 10 μ M ionomycin was added at the end of each experiment to obtain the maximum ratio (340/380) in each region of interest. To reduce variability between experiments performed on different days, raw data were normalized as follows: Normalized Ratio = $(R - R_0)/(R_{\max} - R_0)$, where R is individual ratio value, R_{\max} is the peak ratio after addition of ionomycin, R_0 is the average of the prestimulation baseline ratio. All the data in figure 6E-I represent normalized ratios. Ionomycin was from Calbiochem (San Diego, CA), and bisphenol, EGTA, ATP, ADP, UTP, and ADP were from Sigma (St. Louis, MO).

Results

Otopetrin 1 (Otop1) deficiency results in otoconial agenesis.

To generate a null allele for *Otop1* and to create a histochemical tag to identify OTOP1-expressing cells the *Otop1* gene was targeted by insertion of the β -galactosidase (β gal) coding sequence. *Otop1* has seven exons and three identified amino terminal alternative splice variants, *Otop1a*, *1b* and *1c* (Figure 1A, B). Although *Otop1a* is the most abundant splice variant expressed in the inner ear (Hurle et al., 2003), to ensure generation of a null allele, the β gal cDNA was inserted in frame in exon 2 such that all

known splice variants would be captured as fusion proteins with β GAL. This configuration created an OTOPI1- β GAL fusion protein that includes 109 amino acid residues of OTOPI1a, 107 amino acid residues of OTOPI1b or 41 amino acid residues of OTOPI1c amino terminal coding sequence fused at amino acid residue 5 of β GAL. This design expressed *Otop1* ^{β gal} transcripts under the control of *Otop1* transcriptional regulatory elements. For the *Otop1a* and *Otop1b* transcripts, this fusion protein includes the first two transmembrane (TM) domains of OTOPI1 (Figure 1C). The germ-line transmitted targeted allele was bred to homozygosity (confirmed by Southern blotting and genomic PCR (Figure 1D, E)). Heterozygous *Otop1* ^{β gal/+} mice were phenotypically normal (Figure 1F, G). *Otop1* ^{β gal/ β gal} mice showed vestibular dysfunction (inability to swim) and otoconial agenesis (Figure 1F, H). The sensory epithelium of the utricle and saccule were histologically normal.

OTOPI1 ^{β GAL} expression in the vestibular sensory epithelium.

The spatial and temporal expression pattern of OTOPI1 ^{β GAL} in the inner ear was assessed by X-gal staining. β GAL activity was first apparent at E13.5 in the utricle (Figure 2A). By E16.5, staining intensity increased in the utricle and became apparent in the saccule (Figure 2B). This expression pattern correlated with the onset and maximal rate of otoconial synthesis in the utricle and saccule (Anniko, 1980; Anniko et al., 1987). Importantly, at this stage no expression was observed in any other inner ear organs or structures (semicircular canals or cochlea). At E18.5, however trace β GAL activity was occasionally detected in the endolymphatic sac (data not shown). Examination of whole maculae after X-gal staining revealed a striking absence of expression in the striolar region of the utricle and saccule (Figure 2C, E), a pattern that persisted in adult mice. In

addition to expression in non-striolar regions of the macula, some transitional cells were also positive for β GAL activity (Figure 2D), indicating possible involvement of a subset of transitional cells during otoconial development.

Histological sections through the maculae revealed a staining pattern consistent with expression in supporting cells and transitional cells (Figure 2F, G). Within supporting cells, X-gal staining was observed at three locations; above supporting cell nuclei, in the middle, or at the apex of supporting cells. Because the OTOP1- β GAL protein contains two putative TM domains, it is likely that the fusion protein is tethered to intracellular or surface membranes of supporting cells. From X-gal staining, it cannot be determined whether OTOP1- β GAL is also expressed in hair cells.

In mice, otoconia formation is completed by P7 (Erway et al., 1986; James et al., 1969). Although in the adult otoconia do not continue to grow, there remains a slow turnover of calcium ions (Balsamo et al., 2000; Preston et al., 1975). This suggests that homeostatic mechanisms function to maintain otoconia mineralization. To determine whether OTOP1 could function in otoconia maintenance, OTOP1 ^{β GAL} expression was examined in older animals. Inner ear sections from P7 and 6-month-old mice (Figure 2G, H) showed that *Otop1* continues to be expressed in the supporting and transitional epithelium of the utricle and saccule. To confirm expression in adult mice, endogenous *Otop1* mRNA was detected by quantitative RT-PCR from P2 and 6-month-old utricle and saccule. Consistent with the β GAL activity, both P2 and 6 month-old tissues showed specific expression of *Otop1* in the utricle and saccule but no expression in the cochlea or lung (Figure 2I).

OTOP1 is localized to the apex of supporting cells.

Otoconia are formed within the gelatinous membrane above the utricle and saccule sensory epithelia. We hypothesized that OTOP1 protein would be localized at a subcellular site consistent with a role in the biosynthesis and/or maintenance of otoconia. Polyclonal antibodies, generated to an epitope located in the amino terminal domain of OTOP1 (Figure 1C), were validated by comparing immunohistochemical staining patterns on *Otop1*^{+/+} and *Otop1*^{βgal/βgal} maculae. In *Otop1*^{+/+} maculae, endogenous OTOP1 was localized at the apical membrane of the epithelium (Figure 3A, C). In addition, some signals were also present in a punctate pattern throughout the cell body, suggesting possible trafficking of OTOP1 to the apex. In *Otop1*^{βgal} embryos, the epitope recognized by the antibody is tethered to βGAL (Figure 1C). In *Otop1*^{βgal/βgal} maculae, immunohistochemistry showed co-localization of anti-OTOP1 and anti-βGAL signals in intracellular aggregates (Figure 3D, E, F). OTOP1^{βGAL} signals were more intense than those of the endogenous protein, possibly because the fusion protein forms stable aggregates associated with intracellular membranes, owing to the fused TM domains (Figure 3A, D).

Immunostaining of frozen sections and wholemounts of the utricle and saccule with the anti-OTOP1 antibody was used to identify cell-specific expression of the endogenous OTOP1 protein. Stacked confocal images (Figure 3G) confirmed that anti-OTOP1 signals were localized towards the apex, just beneath the phalloidin signal, which marks the stereocilia bundles of the hair cells. Restricted expression of OTOP1 in supporting cells was demonstrated in both *Otop1*^{+/+} frozen sections and wholemounts. High intensity apical staining was absent above hair cell nuclei but present above supporting cell nuclei (Figure 3H, lines), and the cells beneath the stereocilia (marked by

phalloidin staining) were all negative for OTOPI (Figure 3I, J). Absence of expression of OTOPI in the hair cells was also shown by lack of co-localization of OTOPI^{βGAL} with the hair cell marker, α -parvalbumin (Figure 3K, L).

OTOPI expression alters the purinergic response in chick utricular epithelial cells.

Previous *in vitro* studies (Hughes et al., 2007) identified a potential role for *Otop1* in modulating cytosolic free calcium ion concentration ($[Ca^{2+}]_i$) in response to purinergic signals, such as ATP. Because endolymph is known to contain ATP and purinergic receptors have been identified in several cell types within the inner ear (Housley, 2000; Lee and Marcus, 2008), we hypothesized that OTOPI may also function to regulate purinergic signaling in vestibular supporting cells. Primary chick utricular epithelial cells (Figure 4A) proliferate *in vitro* and express markers consistent with a supporting cell phenotype (Coutinho et al., 1999; Goodyear and Richardson, 2002; Kruger et al., 1999). Quantitative RT-PCR detected *Otop1* expression in acutely dissociated cells (Figure 4B). However, after seven days *in vitro* (DIV), expression of *Otop1* was reduced to a minimal level. This system allowed us to compare the effects of *Otop1* expression in primary vestibular supporting cells to previous studies using heterologous cells (Hughes et al., 2007). To test whether 7 DIV primary chick utricular epithelial cells respond to a purinergic stimulus, cells loaded with the ratiometric Ca^{2+} indicator, fura-2, were imaged to detect changes in single cell cytosolic free Ca^{2+} concentrations ($[Ca^{2+}]_i$) before, during, and after stimulation with 100 μ M ATP (Grynkiewicz et al., 1985; Tsien et al., 1985). Application of 100 μ M ATP resulted in a rapid rise in $[Ca^{2+}]_i$ followed by a steep return to baseline (Figure 4C). This type of response is typical of purinergic receptors of the P2Y family (Carter et al., 1988; Hughes et al., 2007).

To determine if OTOPI1 could modulate the accumulation of Ca^{2+} in 7 DIV primary chick utricular epithelial cells, changes in $[\text{Ca}^{2+}]_i$ in response to ATP in cells transfected to express cytosolic *EGFP*, *EGFP-tagged Otop1 (EGFP-Otop1)*, *FLAG-tagged Otop1 (FLAG-Otop1)*, or native *Otop1* were measured. Cells transfected with either *EGFP-Otop1* (data not shown) or *FLAG-Otop1* (co-transfected with cytosolic *EGFP*) responded to ATP with altered characteristics in the duration of $[\text{Ca}^{2+}]_i$ elevation (Figure 4D). Transfection with cytosolic *EGFP* alone did not significantly alter the purinergic response (Figure 4C). In *Otop1* expressing cells, the initial characteristic P2Y mediated spike in $[\text{Ca}^{2+}]_i$ was absent and an increase in $[\text{Ca}^{2+}]_i$ to an elevated plateau was observed. Similar results were seen for untagged *Otop1* co-transfected with *EGFP* (data not shown), suggesting that the alteration in Ca^{2+} mobilization is specific to OTOPI1 activity.

OTOPI1 modulates purinergic response in the utricular maculae.

To determine if endogenous OTOPI1 is necessary to regulate a purinergic response in the utricular epithelium, organotypic utricular macular cultures from *Otop1*^{+/+} and *Otop1*^{βgal/βgal} inner ears were exposed to ATP. $[\text{Ca}^{2+}]_i$ was examined in multiple areas within each organotypic culture (Figure 5A, B, C). In the *Otop1*^{+/+} samples, addition of 100 μM ATP resulted in an increase in $[\text{Ca}^{2+}]_i$, characterized by an elevated plateau that persisted until removal of the agonist (Figure 5D). The shape of this response curve resembled that of *Otop1*-transfected chick macular epithelial cells (Figure 4D), and the globular substance vesicle response to ATP observed by Suzuki et al. (Suzuki et al., 1997a). In contrast, in *Otop1*^{βgal/βgal} maculae, the response to ATP resulted in an initial increase in $[\text{Ca}^{2+}]_i$, forming a peak, followed by a reduction in $[\text{Ca}^{2+}]_i$ to an elevated

plateau (Figure 5D). These observations suggest that OTOPI functions to partially inhibit a purinergic signal in the utricular macula.

Dissociated cultures from *Otop1*^{+/+}, *Otop1* ^{β gal/+}, and *Otop1* ^{β gal/ β gal} maculae were used to further characterize the OTOPI-specific regulation of the purinergic response. Attempts to fully dissociate mouse maculae resulted in cultures that contained regions of epithelial sheets and clusters of cells that formed globule-like structures (Figure 6A). Interestingly, β GAL activity in *Otop1* ^{β gal/+} or *Otop1* ^{β gal/ β gal} cultures was present in cells associated with these globule-like structures, and was less often found in the adjacent epithelial sheets (Figure 6D). Therefore, the regions near the globule-like structures were selected for imaging (Figure 6B, C). The ATP response of organotypic and dissociated macular cells were similar in their shape and kinetics (Figure 5D, 6E). *Otop1*^{+/+} and *Otop1* ^{β gal/+} maculae showed a similar response to ATP, demonstrating that a single *Otop1* allele is sufficient for OTOPI-specific modulation of the purinergic response. This result is consistent with the presence of normal otoconia in *Otop1* ^{β gal/+} mice (Figure 1G). Cells from regions of the cultures that did not express OTOPI (in *Otop1*^{+/+}) or OTOPI- β GAL (in *Otop1* ^{β gal/ β gal}) showed a different response, characterized by a higher initial peak and greater rate of decay in $[Ca^{2+}]_i$ (Figure 6G, J). Importantly, cells from these regions showed identical responses regardless of whether they were derived from *Otop1*^{+/+} or *Otop1* ^{β gal/ β gal} maculae.

Previous studies showed that the initial peak in response to ATP primarily results in the release of inositol-1,4,5-trisphosphate (IP3)-sensitive intracellular stores by activation of P2Y receptors (Carter et al., 1988). Therefore, the reduced peak observed in *Otop1*^{+/+} compared to *Otop1* ^{β gal/ β gal} (Figure 6E) suggested that OTOPI may function *in*

in vivo to inhibit P2Y signaling. To examine whether OTOPI can block P2Y mediated calcium release, we tested the response to UTP, a P2Y receptor-specific agonist (Burnstock, 2007; Ralevic and Burnstock, 1998) (Figure 6F). Interestingly, the rate of decay in response to UTP was greater in both *Otop1*^{+/+} and *Otop1*^{βgal/βgal} experiments when compared to the ATP response (Figure 6J). This is likely because UTP does not activate P2X receptors, which, through influx of extracellular Ca²⁺, maintain the plateau phase of the response curve. Notably, similar to what was observed with ATP, UTP showed a lower peak value in *Otop1*^{+/+} compare to *Otop1*^{βgal/βgal} macular supporting cells, indicating inhibition of P2Y receptor-mediated calcium release by OTOPI. Because multiple P2X and P2Y receptors with different ligand sensitivities were found to be expressed in the dissociated macular culture (Figure 7) we also tested the activity of two major purine analogs (ADP and UDP). Significant difference in the peak values were not observed following treatment with either ADP or UDP (data not shown). This suggested that OTOPI may preferentially inhibit the function of P2Y receptor subtypes featuring high affinity to ATP and UTP, such as P2Y2 and P2Y4 (Dubyak, 2003; Ralevic and Burnstock, 1998). Other purinergic receptors expressed in the macular epithelium, that are not regulated by OTOPI, may also contribute to the observed increase in [Ca²⁺]_I in response to ADP or UDP. Alternatively, the inhibitory function of *Otop1* may require ATP and UTP but not ADP or UDP.

To examine whether purinergic responses observed in *Otop1*^{+/+} and *Otop1*^{βgal/βgal} maculae are dependent on intracellular calcium stores, cultures were incubated with bis-phenol prior to addition of ATP. Bis-phenol induces release of Ca²⁺ from intracellular stores by inhibiting Ca²⁺ reuptake by intracellular Ca²⁺ATPases (Brown et al., 1994;

Harper et al., 2005). Because a P2Y receptor-mediated increase in $[Ca^{2+}]_i$ is dependent on intracellular Ca^{2+} stores, incubation with bis-phenol should uncouple P2Y receptor signaling from the release of intracellular Ca^{2+} stores. In the presence of bis-phenol, *Otop1*^{+/+} and *Otop1*^{βgal/βgal} cultures responded to ATP in a similar manner with a peak and rate of decay comparable to that of *Otop1*^{+/+} in normal media (Figure 6H, J). This is consistent with a loss of P2Y receptor response and retained P2X receptor-like response in *Otop1*^{+/+} and *Otop1*^{βgal/βgal} cultures in the presence of bis-phenol.

Previous *in vitro* studies (Hughes et al., 2007) and the gain-of-function experiments in cultured chick macular supporting cells (Figure 4), suggested that OTOPI might have a secondary P2X-like function to mediate influx of extracellular Ca^{2+} in response to ATP. To determine whether OTOPI functions *in vivo* to mediate influx of Ca^{2+} , *Otop1*^{+/+} and *Otop1*^{βgal/βgal} cultures were assayed for changes in $[Ca^{2+}]_i$ in response to a purinergic stimulus in the absence of extracellular Ca^{2+} . Imaging in “nominally” calcium free media (containing 10-20 μ M Ca^{2+} , determined with a Ca^{2+} -selective electrode and fura-2 fluorimetry) (Figure 6I) or normal media with 10 mM EGTA (containing less than 1 nM Ca^{2+} , data not shown) showed a similar response. In both *Otop1*^{+/+} and *Otop1*^{βgal/βgal} cultures, the plateau phase, which represents a balance between an influx of extracellular Ca^{2+} and efflux of cytosolic Ca^{2+} into intracellular stores, is greatly reduced. This results in a faster decay of the initial P2Y peak (Figure 6J) compared to cultures stimulated with ATP in normal media. Importantly, the difference in the initial peak value between *Otop1*^{+/+} and *Otop1*^{βgal/βgal} cultures was no longer observed when extracellular Ca^{2+} was removed. This suggests that the function of OTOPI to inhibit P2Y activity is dependent on extracellular Ca^{2+} (at concentrations higher than

that in nominally Ca^{2+} free media). These data support a model in which OTOPI inhibits P2Y receptor-mediated Ca^{2+} release in macular epithelial cells in a Ca^{2+} -dependent manner, and allows or induces an extracellular influx of Ca^{2+} in response to ATP.

Conclusion

Otop1 is essential for otoconia formation and thus for the normal physiological function of the gravity receptor organs in the inner ear. Several missense alleles in *Otop1* have been identified (*tilted*, *mergulhador*, *backstroke*) and all lead to otoconial agenesis in the mouse or otolith agenesis in the zebrafish (Hurle et al., 2003; Sollner et al., 2004). The biochemical function(s) of OTOPI are poorly understood and the biochemical consequences of these missense mutations are not known. To interpret phenotype in relation to the biochemical function of *Otop1* alleles requires knowledge of the genetic null allele and its phenotype. To this end, we have created a genetic null allele for *Otop1*, tagged with β -galactosidase (*Otop1* ^{β gal}). Homozygous *Otop1* ^{β gal/ β gal} mice have otoconial agenesis, similar to that seen in *tilted* and *mergulhador* mice.

The *Otop1* ^{β gal} allele permitted a highly sensitive assay to identify spatial and temporal patterns of *Otop1* expression and to validate an antibody directed against OTOPI. Staining whole maculae for β -galactosidase activity revealed several novel features of *Otop1* expression. Most remarkably, *Otop1* is excluded from the striola in both the utricle and saccule, while intensely expressed in the remaining regions of the maculae. Otoconia size range from 0.5 to 30 μm in mammals, and the striola is known to have fewer and smaller otoconia (Lindeman, 1973). Thus, otoconia formed above the site

where *Otop1* is expressed are likely to be larger in size and number, correlating *Otop1* expression with its proposed role in the regulation of otoconia growth or calcification.

Staining histological sections of the maculae for β -galactosidase activity and immunohistochemical detection of endogenous OTOP1 revealed that OTOP1 is expressed in the supporting and a subset of transitional cells of the mouse utricle and saccule, but not in hair cells. In contrast, zebrafish *Otop1* mRNA was localized to hair cells during otolith growth (Sollner et al., 2004). This disparity between mouse and zebrafish could reflect differences in the cell types that are critical for otolith and otoconia formation. Importantly, it has been shown that hair cells in mice (Bermingham et al., 1999; Hughes et al., 2006; Lundberg et al., 2006) and supporting cells in zebrafish (Haddon et al., 1999; Hughes et al., 2006; Lundberg et al., 2006) are not required for otoconia/otolith formation.

Otoconia are formed during embryonic and perinatal development and *Otop1* is expressed throughout this time. Once formed, the initial complement of otoconia is thought to last throughout the life of the organism, with only limited amounts of Ca^{2+} turnover (Balsamo et al., 2000; Preston et al., 1975). However, the observation that *Otop1* expression persists in the adult (mouse) suggests a possible role for OTOP1 in the maintenance and/or repair of otoconia. In humans, otoconia are prone to degeneration and displacement due to aging, exposure to ototoxic drugs and head trauma, leading to benign positional vertigo and progressive loss of balance (House and Honrubia, 2003; Ross et al., 1976; Welling et al., 1997). It is not known whether, in humans, *Otop1* is expressed throughout life and whether OTOP1, alone, is necessary to maintain or repair otoconia. Analysis of *Otop1* expression in human gravity sensing organs could provide a clue as to

whether OTOPI has a conserved role in the maintenance of otoconia in different species. It will also be interesting to investigate whether deformation and fragmentation of otoconia, a frequent occurrence in old animals (Jang et al., 2006) and humans (Walther and Westhofen, 2007), results from diminished expression or activity of OTOPI.

Previous studies showed that OTOPI expression in heterologous cells could modify the cellular response to purinergic signals resulting in altered concentrations of cytosolic Ca^{2+} (Hughes et al., 2007). To determine whether a similar OTOPI-dependent biochemical activity exists in inner ear supporting cells *in vivo*, we examined OTOPI function in primary chick and mouse utricular epithelial cultures. Restoring *Otop1* expression in chick and comparing wild type and *Otop1* ^{β gal/ β gal} mouse utricular macular epithelial cultures identified distinct functions by which OTOPI modulates purinergic signaling *in vivo*. Most importantly, we found that endogenous OTOPI functions to inhibit P2Y receptor activity and subsequent release of Ca^{2+} from intracellular stores in response to purinergic stimuli *in vivo*. This function was closely phenocopied by depleting intracellular Ca^{2+} stores by application of bis-phenol, an inhibitor of all microsomal Ca^{2+} ATPases that effectively uncouples Ca^{2+} release from P2Y signaling (Brown et al., 1994; Harper et al., 2005).

The function of P2Y signaling during otoconia formation is not known. However, recent studies have identified a role for P2Y in bone mineralization, and otoconia and bone mineralization share a number of common features (Hughes et al., 2006; Orriss et al., 2007). In osteoblasts, P2Y2 receptor activation by ATP and UTP functions to inhibit mineralization *in vitro* and P2Y2^{-/-} mice show increased bone mineral density (Hoebertz et al., 2002; Orriss et al., 2007). In the inner ear, P2Y receptors are expressed in the

sensory epithelium (Figure 7) and nonsensory epithelium (Piazza et al., 2007; Sage and Marcus, 2002; Vlajkovic et al., 2007), and could function to inhibit ectopic mineralization in the inner ear. Suppressing ectopic mineralization would be an essential function because ectopic mineral deposits or otoconia fragments in the semicircular canals (cupulolithiasis) is thought to be a major cause of positional vertigo (Hughes et al., 2006; Marom et al., 2009) and ectopic mineralization in the cochlea could impair auditory function. Inhibition of P2Y receptor signaling by OTOPI in the macular epithelium could serve to locally suppress P2Y activity and thus be permissive to localized mineralization of otoconia.

An additional passive mechanism that could prevent ectopic mineralization in the inner ear is the very low concentration of Ca^{2+} ions normally found in endolymph (10-20 μM) (Anniko, 1980; Salt et al., 1989). However, a consequence of low endolymph $[\text{Ca}^{2+}]$ is the requirement to locally increase $[\text{Ca}^{2+}]$ at the site of otoconia nucleation and growth. This could be achieved by nucleating otoconia within Ca^{2+} -rich vesicles released from supporting cells and/or by maintaining local high concentrations of calcium in the otoconial membrane. The presence of globular substance vesicles (Suzuki et al., 1995, 1997b), and Ca^{2+} ATPase activity in the apical end of the supporting cells (Yoshihara et al., 1987) support both mechanisms. The observation that endogenous or overexpressed OTOPI induces a P2X receptor-like influx of extracellular Ca^{2+} suggests a direct role for OTOPI in sequestration or trafficking of Ca^{2+} in the maculae. OTOPI could itself function as a Ca^{2+} channel or it may induce activity of other P2X-like channels. It is possible that OTOPI regulated flux of Ca^{2+} in supporting cells is a prerequisite for locally increasing $[\text{Ca}^{2+}]$, either directly in the extracellular space of the otoconial membrane or

within globular substance vesicles. Notably, the characteristics of the increase in $[Ca^{2+}]_i$ by OTOPI was very similar to the atypical purinergic response described by Suzuki et al in isolated globular substance vesicles (Suzuki et al., 1997a), suggesting that OTOPI may be responsible for the ATP-mediated increases in intravesicular $[Ca^{2+}]_i$ seen in these studies. In addition to Otop1, plasma membrane Ca^{2+} -ATPase 2 (PMCA2) is expressed on the apical surface of sensory hair cells (Dumont et al., 2001) and *PMCA2*^{-/-} mice show agenesis of otoconia (Kozel et al., 1998). Notably, $[Ca^{2+}]_i$ is lower in *Deafwaddler* (*Pmca2* frameshift mutation) endolymph compared to controls (Wood et al., 2004). Thus, both OTOPI and PMCA2 may cooperate to regulate local concentrations of Ca^{2+} above the macular epithelium.

To investigate the requirement for extracellular Ca^{2+} for OTOPI activity, wild type and *Otop1* ^{β gal/ β gal} macular epithelial cultures were assayed for purinergic responses in “nominally” Ca^{2+} free media and Ca^{2+} free media (10 mM EGTA). The $[Ca^{2+}]_i$ in “nominally” Ca^{2+} free media is similar to the $[Ca^{2+}]_i$ in the endolymph. The observation that OTOPI could no longer inhibit P2Y function in “nominally” Ca^{2+} free media (or in the presence of 10 mM EGTA) suggests that OTOPI is very sensitive to $[Ca^{2+}]_i$ and that apically localized OTOPI could act as a sensor for extracellular $[Ca^{2+}]_i$ or interact with other sensor molecules to form a feedback signal to regulate $[Ca^{2+}]_i$ above the macular sensory epithelium.

The studies presented here demonstrate that one function of OTOPI is to modulate purinergic signaling in macular supporting cells. This raises the important question of the role of ATP in endolymph. ATP is thought to be stored and released from vesicles in the marginal cells of the stria vascularis. In the vestibular system non-sensory

epithelium, dark cells (which are functionally similar to strial marginal cells) are a possible source of ATP (Lee and Marcus, 2008). Because OTOPI responds to ATP in a dose-dependent manner (Hughes et al., 2007), it may serve as an apical sensor of local ATP concentrations. For example, during otoconia formation, release of ATP containing vesicles might increase and maintain active OTOPI and active otoconial growth. Alternatively, ATP may function to activate purinergic receptors throughout the inner ear (to suppress ectopic mineralization) and through OTOPI activity, permit mineralization in the otoconial membrane. Lastly, it remains possible that the OTOPI response to purinergic signals and the modulation of cellular or extracellular Ca^{2+} may not be the central role for OTOPI during otoconia formation. For example, in zebrafish, OTOPI was shown to regulate the trafficking of *starmaker*, a protein required for otolith formation (Sollner et al., 2004).

Acknowledgements

We thank C. Smith for technical help and R. Thalmann for critically reading the manuscript. This work was funded by NIH grant DC02236 (DMO) and DC008603 (YWL).

References

- Anniko, M. (1980). Development of otoconia. *Am J Otolaryngol* 1, 400-410.
- Anniko, M., Wikstrom, S.O., and Wroblewski, R. (1987). X-ray microanalytic studies on developing otoconia. *Acta Otolaryngol* 104, 285-289.

- Balsamo, G., Avallone, B., Del Genio, F., Trapani, S., and Marmo, F. (2000). Calcification processes in the chick otoconia and calcium binding proteins: patterns of tetracycline incorporation and calbindin-D28K distribution. *Hear Res* 148, 1-8.
- Bermingham, N.A., Hassan, B.A., Price, S.D., Vollrath, M.A., Ben-Arie, N., Eatock, R.A., Bellen, H.J., Lysakowski, A., and Zoghbi, H.Y. (1999). Math1: an essential gene for the generation of inner ear hair cells. *Science* 284, 1837-1841.
- Brown, G.R., Benyon, S.L., Kirk, C.J., Wictome, M., East, J.M., Lee, A.G., and Michelangeli, F. (1994). Characterisation of a novel Ca²⁺ pump inhibitor (bis-phenol) and its effects on intracellular Ca²⁺ mobilization. *Biochim Biophys Acta* 1195, 252-258.
- Burnstock, G. (2007). Purine and pyrimidine receptors. *Cell Mol Life Sci* 64, 1471-1483.
- Carter, T.D., Hallam, T.J., Cusack, N.J., and Pearson, J.D. (1988). Regulation of P2y-purinoceptor-mediated prostacyclin release from human endothelial cells by cytoplasmic calcium concentration. *Br J Pharmacol* 95, 1181-1190.
- Coutinho, P., Goodyear, R., Legan, P.K., and Richardson, G.P. (1999). Chick alpha-tectorin: molecular cloning and expression during embryogenesis. *Hear Res* 130, 62-74.
- Dubyak, G.R. (2003). Knock-out mice reveal tissue-specific roles of P2Y receptor subtypes in different epithelia. *Mol Pharmacol* 63, 773-776.
- Dumont, R.A., Lins, U., Filoteo, A.G., Penniston, J.T., Kachar, B., and Gillespie, P.G. (2001). Plasma membrane Ca²⁺-ATPase isoform 2a is the PMCA of hair bundles. *J Neurosci* 21, 5066-5078.
- Erway, L.C., Purichia, N.A., Netzler, E.R., D'Amore, M.A., Esses, D., and Levine, M. (1986). Genes, manganese, and zinc in formation of otoconia: labeling, recovery, and maternal effects. *Scanning Electron Microscopy*, 1681-1694.
- Goodyear, R.J., and Richardson, G.P. (2002). Extracellular matrices associated with the apical surfaces of sensory epithelia in the inner ear: molecular and structural diversity. *J Neurobiol* 53, 212-227.
- Grynkiewicz, G., Poenie, M., and Tsien, R.Y. (1985). A new generation of Ca²⁺ indicators with greatly improved fluorescence properties. *J Biol Chem* 260, 3440-3450.
- Haddon, C., Mowbray, C., Whitfield, T., Jones, D., Gschmeissner, S., and Lewis, J. (1999). Hair cells without supporting cells: further studies in the ear of the zebrafish mind bomb mutant. *J Neurocytol* 28, 837-850.
- Harper, C., Wootton, L., Michelangeli, F., Lefievre, L., Barratt, C., and Publicover, S. (2005). Secretory pathway Ca(2+)-ATPase (SPCA1) Ca(2+) pumps, not SERCAs, regulate complex [Ca(2+)](i) signals in human spermatozoa. *J Cell Sci* 118, 1673-1685.

- Hayato, R., Ohtubo, Y., and Yoshii, K. (2007). Functional expression of ionotropic purinergic receptors on mouse taste bud cells. *J Physiol* 584, 473-488.
- Hoebertz, A., Mahendran, S., Burnstock, G., and Arnett, T.R. (2002). ATP and UTP at low concentrations strongly inhibit bone formation by osteoblasts: a novel role for the P2Y2 receptor in bone remodeling. *J Cell Biochem* 86, 413-419.
- House, M.G., and Honrubia, V. (2003). Theoretical models for the mechanisms of benign paroxysmal positional vertigo. *Audiol Neurootol* 8, 91-99.
- Housley, G.D. (2000). Physiological effects of extracellular nucleotides in the inner ear. *Clin Exp Pharmacol Physiol* 27, 575-580.
- Hughes, I., Binkley, J., Hurle, B., Green, E.D., NISC Comparative Sequencing Program, Sidow, A., and Ornitz, D.M. (2008). Identification of the Otopetrin Domain, a conserved domain in vertebrate otopetrins and invertebrate otopetrin-like family members. *BMC Evolutionary Biology* 8:41.
- Hughes, I., Blasiole, B., Huss, D., Warchol, M.E., Rath, N.P., Hurle, B., Ignatova, E., Dickman, J.D., Thalmann, R., Levenson, R., *et al.* (2004). Otopetrin 1 is required for otolith formation in the zebrafish *Danio rerio*. *Dev Biol* 276, 391-402.
- Hughes, I., Saito, M., Schlesinger, P.H., and Ornitz, D.M. (2007). Otopetrin1 activation by purinergic nucleotides regulates intracellular calcium. *Proc Natl Acad Sci U S A* 104, 12023-12028.
- Hughes, I., Thalmann, I., Thalmann, R., and Ornitz, D.M. (2006). Mixing model systems: Using zebrafish and mouse inner ear mutants and other organ systems to unravel the mystery of otoconial development. *Brain Res* 1091, 58-74.
- Hurle, B., Ignatova, E., Massironi, S.M., Mashimo, T., Rios, X., Thalmann, I., Thalmann, R., and Ornitz, D.M. (2003). Non-syndromic vestibular disorder with otoconial agenesis in tilted/mergulhador mice caused by mutations in otopetrin 1. *Hum Mol Genet* 12, 777-789.
- James, J., Schellens, J.P., and Veenhof, V.B. (1969). Electron microscopy of formation of statoconia. *Experientia* 25, 1173-1174.
- Jang, Y.S., Hwang, C.H., Shin, J.Y., Bae, W.Y., and Kim, L.S. (2006). Age-related changes on the morphology of the otoconia. *Laryngoscope* 116, 996-1001.
- Kozel, P.J., Friedman, R.A., Erway, L.C., Yamoah, E.N., Liu, L.H., Riddle, T., Duffy, J.J., Doetschman, T., Miller, M.L., Cardell, E.L., *et al.* (1998). Balance and hearing deficits in mice with a null mutation in the gene encoding plasma membrane Ca²⁺-ATPase isoform 2. *J Biol Chem* 273, 18693-18696.

- Kruger, R.P., Goodyear, R.J., Legan, P.K., Warchol, M.E., Raphael, Y., Cotanche, D.A., and Richardson, G.P. (1999). The supporting-cell antigen: a receptor-like protein tyrosine phosphatase expressed in the sensory epithelia of the avian inner ear. *J Neurosci* *19*, 4815-4827.
- Lee, J.H., and Marcus, D.C. (2008). Purinergic signaling in the inner ear. *Hear Res* *235*, 1-7.
- Lim, D.J. (1973). Formation and fate of the otoconia. Scanning and transmission electron microscopy. *Ann Otol Rhinol Laryngol* *82*, 23-35.
- Lindeman, H.H. (1973). Anatomy of the otolith organs. *Adv Otorhinolaryngol* *20*, 405-433.
- Lins, U., Farina, M., Kurc, M., Riordan, G., Thalmann, R., Thalmann, I., and Kachar, B. (2000). The otoconia of the guinea pig utricle: internal structure, surface exposure, and interactions with the filament matrix. *J Struct Biol* *131*, 67-78.
- Liu, P., Jenkins, N.A., and Copeland, N.G. (2003). A highly efficient recombineering-based method for generating conditional knockout mutations. *Genome Res* *13*, 476-484.
- Lundberg, Y.W., Zhao, X., and Yamoah, E.N. (2006). Assembly of the otoconia complex to the macular sensory epithelium of the vestibule. *Brain Res* *1091*, 47-57.
- Mann, S., Parker, S.B., Ross, M.D., Skarnulis, A.J., and Williams, R.J. (1983). The ultrastructure of the calcium carbonate balance organs of the inner ear: an ultra-high resolution electron microscopy study. *Proc R Soc Lond B Biol Sci* *218*, 415-424.
- Marom, T., Oron, Y., Watad, W., Levy, D., and Roth, Y. (2009). Revisiting benign paroxysmal positional vertigo pathophysiology. *Am J Otolaryngol* *30*, 250-255.
- North, R.A. (2002). Molecular physiology of P2X receptors. *Physiol Rev* *82*, 1013-1067.
- Oghalai, J.S., Manolidis, S., Barth, J.L., Stewart, M.G., and Jenkins, H.A. (2000). Unrecognized benign paroxysmal positional vertigo in elderly patients. *Otolaryngol Head Neck Surg* *122*, 630-634.
- Ornitz, D.M., Bohne, B.A., Thalmann, I., Harding, G.W., and Thalmann, R. (1998). Otoconial agenesis in *tilted* mutant mice. *Hearing Res* *122*, 60-70.
- Orriss, I.R., Utting, J.C., Brandao-Burch, A., Colston, K., Grubb, B.R., Burnstock, G., and Arnett, T.R. (2007). Extracellular nucleotides block bone mineralization in vitro: evidence for dual inhibitory mechanisms involving both P2Y2 receptors and pyrophosphate. *Endocrinology* *148*, 4208-4216.

- Piazza, V., Ciubotaru, C.D., Gale, J.E., and Mammano, F. (2007). Purinergic signalling and intercellular Ca²⁺ wave propagation in the organ of Corti. *Cell Calcium* *41*, 77-86.
- Preston, R.E., Johnsson, L.G., Hill, J.H., and Schacht, J. (1975). Incorporation of radioactive calcium into otolithic membranes and middle ear ossicles of the gerbil. *Acta Otolaryngol* *80*, 269-275.
- Ralevic, V., and Burnstock, G. (1998). Receptors for purines and pyrimidines. *Pharmacol Rev* *50*, 413-492.
- Ross, M.D., Peacor, D., Johnsson, L.G., and Allard, L.F. (1976). Observations on normal and degenerating human otoconia. *Ann Otol Rhinol Laryngol* *85*, 310-326.
- Ross, M.D., Pote, K.G., and Perini, F. (1985). Analytical studies of the organic material of otoconial complexes, including its amino acid and carbohydrate composition. In *Auditory Biochemistry*, i.D.G.D.e.a. (eds.), ed. (Springfield, IL, in D.G. Drescher et al. (eds.)), pp. 500-514.
- Sage, C.L., and Marcus, D.C. (2002). Immunolocalization of P2Y₄ and P2Y₂ purinergic receptors in strial marginal cells and vestibular dark cells. *J Membr Biol* *185*, 103-115.
- Salt, A.N., Inamura, N., Thalmann, R., and Vora, A. (1989). Calcium gradients in inner ear endolymph. *Am J Otolaryngol* *10*, 371-375.
- Sollner, C., Schwarz, H., Geisler, R., and Nicolson, T. (2004). Mutated otopetrin 1 affects the genesis of otoliths and the localization of Starmaker in zebrafish. *Dev Genes Evol* *214*, 582-590.
- Suzuki, H., Ikeda, K., Furukawa, M., and Takasaka, T. (1997a). P₂ purinoceptor of the globular substance in the otoconial membrane of the guinea pig inner ear. *Am J Physiol* *273*, C1533-1540.
- Suzuki, H., Ikeda, K., and Takasaka, T. (1995). Biological characteristics of the globular substance in the otoconial membrane of the guinea pig. *Hear Res* *90*, 212-218.
- Suzuki, H., Ikeda, K., and Takasaka, T. (1997b). Age-related changes of the globular substance in the otoconial membrane of mice. *Laryngoscope* *107*, 378-381.
- Tateda, M., Suzuki, H., Ikeda, K., and Takasaka, T. (1998). pH regulation of the globular substance in the otoconial membrane of the guinea-pig inner ear. *Hear Res* *124*, 91-98.
- Thalmann, I., Hughes, I., Tong, B.D., Ornitz, D.M., and Thalmann, R. (2006). Microscale analysis of proteins in inner ear tissues and fluids with emphasis on endolymphatic sac, otoconia, and organ of Corti. *Electrophoresis* *27*, 1598-1608.

- Tsien, R.Y., Rink, T.J., and Poenie, M. (1985). Measurement of cytosolic free Ca²⁺ in individual small cells using fluorescence microscopy with dual excitation wavelengths. *Cell Calcium* 6, 145-157.
- Vlajkovic, S.M., Abi, S., Wang, C.J., Housley, G.D., and Thorne, P.R. (2007). Differential distribution of adenosine receptors in rat cochlea. *Cell Tissue Res* 328, 461-471.
- Walther, L.E., and Westhofen, M. (2007). Presbyvertigo-aging of otoconia and vestibular sensory cells. *J Vestib Res* 17, 89-92.
- Welling, D.B., Parnes, L.S., O'Brien, B., Bakaletz, L.O., Brackmann, D.E., and Hinojosa, R. (1997). Particulate matter in the posterior semicircular canal. *Laryngoscope* 107, 90-94.
- Wood, J.D., Muchinsky, S.J., Filoteo, A.G., Penniston, J.T., and Tempel, B.L. (2004). Low endolymph calcium concentrations in deafwaddler2J mice suggest that PMCA2 contributes to endolymph calcium maintenance. *J Assoc Res Otolaryngol* 5, 99-110.
- Yoshihara, T., Igarashi, M., Usami, S., and Kanda, T. (1987). Cytochemical studies of Ca⁺⁺-ATPase activity in the vestibular epithelia of the guinea pig. *Arch Otorhinolaryngol* 243, 417-423.
- Zhao, X., Yang, H., Yamoah, E.N., and Lundberg, Y.W. (2007). Gene targeting reveals the role of Oc90 as the essential organizer of the otoconial organic matrix. *Dev Biol* 304, 508-524.

Figure 1. Targeting the *Otopetrin 1 (Otop1)* gene. (A) *Otop1* spans over 28 kb of genomic DNA on mouse chromosome 5 and contains seven exons. (B) *Otop1a* coding sequence starts within exon 2 and is the major splice form of *Otop1*. *Otop1b* and *1c* are transcribed from exon 1 and splice to different sites in exon 2. In the targeting vector, the β -galactosidase (β gal) gene and LoxP-neo cassette was inserted in frame to exon 2 after the *Otop1c* splice site. (C) The targeted allele, *Otop1* ^{β gal}, created a fusion protein with the first two transmembrane (TM) domains of OTOPI1 at the N-terminus of β Gal. The epitope to which OTOPI1 antibody was made is located within the N-terminal tail (red line, arrow). (D) Southern blot digested with EcoRV. The wild type allele produces a 17 kb fragment with both 5' and 3' probes. Targeted allele produces a 5' 8 kb and 3' 9 kb restriction fragment. (E) PCR genotyping with primers shown in panel C. Wild type allele, 545 bp; Targeted allele, 369 bp. (F-H) Histological sections through the utricle and saccule. (F,G) Otoconia are normally formed above the sensory epithelia (SE) of *Otop1*^{+/+} and *Otop1* ^{β gal/+} utricle (upper) and saccule (lower). (H) no otoconia are observed in *Otop1* ^{β gal/ β gal} otolithic organs. Scale bar, 100 μ m.

Figure 1

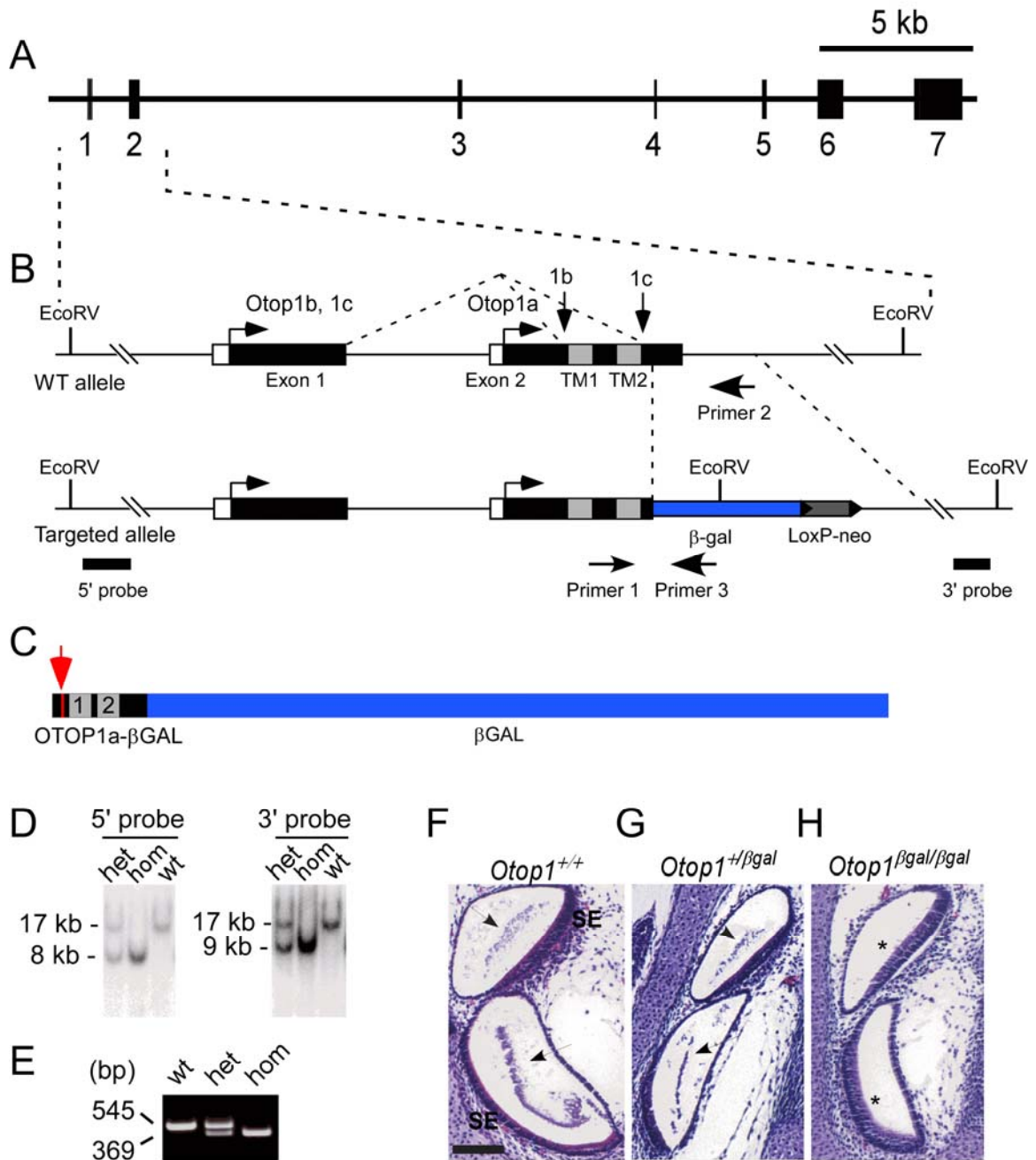


Figure 2. Spatial and temporal expression of OTOP1^{βGAL}. (A) At E13.5 X-gal staining is observed in the utricle of *Otop1^{βgal/+}* inner ears. (B) At E16.5 both the utricle and saccule are positive for βGAL activity. No staining was observed in the cochlea or semicircular canals. (C-E) X-gal stained whole mounts of P0 maculae of the utricle and saccule. OTOP1^{βGAL} expression is absent from the striola region (S) in the utricle (C) and saccule (E). (D) High magnification of the boxed region in (C) showing OTOP1^{βGAL} expression in some transitional cells (region below the white dotted line). (F-H) Histological sections through the maculae of the utricle. (F) At P0, OTOP1^{βGAL} is expressed in supporting cells (black arrowheads) and transitional cells (white arrowheads). Similar expression patterns are maintained in P7 (G) and adult (H) mice. (I) Quantitative RT-PCR showing endogenous *Otop1* expression in P2 utricle/saccule and adult inner ear. Error bars are standard deviations of three replicates. Scale bars in C, E, 100 μm; D, F, G, H, 20 μm.

Figure 2

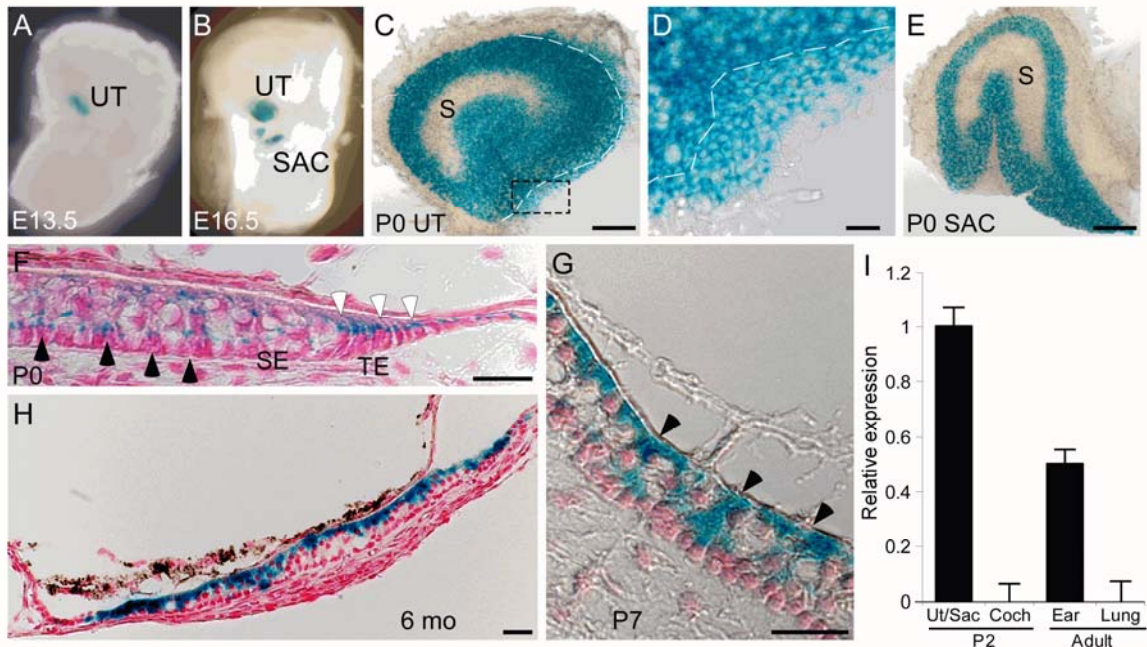


Figure 3. OTOP1 is localized at the apex of supporting cells. (A-F) Frozen sections stained with antibodies against the OTOP1 5' epitope (red) and β GAL (green). (A-C) *Otop1*^{+/+} utricle showing endogenous OTOP1 localization near the apical sensory epithelium. (D) *Otop1* ^{β gal/ β gal} utricle showing OTOP1 ^{β GAL} expression in an intracellular vesicular pattern. (E) The staining pattern with an anti- β GAL antibody matches that of the anti-OTOP1 antibody, confirming the specificity of the OTOP1 antibody. (G) Confocal image of a wholemount wild type utricle, stacked in the XY plane, showing OTOP1 (green) localization just beneath the stereocilia (phalloidin staining, red). (H) Frozen section of an *Otop1*^{+/+} utricle showing apical staining above supporting cells (SC) and no apical staining above hair cells (HC) (red bars). (I, J) Z-stacked image of a wholemount utricle showing absence of staining in regions beneath the stereocilia (star). (K, L) OTOP1 ^{β GAL} protein does not colocalize with the hair cell-specific marker α -parvalbumin. Scale bars, 20 μ m.

Figure 3

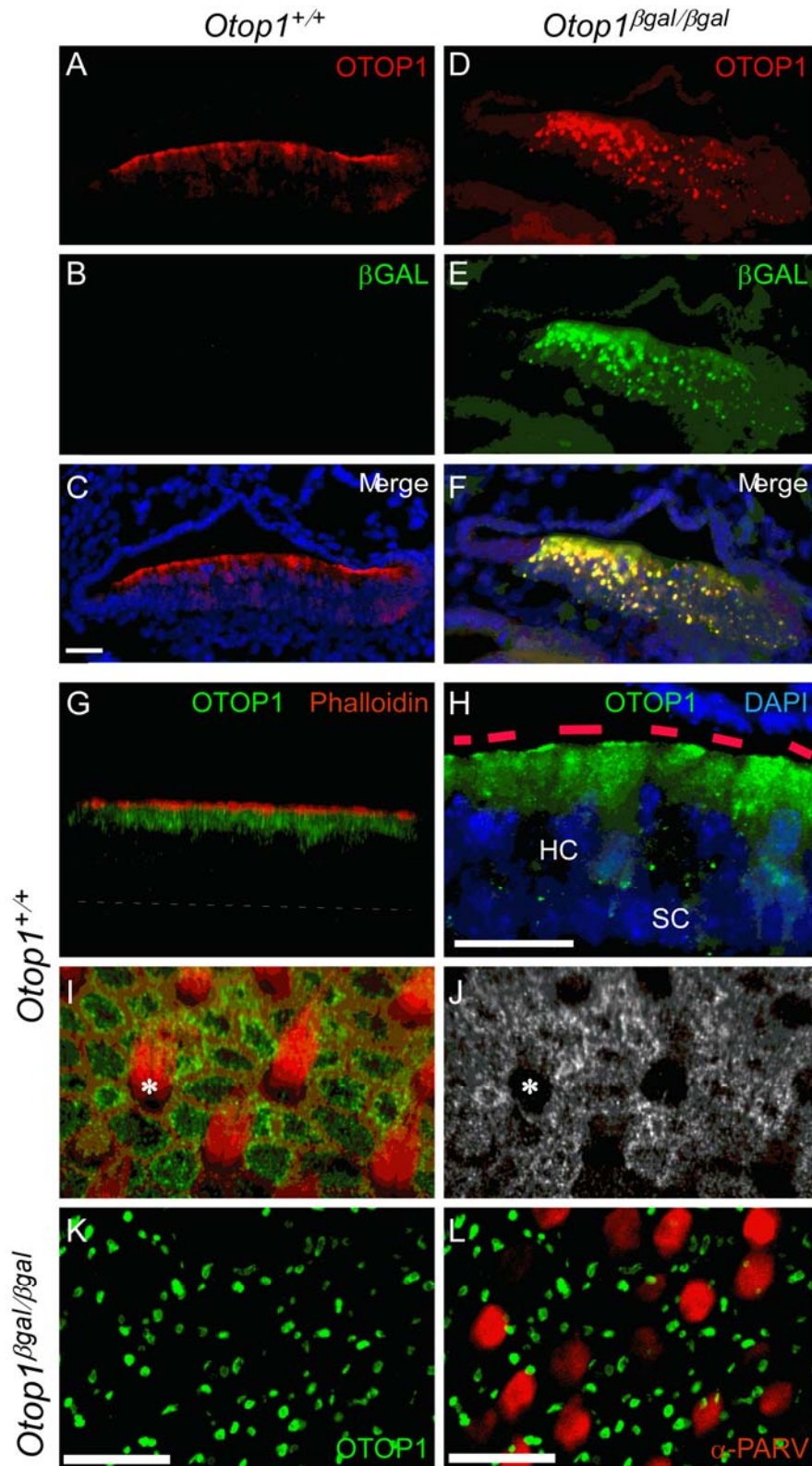


Figure 4. Otop1 regulation of the purinergic response in primary chick utricular macular cultures. (A) Bright field image of a chick utricular macular culture after 7 days in culture. (B) Expression of *Otop1* was assayed in 1 and 7 DIV chick utricular macular cultures (n=2 cultures). After 7 DIV, *Otop1* expression is no longer detectable (p<0.005). (C,D) Transfection of 7 DIV cells to express EGFP and Flag-OTOP1. (C) Wild type (WT) (n=16) and EGFP transfected cells (n=11) show similar responses to 200 μ M ATP, characterized by a sharp increase in $[Ca^{2+}]_i$ and rapid return to prestimulation baseline before removal of ATP (wash). (D) Compared to untransfected control (n=11), transfected cells expressing EGFP and Flag-OTOP1 (n=5) respond to ATP with an increase in $[Ca^{2+}]_i$ to an elevated plateau that persists until removal of the agonist (wash). The data shown here is representative of at least three independent experiments.

Figure 4

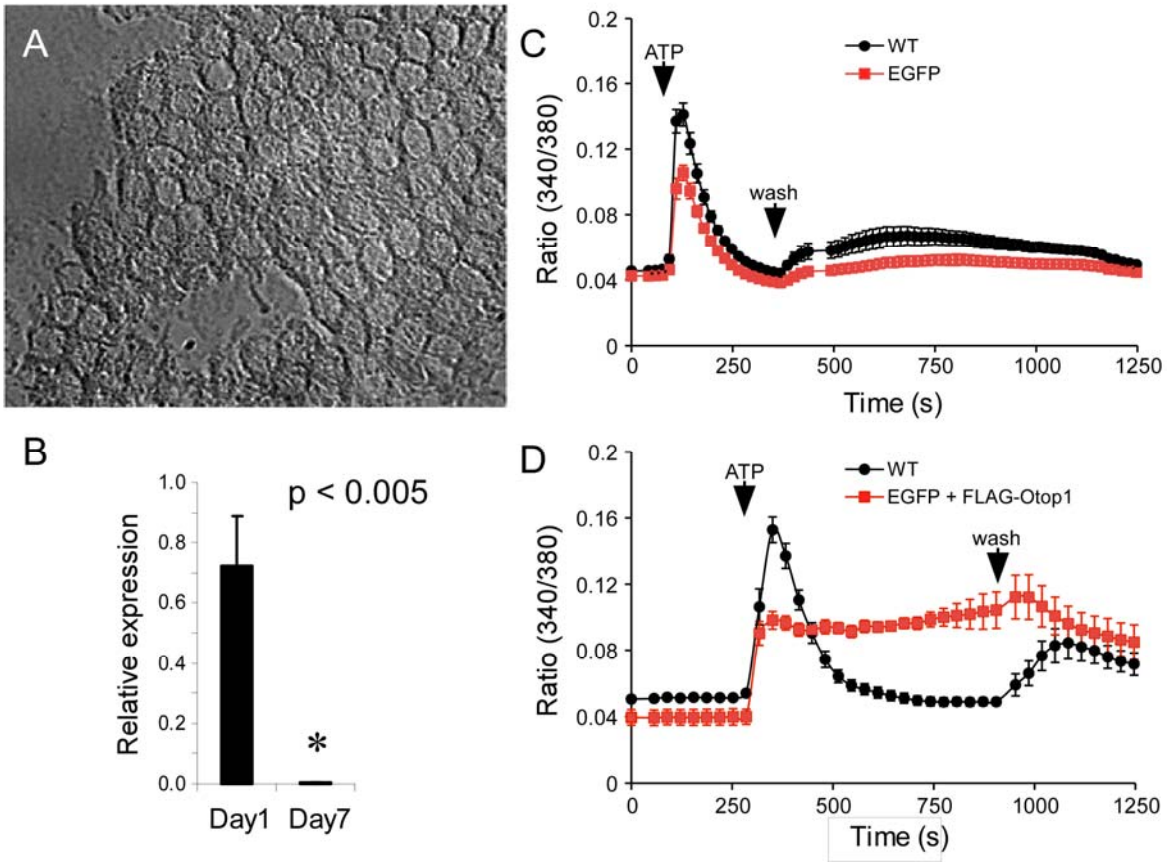


Figure 5. Purinergic response of organotypic macular cultures from the utricle of P0-P3 mice. (A) Bright field image of a utricular macula in culture for 24 hr. Scale bar, 200 μ m. (B) Ratio (340/380) image of a culture loaded with fura-2 before stimulation with ATP. Circles show areas selected for analysis. (C) Addition of 100 μ M ATP results in an increase in $[Ca^{2+}]_i$ as indicated by change in color (red: high, purple: low). (D) *Otop1*^{+/+} (n=2) responded to ATP with an increase in $[Ca^{2+}]_i$ to an elevated plateau, whereas *Otop1* ^{β gal/ β gal} (n=4) maculae showed a biphasic response to 100 μ M ATP characterized by a sharp peak in $[Ca^{2+}]_i$ and a rapid reduction in $[Ca^{2+}]_i$ to an elevated plateau. $[Ca^{2+}]_i$ returned to baseline after removal of agonist (wash). The data shown here is representative of four independent experiments.

Figure 5

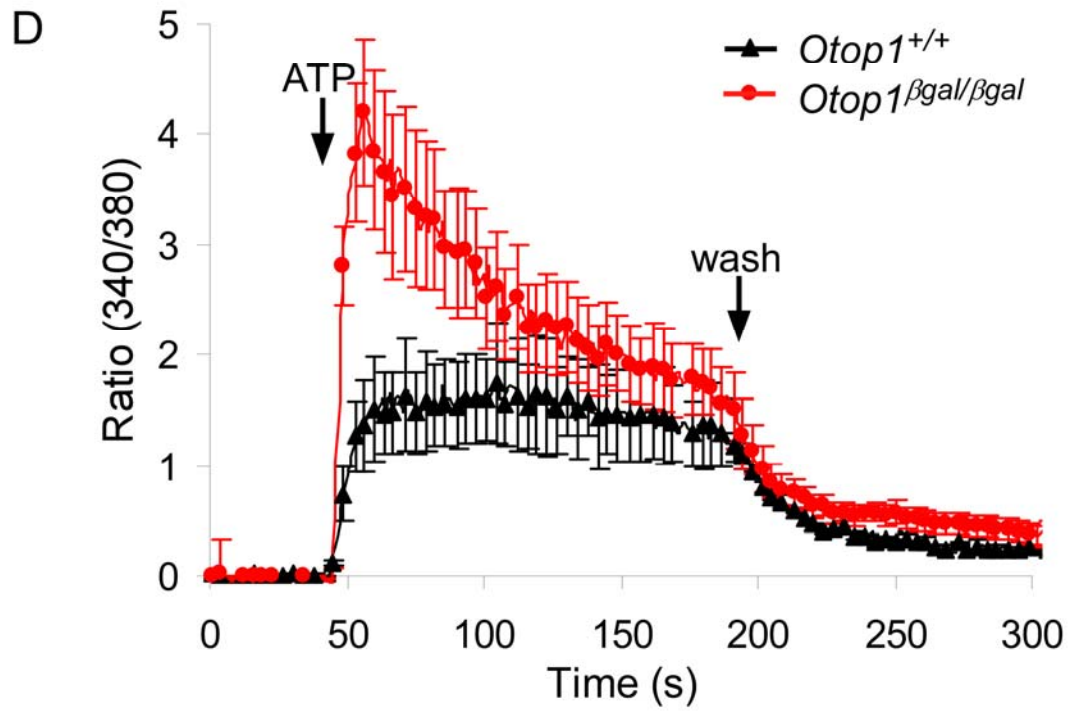
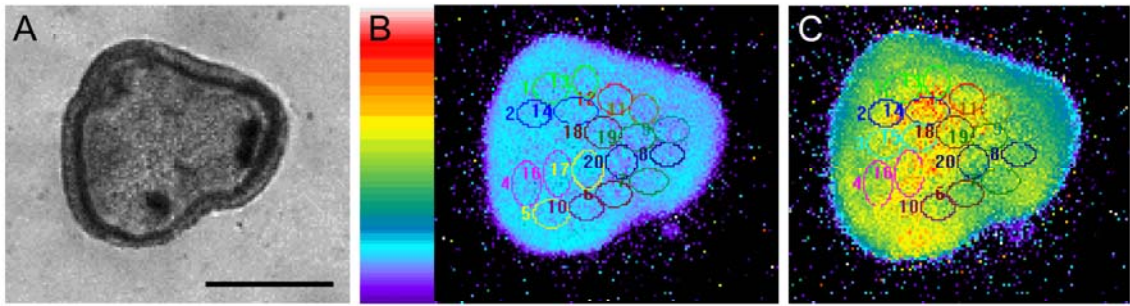


Figure 6. Purinergic response of dissociated macular cultures from the utricles of P0-P3 mice. (A) Bright field view of a dissociated utricular epithelial cells after 24 hr in culture. Note regions of flattened epithelial-like cells (*) and clumps of cells associated with globule-like structures (arrow). Scale bar, 50 μm . (B) Ratio (340/380) image of a culture loaded with fura-2. Circles show areas selected for analysis. (C) Addition of 100 μM ATP results in an increase in $[\text{Ca}^{2+}]_i$ as indicated by change in color (red: high, purple: low). (D) *Otop1* expressing cells, identified in heterozygous and homozygous cultures (marked by X-gal staining), are predominantly associated with globule-like structures (arrow). These cultures also contain *Otop1* negative regions (*). (E) *Otop1*^{+/+} (n=57) and *Otop1* ^{$\beta\text{gal}/+$} (n=31) cultures respond to 100 μM ATP by increasing $[\text{Ca}^{2+}]_i$ to an elevated plateau. *Otop1* ^{$\beta\text{gal}/\beta\text{gal}$} (n=36) cultures respond to 100 μM ATP by increasing $[\text{Ca}^{2+}]_i$ to an elevated peak followed by a faster rate of decay compared to the *Otop1*^{+/+} cells. (F) Dissociated cultures stimulated with P2Y receptor-specific agonist UTP showing an increased rate of decay (UTP should not activate P2X receptors) in all genotypes. Note that *Otop1*^{+/+} (n=18) and *Otop1* ^{$\beta\text{gal}/+$} (n=43) cultured cells still show a decreased peak compared to the *Otop1* ^{$\beta\text{gal}/\beta\text{gal}$} (n=26) cultures. (G) Cultured macular epithelial cells which do not normally express OTOPI (negative for βGal activity and not associated with globule-like structures) (*Otop1*^{+/+} (n=15), *Otop1* ^{$\beta\text{gal}/\beta\text{gal}$} (n=12)) show a biphasic response to 100 μM ATP with a sharp peak with a fast decay to an elevated plateau which persists until wash. (H) Cultures were treated with 40 μM bis-phenol (arrowhead) to release Ca^{2+} from intracellular stores. After incubation with bis-phenol, *Otop1*^{+/+} (n=13) and *Otop1* ^{$\beta\text{gal}/\beta\text{gal}$} (n=20) cultures no longer showed differences in peak and rate of decay in response to 100 μM ATP. (I) In nominally Ca^{2+} free media, *Otop1*^{+/+}

(n=49) and *Otop1* ^{β gal/ β gal} (n=50) cultures show a similar response to 100 μ M ATP with a distinct peak and increased rate of decay compared to normal media (E). Note that the difference in initial peak value observed in normal media (E) is lost in the absence of extracellular Ca²⁺. (J) Comparison of rates of decay of *Otop1*^{+/+} and *Otop1* ^{β gal/ β gal} cultures in different experimental conditions. *, p < 0.05; **, p < 0.02. The data in E-J are the combined results of at least three independent experiments.

Figure 6

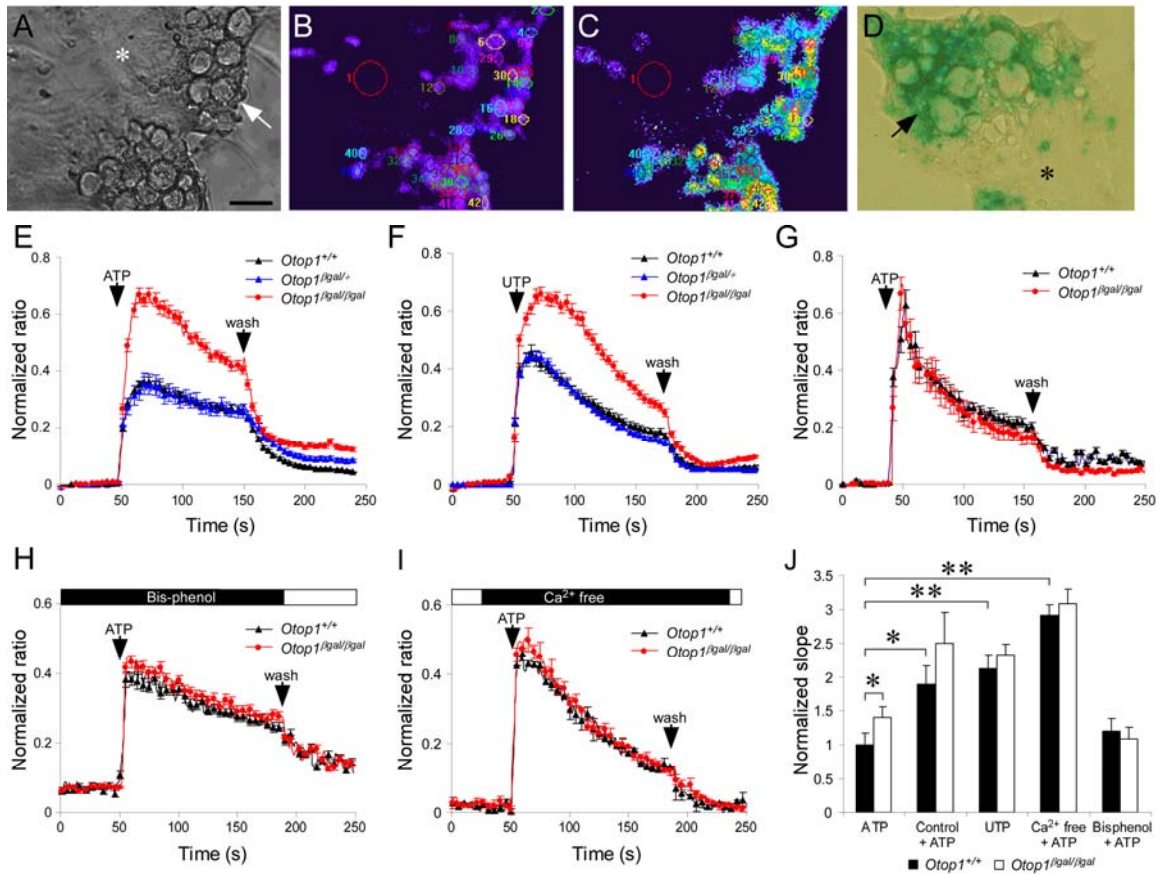
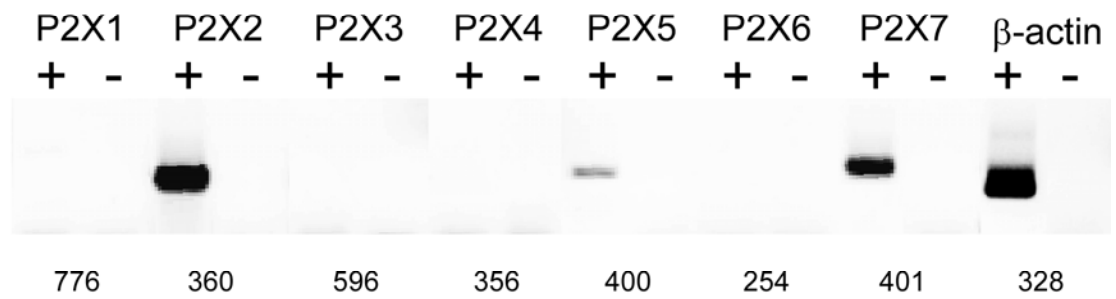


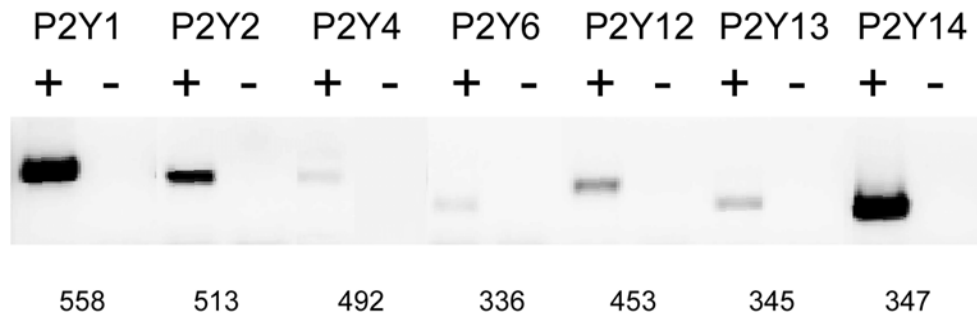
Figure 7. Semi-quantitative RT-PCR analysis of P2X and P2Y receptors in *Otop1*^{+/+} mouse dissociated culture cells. Expected size of each PCR product is shown below the bands. β -actin was used as an endogenous control. P2X2, P2X5, P2X7, P2Y1, P2Y2, P2Y4, P2Y6, P2Y12, P2Y13, P2Y14 are expressed. +, with reverse transcriptase (RT); -, without RT.

Figure 7

A



B



Chapter II

***Tlt* and *mlh* differentially disrupt OTOP1 function**

Introduction

Otopetrin 1 (Otop1) is a member of a new gene family and previous studies have shown that OTOP1 is required for formation of normal otoconia, the calcium carbonate crystals present in the utricle and saccule (Hurle et al., 2003). The observation that *Otop1* is found in all vertebrates and is phylogenically conserved suggests that OTOP1 has a conserved role in biomineralization in vertebrates (Hughes et al., 2008). Ideal for its putative function, *Otop1* mRNA is expressed in the mouse sensory epithelium (macula) of the utricle and saccule (Hurle et al., 2003). Since OTOP1 is predicted to encode a 12-transmembrane (TM) protein (Hughes et al., 2008), OTOP1, synthesized in the macula, may be trafficked to the apex of the epithelium and ultimately interact with proteins in the endolymph (the extracellular fluid filling the inner ear labyrinth) to induce or allow formation of the crystals.

Each otoconium is composed of a proteinaceous core surrounded by calcium carbonate crystals. Proteins forming the proteinaceous core (Thalmann et al., 2006) and the enzyme catalyzing formation of carbonate ions are known (Hughes et al., 2006; Lim et al., 1983; Shiao et al., 2005), but little information is available on the genes important for modulating calcium ions during otoconia formation.

Notably, Suzuki et al (Suzuki et al., 1997) observed that when isolated guinea pig globular substance vesicles (putative precursor of otoconia) were stimulated with ATP (abundant in endolymph), there was a 5-6 fold increase in intravesicular Ca^{2+} , suggesting a possible mechanism by which an increase in $[\text{Ca}^{2+}]$ could occur and possibly be maintained during the mineralization process. This result also indicated that a protein or a

protein complex, with the ability to modulate Ca^{2+} , may be localized within the globular substance vesicles, and OTOPI could potentially be a candidate.

Indeed, when OTOPI was transfected to heterologous systems and tested for response to ATP, a similar rise in $[\text{Ca}^{2+}]_i$ was observed as in the study with globular substance vesicles (Hughes et al., 2007). Further studies revealed that OTOPI can specifically modulate purinergic signaling *in vitro*.

Quintessential to fully understanding how OTOPI functions in the biosynthesis of otoconia is to understand the mechanism(s) by which OTOPI function is altered or disrupted by mutations that result in non-syndromic failure to form otoconia. Mutant alleles of *Otop1* (Hurle et al., 2003), *tilted* (*tlt*) and *mergulhador* (*mlh*) cause a balance problem in mice with 100% penetrance due to otoconia agenesis with no other abnormalities in the inner ear. Both mutants carry single missense mutations leading to non-conservative amino acid substitutions that affect two putative TM (*tlt*, Ala₁₅₁->Glu in TM3; *mlh*, Leu₄₀₈->Gln in TM9) domains. The TM domains bearing the *tlt* and *mlh* mutations are part of the highly conserved domains (Otopetrin Domain-I, II and III (OD-I, II, and III)) found in all the homologues of *Otop1* (Hughes et al., 2008), which could be functional domains. Investigating how these mutations affect normal expression and biochemical functions (especially modulation of purinergic signaling (Hughes et al., 2007)) may also reveal the function(s) of the highly conserved domains of OTOPI. The *tlt* and *mlh* mutations are predicted to alter the hydrophobicity of the putative transmembrane domains, suggesting that the mutations may alter protein topology, membrane trafficking, or biochemical activity.

Materials and Methods

Construction of Otop1^{tlt} and Otop1^{mlh} expression vector

The full length cDNA clone of *Otopetrin 1* (A530025J20) was obtained from Riken Laboratories (Japan). To make an N-terminal EGFP fusion constructs of *Otop1* with pCS2EGFP vector, EcoRI and XbaI enzyme linker sites were added by PCR. Due to the G-C rich region in the N-terminal loop, a short linker region consisting of the amino acids DWK (found in the 3'UTR just upstream of the Otop1 transcription start site) was added. The following primers were used to clone EGFP*Otop1*; primer 1 (5'-TTTGAATTCAGACTGGAAGATGCCTGG -3' (forward)), primer 2 (5'-CCCTCTAGACTAGATCTTACAATAGACCTCAAAGAGG -3' (reverse)). 25 cycles of denaturation at 92°C for 30 sec, annealing at 62°C for 30 sec, and extension at 68°C for 30 sec were used to amplify 1800 bp fragments. pCS2EGFP empty vector was used as a cytosolic EGFP control in all of the following experiments. To construct *Otop1^{tlt}* and *Otop1^{mlh}* expression vectors, PCR-based site-directed mutagenesis was performed to induce these mutations in EGFP*Otop1* constructs. Primers used to induce *tlt* and *mlh* mutations were as follows; *tlt*, primer 1 (5'-ATGAAGTATTCGACTTTCAAGCATCCCAGGACG -3' (reverse)), primer 2 (5'-AAAGTCGAATACTTCATTGGATTCTCGGAGTGC -3' (forward)), *mlh*, primer 1 (5'-ATGGCCTGAATGGAGCCCCAGGAGAGG -3' (reverse)), primer 2 (5'-TCCATTCAGGCCATCGCCTGTGCTGAG -3' (forward)). 25 cycles of denaturation at 94°C for 1 min, annealing at 63°C for 1 min, and extension at 72°C for 2 min were used to amplify each mutant forms.

Cell culture and transfection

COS7 cells were maintained in Dulbecco's Modified Eagle Media (Gibco) supplemented with 10% fetal calf serum (Gibco), 2mM L-glutamine, and 1X penicillin/streptomycin. Cells were plated on 35 mm plates with glass coverslips (MatTek Cultureware) 24-48 hours before transfection. Cells were transfected using Lipofectamine 2000 (Invitrogen) and approximately 1 µg plasmid DNA in OptiMEM (Invitrogen) for 4-5 hours following manufacturer's instructions. Cultures were allowed to recover overnight in growth media.

Preparation of mouse utricular macular dissociated culture

P0-P3 utricles were dissected in medium 199 (Gibco #12350039), and the nonsensory epithelium and otoconial layer were completely removed. After incubation in thermolysin (Sigma) at 37°C for 50 min, the underlying stroma was removed and the remaining epithelial sheet was attached to a MatTek dish using ECM gel (Sigma). The tissue was incubated in growth media overnight at 37°C. For dissociated culture, isolated epithelial sheets were treated with Trypsin/EDTA (0.05%, 0.02%) for 15 min at 37 °C. After replacing Trypsin/EDTA with Medium 199 (Gibco #12340030) cells were triturated 5 to 10 times and plated on laminin coated MatTek dishes and incubated overnight at 37°C. The next day Medium 199 (Gibco #12340030) containing 10% fetal bovine serum (Gibco) was added.

Ratiometric calcium imaging and data analysis

All imaging experiments were carried out at room temperature in a HEPES-buffered salt solution (HCSS) containing, in mM: 140 NaCl, 5.4 KCl, 1 NaH₂PO₄, 1.8 CaCl₂, 1 MgSO₄, 12 HEPES, and 5.5 D-glucose, pH 7.4±0.1. COS7 cells or dissociated utricular macular cultures were loaded with fura-2 by incubation for 60 min with 5-10 μM acetoxymethyl (AM) ester (Invitrogen, Eugene, OR) and 0.1% Pluronic F-127 (Invitrogen, Eugene, OR) in HCSS (pH=7.2) at room temperature, washed with HCSS and incubated for another 60 min to allow for ester hydrolysis. After loading, cells were imaged on an inverted microscope (Nikon Eclipse TE300, Nikon Inc., Melville, NY) equipped with a cooled CCD camera (Cooke Corp., Auburn Hill, MI) using a 20x/0.45 Plan Fluor objective (Nikon). The fluorescence excitation (75 W xenon arc lamp) was provided by band-specific filters (340 and 380 nm; Semrock, Rochester, NY) in combination with a XF73 dichroic beam splitter (Omega Optical, Brattleboro, VA). Pairs of images were collected constantly at alternate excitation wavelengths. After subtracting the matching background, the image intensities were divided by one another to yield ratio values for individual cells. Ionomycin was from Calbiochem (San Diego, CA), ATP was from Sigma (St. Louis, MO).

For COS7 cells, fluorescent intensities of GFP (485 nm) and fura-2 (340 and 380 nm) channels were recorded. Analysis of fura-2 signal intensities in unloaded GFP-expressing cells showed that approximately 4% and 23% of the GFP signal bleeds through 340 and 380 fura-2 channels, respectively. Therefore, the signal intensity contributed by the presence of GFP was subtracted from each value before analysis of each experiment. Each point was then normalized to the average of the baseline points

(before adding an agonist). For studies done with mouse macular dissociated cultures, 10 μ M ionomycin was added at the end of each experiment to obtain the maximum level of $[Ca^{2+}]_i$ in each region of interest. To make data points comparable between experiments performed on different days, raw data (ratio of 340/380 fluorescent intensity) was normalized as follows: Normalized Ratio = $(R - R_0)/(R_{max} - R_0)$, where R is the individual ratio value, R_{max} is the peak ratio after addition of ionomycin, R_0 is the average of the prestimulation baseline ratio.

Production of anti-Otop1 antibody

A rabbit polyclonal antibody was made using a 16-amino acid peptide epitope (ARGSPQASGPRRGASV) derived from the N-terminus of OTOPI1 (Fig 1C). The synthetic peptide was conjugated to maleimide-activated keyhole limpet hemocyanin prior to injection into the rabbit. The resulting antibody was purified on the peptide affinity column, and validated by Western blotting of extracts from inner ear tissues. Further validation was performed in this study by comparing the immunostaining patterns with those of X-gal staining.

Wholemout immunohistochemistry

Temporal bones were isolated in Leibovitz's medium L15 (Sigma) and fixed in 4% paraformaldehyde for 1-2hr at RT. Utricular and saccular maculae were dissected from the temporal bones in cold PBS, incubated in 0.5% Triton X-100 for 30 min at room temperature, and then washed with PBS. Samples were blocked using 4% BSA/PBS overnight at 4°C, and incubated with rabbit α -Otop1 (1:800) and/or mouse α -parvalbumin

(Sigma- 1:500) for 90 min at room temperature in a humidified chamber. After washing with PBS, samples were incubated with secondary antibodies, Alexa 488 anti-rabbit IgG (Invitrogen- 1:600) and Alexa 555 anti-mouse IgG (Invitrogen- 1:600), respectively for 45 min at room temperature. For stereocilia staining, samples were further incubated with rhodamine-phalloidin (Invitrogen- 1:200) for 15 min at room temperature. After washing with PBS, samples were transferred to a superfrost slide, mounted with vectashield (Vector labs), and coverslipped before imaging with an Olympus FV500a multi-channel confocal microscope.

Results

EGFP^{Otop1^{tlt}} and EGFP^{Otop1^{mlh}}-expressing COS7 cells show a reduced purinergic response to ATP.

The phenotypes of the *tlt* and *mlh* mice are the result of single base pair mutations in the *Otop1* coding region leading to non-conservative amino acid changes in TM5 and TM9, respectively (Figure 3A). Both mutations are predicted to alter the hydrophobicity of their putative transmembrane domains, suggesting that they may alter the subcellular localization of the mutant protein and/or may affect its activity. To assess this possibility, COS7 cells were transfected with EGFP^{Otop1^{tlt}} and EGFP^{Otop1^{mlh}}, and their localization and response to exogenous ATP was observed. The tagged EGFP protein allowed us to effectively mark subcellular localization of the mutant protein in COS7 cells. Surprisingly, presence of either mutation did not alter the localization of the EGFP signal. Wildtype OTOPI and the mutant proteins were found extensively in the endoplasmic reticulum (ER) and a dimmer signal was also positive in the plasma

membrane (PM) (Figure 1B, C, D). This is consistent with the fact that OTOPI does not have any known signal peptide (Hurle et al., 2003) with which OTOPI may have been trafficked to other subcellular compartments. Whether Otop1 functions in the ER needs to be studied in further detail, but nonspecific localization of overexpressed transmembrane domain proteins in the ER have been previously observed (Brostrom and Brostrom, 2003; Dellis et al., 2006).

To test whether OTOPI^{TLT} and OTOPI^{MLH} could respond to purinergic stimuli in a similar manner to the wildtype OTOPI, time lapse fluorescence microscopy was used to monitor change in cytosolic $[Ca^{2+}]_i$ in COS7 cells transfected with EGFP^{Otop1^{tlt}} and EGFP^{Otop1^{mlh}} after loading with fura-2 acetoxymethyl ester. Untransfected COS7 cells (WT) and those transfected with cytosolic EGFP responded to ATP (Figure 2 and data not shown) with a rapid peak in $[Ca^{2+}]_i$, which is due to Gαq-coupled P2Y receptor signaling (Hughes et al., 2007). Cells expressing EGFP^{Otop1} showed a dramatic absence of this peak in response to ATP. The plateau phase following the initial peak shown in the WT cells is mainly mediated by influx of extracellular calcium (Hughes et al., 2007). In EGFP^{Otop1}-positive cells, the level of the plateau phase was also reduced compared to the WT (Figure 2A). In response to ATP, EGFP^{Otop1^{tlt}} and EGFP^{Otop1^{mlh}}-positive cells showed a reduced increase in $[Ca^{2+}]_i$ compared to the WT (Figure 2B, C). However, the way the response changed due to expression of the mutant proteins was subtly different from the effect seen by expressing EGFP^{Otop1}. The initial peak was more apparent (dotted circle) and the level of extracellular Ca^{2+} influx, depicted in the following plateau phase, was slightly higher in mutant expressing cells. These data

suggested that the presence of *tlt* and *mlh* mutations most likely reduces OTOPI1 less inhibition of P2Y receptor function.

Tlt and mlh mutations affect trafficking of endogenous OTOPI1.

It was still possible that the overexpression system may have forced the wildtype and mutant proteins to be localized differently from the endogenous OTOPI1. Therefore, OTOPI1 localization was further investigated in P0 *Otop1^{tlt/tlt}* and *Otop1^{mlh/mlh}* utricles with wholemount immunohistochemistry. A new anti-OTOPI1 antibody was generated, against an epitope located at the N-terminus of the protein before the first putative TM domain (Figure 3A). According to the predicted secondary structure (Hughes et al., 2008), this epitope is likely to be located in the cytosol. The specificity of this antibody had been previously confirmed by co-localization with β GAL signal in a homozygous null allele of *Otop1* (*Otop1 ^{β gal/ β gal}*).

XY-plane stacked images of the wholemount utricles were obtained after confocal imaging to compare the location of OTOPI1 signals with respect to the apical and basal sides of the macular epithelium. In *Otop1^{+/+}*, signals were in a punctate pattern, possibly due to localization within intracellular vesicles (Figure 3B). Signals were located just underneath the apical end (marked by the stereocilia bundles stained with phalloidin); almost no signal was detected below the mid region of the epithelium (Figure 3F). Because *Otop1 ^{β gal}* allele still expresses the first two TM domains we were able to detect the localization of the β -galactosidase (β GAL) fusion protein using the Otop1 antibody made against the N-terminal epitope. Signal intensity in *Otop1 ^{β gal/ β gal}* tissue is greatly increased (Figure 3C, F); signals were highly localized at the mid region of the

epithelium. This suggested that the fusion proteins formed aggregates within the intracellular vesicles and could no longer be trafficked to the apical end. OTOPI1 signal pattern in *Otop1^{tl/tl}* (Figure 3D) and *Otop1^{mlh/mlh}* (Figure 3E) tissue clearly showed mislocalization of the mutant proteins. The signals were spread out throughout the epithelium in a punctate pattern, and most of them did not reach the apical end (Figure 3F). These results suggest that both *tlt* and *mlh* mutations were sufficient to alter the localization of OTOPI1 and therefore the TM domains (TM3 and 9) and/or the Otopetrin Domains (OD-I and II) bearing these mutations might be important for subcellular localization of OTOPI1. Impaired localization in *Otop1^{tl/tl}* and *Otop1^{mlh/mlh}* tissue suggests the importance of apical localization for the normal function of OTOPI1.

Ratiometric Ca²⁺ imaging with primary cultures of macular epithelial cells.

To determine if endogenous OTOPI1^{TLT} can alter the *in vivo* function of OTOPI1 in modulating purinergic signaling, dissociated macular supporting cell cultures from *Otop1^{+/+}*, *Otop1^{βgal/βgal}*, *Otop1^{tl/+}*, *Otop1^{tl/tl}* inner ears were exposed to 100 μM ATP. In the *Otop1^{+/+}* samples, addition of ATP resulted in an increase in [Ca²⁺]_i, characterized by an elevated plateau that persisted until removal of the agonist (Figure. 4). The shape of this response curve resembled that of the globular substance vesicle response to ATP observed by Suzuki et al. (Suzuki et al., 1997). In contrast, in *Otop1^{βgal/βgal}* maculae, the response to ATP showed a higher peak, followed by a reduction in [Ca²⁺]_i to an elevated plateau. Detailed study on the source of calcium that mediates such an increase in [Ca²⁺]_i in mouse dissociated macular cultures showed that the peak represented P2Y receptor-mediated Ca²⁺ release from intracellular stores, whereas the plateau phase indicated a

balance between an influx of extracellular Ca^{2+} and efflux of cytosolic Ca^{2+} into intracellular stores. Therefore, the different response to ATP in *Otop1*^{+/+} and *Otop1* ^{$\beta\text{gal}/\beta\text{gal}$} cultures suggested that OTOPI functions to inhibit P2Y function and induces/allows influx of extracellular Ca^{2+} .

Otop1^{+/+} and *Otop1*^{*tlt*/+} macular cultures showed a similar response to ATP, demonstrating that a single *Otop1* allele is sufficient for OTOPI-specific modulation of the purinergic response. This result is consistent with the presence of normal otoconia in *Otop1*^{*tlt*/+} mice (Ornitz et al., 1998). Interestingly, *Otop1*^{*tlt*/*tlt*} macular cultures also showed a similar response to ATP as *Otop1*^{+/+} samples, indicating that the *tlt* mutation does not interfere with the function of OTOPI to modulate purinergic response in macular supporting cells. The *tlt* mutation may primarily influence protein localization (Figure 3B, D) or another unknown biochemical function of OTOPI.

Conclusions

Otopetrin 1 (*Otop1*) is essential for the formation of otoconia in the otolithic organs in the inner ear as the primary phenotype found in all the mutants of *Otop1* is otoconial agenesis (Hughes et al., 2004; Hurle et al., 2003; Ornitz et al., 1998; Sollner et al., 2004). *Tlt* and *mlh* are two mouse mutations in *Otop1* caused by single amino acid substitutions in the highly conserved putative transmembrane (TM) domains (TM3 for *tlt* and TM9 for *mlh*) (Hughes et al., 2008; Hurle et al., 2003). Since these mutations are predicted to alter the hydrophobicity of different TM domains, which are parts of highly conserved but distinct Otopetrin Domains (Hughes et al., 2008), the mechanism by which each mutation affects OTOPI protein function may also be different. To assess this

possibility we studied protein localization, and the ability to modulate purinergic response in *in vitro* and *in vivo*.

Introduction of the *tlt* and *mlh* mutations into the full-length Otop1 construct did not significantly alter the localization of the overexpressed protein in COS7 cells. However, comparison of the *Otop1*^{+/+}, *Otop1*^{tlt/tlt}, and *Otop1*^{mlh/mlh} utricles revealed that the apical localization of endogenous OTOP1 is impaired in both mutant samples, a phenotype that could not be assessed in COS7 cells grown in monolayer culture. In terms of modulating the purinergic response, the *mlh* mutation seems to impair OTOP1 function more than the *tlt* mutation as we observed less inhibition of P2Y- mediated function in EGFP^{Otop1}^{mlh}-expressing COS7 cells compared to EGFP^{Otop1}^{tlt}-expressing COS7 cells. Further ratiometric calcium studies with *Otop1*^{mlh/mlh} macular epithelial cells needs to be done to confirm this point. Similar purinergic response in *Otop1*^{+/+} and *Otop1*^{tlt/tlt} samples suggests that the *tlt* mutation impairs localization of the rather biochemical function, thus blocking the access of a functional protein. Alternatively, *tlt* mutation may affect other biochemical function(s) of OTOP1 which were not revealed in our ratiometric calcium assays. These data suggested that *tlt* and *mlh* mutations may differentially affect OTOP1 function and define distinct functions of each conserved Otopetrin Domain.

References

- Brostrom, M. A., and Brostrom, C. O. (2003). Calcium dynamics and endoplasmic reticular function in the regulation of protein synthesis: implications for cell growth and adaptability. *Cell Calcium* 34, 345-363.
- Dellis, O., Dedos, S. G., Tovey, S. C., Taufiq Ur, R., Dubel, S. J., and Taylor, C. W. (2006). Ca²⁺ entry through plasma membrane IP3 receptors. *Science* 313, 229-233.

Hughes, I., Binkley, J., Hurle, B., Green, E. D., NISC Comparative Sequencing Program, Sidow, A., and Ornitz, D. M. (2008). Identification of the Otopetrin Domain, a conserved domain in vertebrate otopetrins and invertebrate otopetrin-like family members. *BMC Evolutionary Biology* 8:41.

Hughes, I., Blasiolo, B., Huss, D., Warchol, M. E., Rath, N. P., Hurle, B., Ignatova, E., Dickman, J. D., Thalmann, R., Levenson, R., and Ornitz, D. M. (2004). Otopetrin 1 is required for otolith formation in the zebrafish *Danio rerio*. *Dev Biol* 276, 391-402.

Hughes, I., Saito, M., Schlesinger, P. H., and Ornitz, D. M. (2007). Otopetrin1 activation by purinergic nucleotides regulates intracellular calcium. *Proc Natl Acad Sci U S A* 104, 12023-12028.

Hughes, I., Thalmann, I., Thalmann, R., and Ornitz, D. M. (2006). Mixing model systems: Using zebrafish and mouse inner ear mutants and other organ systems to unravel the mystery of otoconial development. *Brain Res* 1091, 58-74.

Hurle, B., Ignatova, E., Massironi, S. M., Mashimo, T., Rios, X., Thalmann, I., Thalmann, R., and Ornitz, D. M. (2003). Non-syndromic vestibular disorder with otoconial agenesis in tilted/mergulhador mice caused by mutations in otopetrin 1. *Hum Mol Genet* 12, 777-789.

Lim, D. J., Karabinas, C., and Trune, D. R. (1983). Histochemical localization of carbonic anhydrase in the inner ear. *Am J Otolaryngol* 4, 33-42.

Ornitz, D. M., Bohne, B. A., Thalmann, I., Harding, G. W., and Thalmann, R. (1998). Otoconial agenesis in *tilted* mutant mice. *Hearing Res* 122, 60-70.

Shiao, J. C., Lin, L. Y., Horng, J. L., Hwang, P. P., and Kaneko, T. (2005). How can teleostean inner ear hair cells maintain the proper association with the accreting otolith? *J Comp Neurol* 488, 331-341.

Sollner, C., Schwarz, H., Geisler, R., and Nicolson, T. (2004). Mutated otopetrin 1 affects the genesis of otoliths and the localization of Starmaker in zebrafish. *Dev Genes Evol* 214, 582-590.

Suzuki, H., Ikeda, K., Furukawa, M., and Takasaka, T. (1997). P2 purinoceptor of the globular substance in the otoconial membrane of the guinea pig inner ear. *Am J Physiol* 273, C1533-1540.

Thalmann, I., Hughes, I., Tong, B. D., Ornitz, D. M., and Thalmann, R. (2006). Microscale analysis of proteins in inner ear tissues and fluids with emphasis on endolymphatic sac, otoconia, and organ of Corti. *Electrophoresis* 27, 1598-1608.

Figure 1. Localization of EGFPOTop1^{ttt} and EGFPOTop1^{mlh} in COS7 cells. A) EGFP is fused throughout the whole cytoplasm. B) EGFPOTop1 predominantly localizes to the endoplasmic reticulum (ER) and a fainter signal is detected in the plasma membrane (PM). C and D) Presence of *tlt* or *mlh* mutations does not affect localization of the transfected OTOP1 protein.

Figure 1

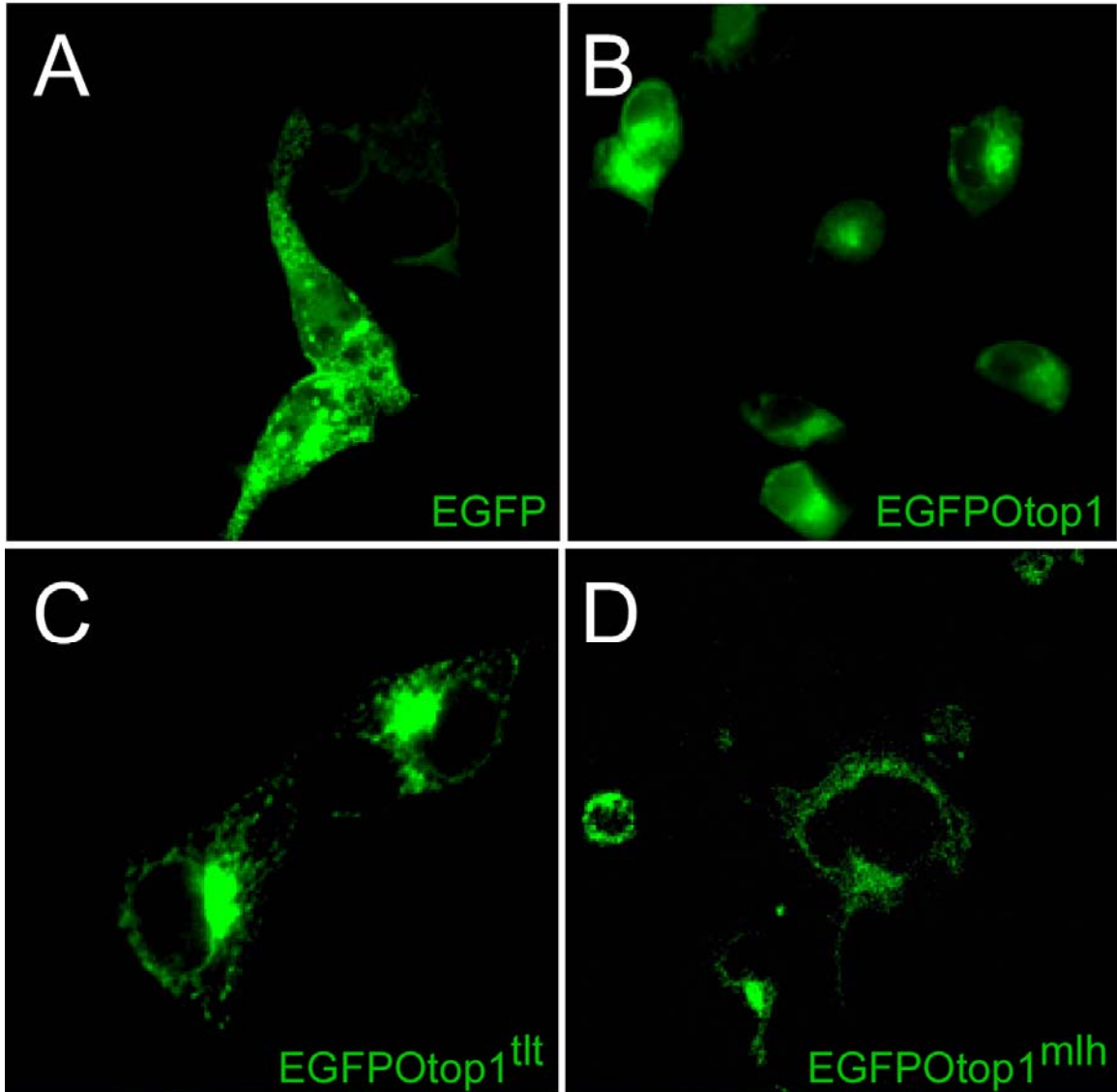


Figure 2. Overexpression of EGFP^{Otop1}, EGFP^{Otop1^{tt}}, and EGFP^{Otop1^{mlh}} in COS7 cells alters the purinergic response. A) WT (n=26) showed a biphasic response to 100 μ M ATP with an initial peak followed by a plateau phase which persisted until removal of the agonist (wash). The initial peak (rise) in $[Ca^{2+}]_i$ was much lower in the presence of EGFP^{Otop1} (n=19) where a sharp peak was absent. B) EGFP^{Otop1^{tt}}-positive cells (n=26) showed a reduced initial rise in $[Ca^{2+}]_i$ compared to the WT (n=24) cells. Presence of the peak was apparent (dotted circle) compared to EGFP^{Otop1}-expressing cells (A). C) GFPO^{top1^{mlh}}-positive cells (n=20) showed a biphasic response with a peak and a plateau phase, however the overall response was lower than with WT cells (n=20).

Figure 2

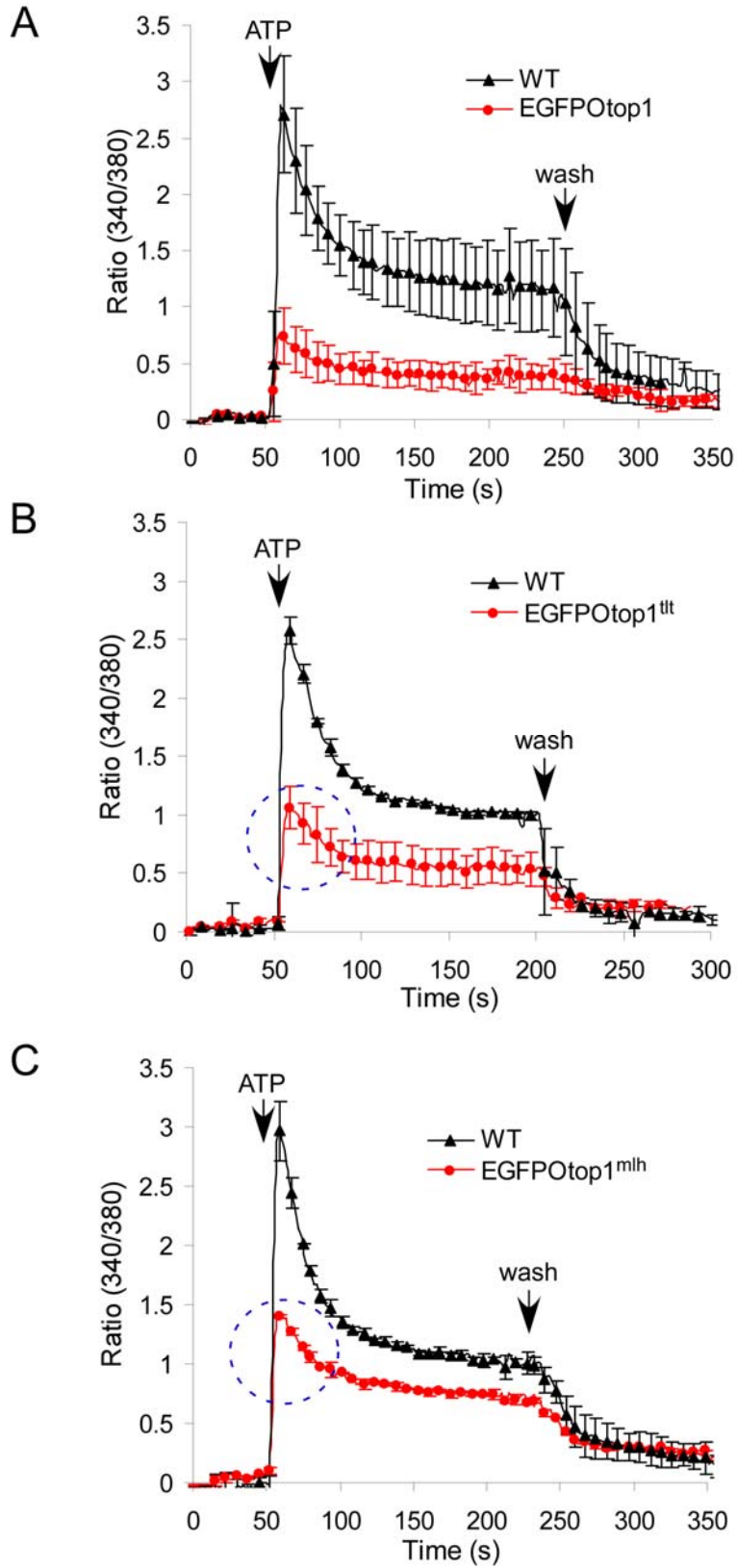


Figure 3. Apical trafficking of endogenous OTOP1 is affected in *Otop1^{tlt}* and *Otop1^{mlh}* utricular maculae. A) Schematic diagram showing the location of *tlt* and *mlh* mutations with respect to the putative transmembrane (TM) domains of OTOP1. *Tlt* and *mlh* are present within TM 3 and 9, which are parts of Otopetrin Domain I and II, respectively. The epitope for the OTOP1 antibody is located N-terminal to the putative TM domains. B-E) XY plane-stacked image of wholemount utricles stained with phalloidin and the anti-OTOP1 antibody. Phalloidin, shown in red, depicts the stereocilia bundles and actins at the apical (A) and basal (B) end, respectively. OTOP1 signals are shown in green. B) Wildtype OTOP1 is localized near the apex of the epithelium. C) In *Otop1^{βgal/βgal}* tissue, the β-galactosidase fusion protein is mis-localized and forms aggregates with each other possibly in intracellular vesicles. D, E) OTOP1^{TLT} and OTOP1^{MLH} are not get properly targeted to the apex and the signal is concentrated in the mid to basal end of the epithelium. F) Quantitation of OTOP1 signal intensities with respect to its location in the wholemount utricles (shown in B-E). X-axis depicts distance from apical to basal end, where ‘0’ indicates the most apical region.

Figure 3

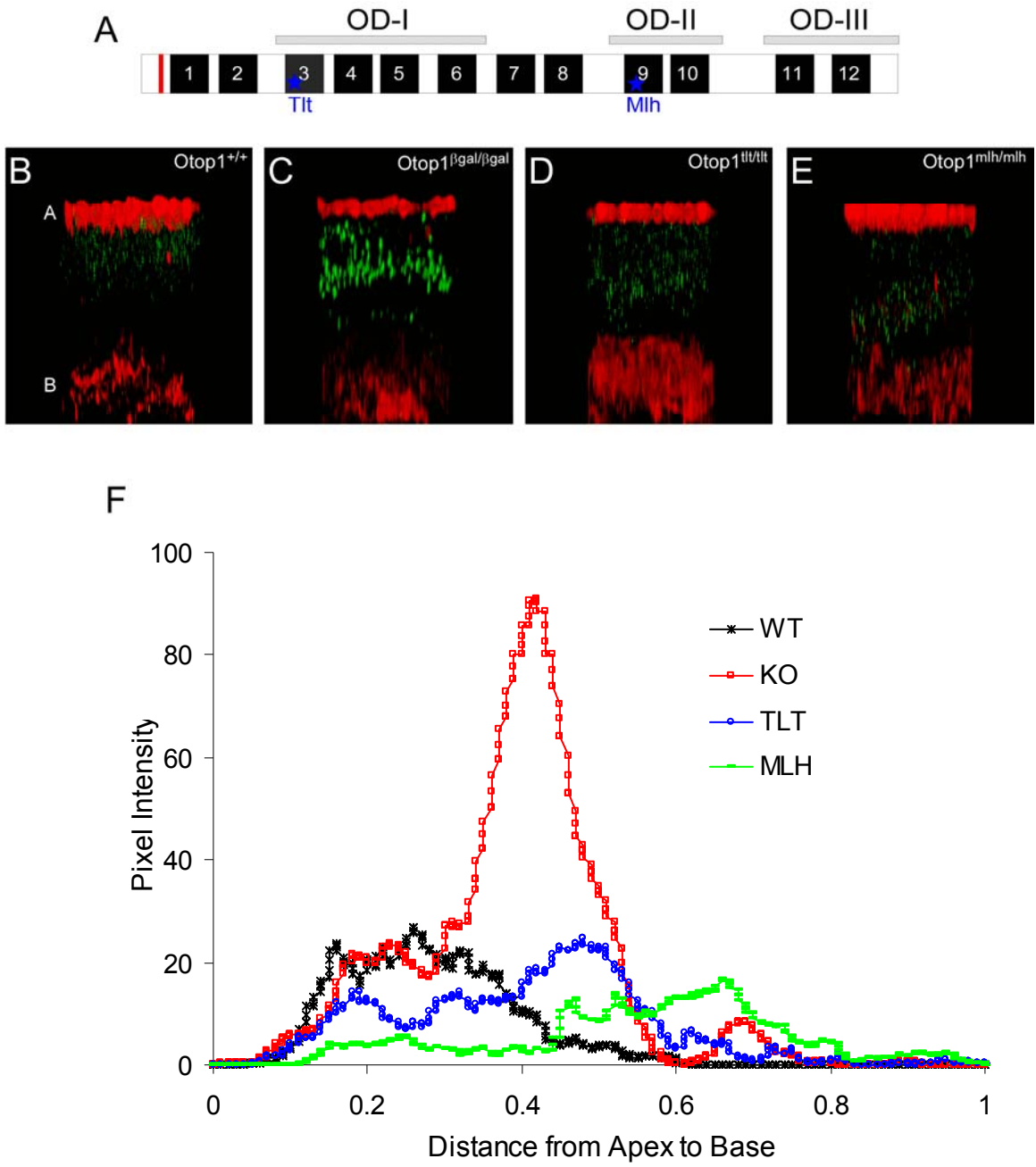
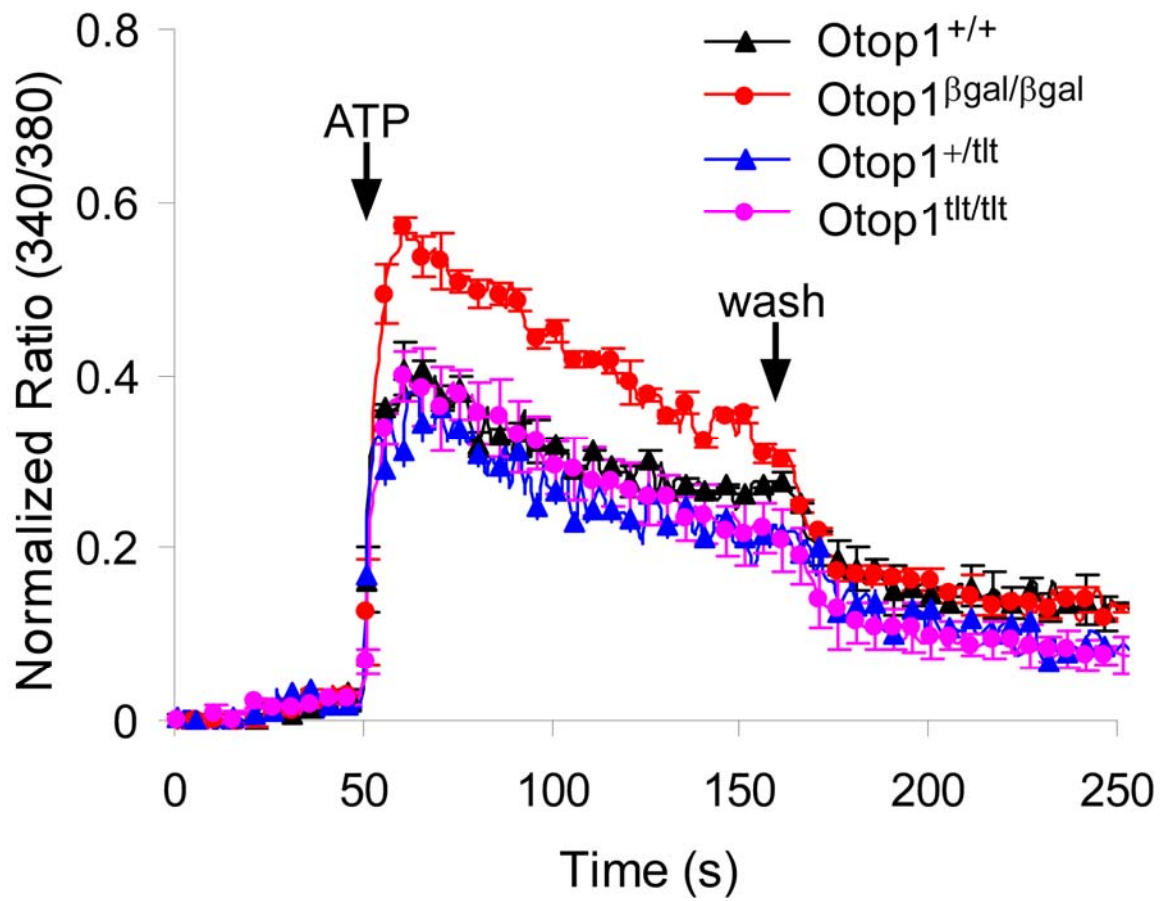


Figure 4. *Otop1^{tlt}* macular culture cells respond to ATP in a similar manner to *Otop1^{+/+}*. In response to 100 μ M ATP, OTOP1 inhibits P2Y receptor function, while allowing P2X-like influx of Ca^{2+} . This is shown as a reduced peak level compared to *Otop1 ^{β gal/ β gal}* culture cells and a sustained increase in $[\text{Ca}^{2+}]_i$ until wash. Unlike with the null allele (*Otop1 ^{β gal/ β gal}*), the *tlt* mutation does not disrupt the function of OTOP1 to modulate the purinergic response *in vivo*.

Figure 4



Chapter III

Generation and characterization of *Otop2*^{nβgal} mice

Introduction

In preliminary studies focused on identifying the genetic etiology of otoconial agenesis in *tilted (tlt)* mutant mice (Hurle et al., 2003), we identified the *Otopetrin 1 (Otop1)* gene and its paralogues *Otopetrin 2 (Otop2)* and *Otopetrin 3 (Otop3)*. Mouse OTO2 and OTO3 show 34% and 30% amino acid identity with OTO1, respectively. These genes express the highly conserved domains (Otopetrin Domain I, II, and III) (Hughes et al., 2008), which could be the functional domains of this gene family.

Otop1 is expressed in many major organs (Hurle et al., 2003). There is considerable overlap in expression between the three mouse Otopetrins, with Otop3 being the most restricted. Overlapping patterns of expression suggests the potential for functional redundancy. We hypothesized that all Otopetrins have similar biochemical properties. Additionally, functional redundancy may mask other developmental or physiological activities in other organ systems.

Previous studies with *Otop1* mutants suggested that one biochemical function of OTO1 is very likely related to regulating calcium homeostasis, which could be important for calcification during otoconia formation (Hughes et al., 2004; Hurle et al., 2003; Sollner et al., 2004). In support of this idea, OTO1 was shown to have a prominent role in regulating Ca^{2+} levels or Ca^{2+} transit in response to purinergic stimuli in heterologous systems (Hughes et al., 2007). Purinergic signaling is mediated by two classes of P2 receptors, P2Y and P2X receptors, which have distinct pharmacological responses to purines and purine analogs (North and Surprenant, 2000; Ralevic and Burnstock, 1998). P2Y receptors are metabotropic G-protein coupled receptors which mediate release of intracellular Ca^{2+} stores, whereas P2X receptors are ionotropic

channels which allow influx of extracellular Ca^{2+} upon ATP binding. Overexpression of EGFP-Otop1 in COS7 cells had three prominent consequences: 1) nonspecific depletion of endoplasmic reticulum calcium stores, 2) specific inhibition of the purinergic receptor P2Y2, and 3) initiation of a novel influx of extracellular calcium in response to ATP-like nucleotides. In a physiological setting, these activities could direct the formation and growth of otoconia and regulate other biomineralization processes. Investigating whether Otop2 and Otop3 share such biochemical functions of Otop1 in modulating $[\text{Ca}^{2+}]_i$ will help us understand the redundancy between mouse Otopetrins .

To fully understand the *in vivo* role of a protein generation of its null allele is indispensable. In this study, we generated a null allele of *Otop2* (*Otop2^{nβgal}*), which will consequently allow us to determine whether it has unique biological functions by looking for phenotypes in *Otop2^{nβgal/nβgal}* mice. The highly conserved expression of *Otop2* in the digestive tract of mouse and other animals (chicken, cow, fish) suggests that this will be an important site to look for a secretion or absorption phenotype in *Otop2^{nβgal/nβgal}* mice. Generation of an Otop1/Otop2 double null mouse will allow potential functional redundancy between these two genes to be examined in mouse development. The findings from *Otop2^{nβgal/nβgal}* mice and double homozygous null mice may suggest further biochemical activities.

Materials and Methods

Generation of $Otop2^{nlacZ}$ allele

The targeting construct was made using recombineering methods (Liu et al., 2003). First, about 5 kb upstream and downstream of the regions to target was retrieved from BAC clone RP23-117K15 (derived from C57BL/J6 mice), which completely spanned the *Otop2* gene. We designed a deletion of most of exon 2 (306 bp), intron 2 (837 bp), exon 3 and a portion of intron 3 (651 bp). β -galactosidase (*β gal*) gene and *LoxP/pol-2-neo/LoxP* selectable marker (6.1 kb) were ligated in-frame with the first two amino acids of exon 2. The SV40 nuclear transport signal (Lanford et al., 1988) was added at the N-terminus of the β -galactosidase gene to target lacZ expression to the nucleus (nlacZ). To achieve this, 500 bp sequences immediately 5' and 3' of the site that we aimed to target was ligated to the β gal coding sequence and the neo cassette, which was excised from the PL452 vector and cloned into a pBluescript vector. This construct was electroporated into DY380 cells already containing the retrieved BAC plasmid, and heat shock (32°C -> 42°C) was used to induce homologous recombination to generate the targeting vector. The 5' and 3' regions of homology contained a total of 7.6 kb of genomic DNA. The targeting vector was verified by restriction mapping and sequencing.

Before electroporation, the integrity and function of the $OTOP2^{n\beta GAL}$ fusion protein was tested in tissue culture cells. The *Otop2-n β gal* portion of the targeting vector was transiently expressed using lipofectamine (Invitrogen) in COS7 cells under a CMV promoter and cells were stained for β gal activity. $OTOP2^{n\beta GAL}$ positive cells showed X-gal staining consistent with nuclear localization of the chimeric protein.

The targeting construct was linearized and electroporated into SCC-10 ES cells, which were derived from 129X1/SvJ mice. Electroporation was carried out in the Washington University Siteman Cancer Center Murine Embryonic Stem Cell Core facility. G418 resistant clones were screened for homologous recombination by Southern blot using 5' probes. Two positive clones were identified and homologous recombination was verified using a 3' Southern blot probe. ES clones were karyotyped and then microinjected into mouse blastocysts by the Washington University Mouse Genetics Core facility. Chimerism was determined by coat color and high percentage chimeric males were mated with C57BL6/J females. The subsequent F1 mice were intercrossed, and the litters were examined for the germline transmission of the *Otop2^{nβgal}* allele using Southern blotting with 5' and 3' probes extrinsic to the targeting vector and by genomic PCR (Figure 1). The LoxP-neo cassette was excised *in vivo* by mating to a mouse that expressed Cre in the germ line, and then the male progeny were bred to C57BL6/J females to transfer the targeted allele onto a C57BL6/J genetic background.

Southern blotting and genomic PCR

Genomic DNA was extracted with phenol/choloroform and isopropanol precipitation. 10 µg of each sample was digested with either BamHI (5' probe) or Asp718 (3' probe) at 37°C overnight and electrophoresed on 1% agarose gel. Southern blots were probed with 5' and 3' probes, which were labeled with ³²P (Stratagene Prime-It II Random Primer Labeling Kit) and purified (Amersham Biosciences MicroSpin S-200 HR columns). 5' and 3' probes were made by amplification from RP23-117K15 BAC DNA with the following primers: 5' probe: primer 1 (5'- CTTGAGCCACATTGGCCCCT

- 3' (forward)), primer 2 (5' - GGCCAGATGCTGTGACCCTC
- 3' (reverse)), 3' probe: primer 1 (5' - TCTATCGTGGCTGTGGTGGTG
- 3' (forward)), primer 2 (5' - TATGAGGGCTTCTGCTTGGG
- 3' (reverse)). For genotyping PCR, mouse tail DNA was amplified with the following
primers: primer 1 (5'- GACTTAGAATCCTGTCCTTGCCCC
-3' (forward)), primer 2 (5' - TTTGCTCTTCCTTCCCAGGGC
-3' (wild-type reverse)), primer 3 (5' - TCTGCCAGTTTGAGGGGACGA -3' (*Otop2*^{n β gal}
reverse)). 30 cycles of denaturation at 94°C for 1 min, annealing at 65°C for 1 min, and
extension at 68°C for 3 min were used to amplify either 527 (wild-type) or 380
(*Otop2*^{n β gal}) bp fragments.

Construction of Otop2 and Otop3 expression vector

The full length cDNA clone of *Otop2* (4732464P15 or AK028866) and *Otop3*
(A730078K24 or AK043266) was obtained from Riken Laboratories (Japan). To clone
Otop2 and *3* into the pCS2EGFP vector, which makes N-terminal EGFP fusion
constructs, EcoRI (forward) and XbaI (reverse) enzyme linker sites were added with PCR.
The following primers were used to clone EGFP*Otop2*: primer 1 (5'-
TTTGAATTCAATGTCGGAGGAACTGGT -3' (forward)), primer 2 (5'-
CCCTCTAGATCTCTGTGGAGCTTCAGG -3' (reverse)). The following primers were
used to clone EGFP*Otop3*: primer 1 (5'- TTTGAATTCAATGGCTTCGCAGACTTC -3'
(forward)), primer 2 (5'- CCCTCTAGATCAGGCCCCCAGGTA -3' (reverse)). 25
cycles of denaturation at 92°C for 30 sec, annealing at 62°C for 30 sec, and extension at
68°C for 30 sec were used to amplify either 1692 (*Otop2*) or 1790 (*Otop3*) bp fragments.

Cell culture and transfection

COS7 cells were maintained in Dulbecco's Modified Eagle Media (Gibco) supplemented with 10% fetal calf serum (Gibco), 2mM L-glutamine, and 1X penicillin/streptomycin. Cells were plated on 35 mm plates with glass coverslips (MatTek Cultureware) 24-48 hours before transfection. Cells were transfected using Lipofectamine 2000 (Invitrogen) and approximately 1 μ g plasmid DNA in OptiMEM (Invitrogen) for 4-5 hours following manufacturer's instructions. Cultures were allowed to recover overnight in growth media.

Ratiometric calcium imaging

Transfected cells were loaded with the Ca^{2+} sensitive dye Fura 2 acetoxymethyl ester (Invitrogen) for 35 min at 37°C in 5% CO_2 following manufacturer's instructions to examine stimulus-dependent alterations in cytosolic Ca^{2+} concentrations, $[\text{Ca}^{2+}]_i$ (5). Cells were then washed in growth media for 30 min, equilibrated to physiologic recording media (145 mM NaCl/5 mM KCl/1.8 mM CaCl_2 /1 mM MgCl_2 /10 mM Hepes/10 mM glucose, adjusted to pH 7.38-7.44 with 10 N NaOH) for 15 min and washed twice in recording media before analysis. Ca^{2+} -free media contained 3 mM EGTA. For sodium-free media, NaCl was replaced isotonicly with *N*-methyl-D-glucamine and the pH adjusted to 7.4 with HCl. For chloride-free media, chloride was isotonicly replaced with gluconate salts, except MgCl_2 was replaced with MgSO_4 .

Cultures were examined with a Zeiss Axiovert (Carl Zeiss, Thornwood, NY) inverted microscope at room temperature and images were captured with an Intelligent Imaging Innovations digital camera system and analyzed with Slidebook software

(Intelligent Imaging Innovations, Denver, CO). Images of EGFP and Fura 510-nm emission after excitation at 340 nm and 380 nm, respectively, were taken sequentially at 10-s intervals. Dye fluorescence intensity was collected and then measured on a pixel-to-pixel basis to yield a single bitmap field. Images were collected with 8' binning. Cellular fluorescence was defined by measurement windows placed over individual cells. Average pixel fluorescence over the measurement field, which included ER and nucleus, was calculated by the imaging software and then logged to a file. The values for single-cell emission (at 510 nm) ratio (F340/F380 ratio = emission at 340 nm excitation/emission at 380 excitation) were plotted over time.

All cultures were examined in 1 ml of recording media. Agonist was added by pipette to the static bath media. Washes were continuous with full replacement of the media. Pharmacologic agents were added to aliquots of recording media before administration to cells. Cells were observed for 1-2 min before addition of pharmacologic agents to assess stability of the baseline. Untreated media was removed and rapidly replaced with treated media. Cells were examined throughout the pretreatment period and treated with agonist as above. Vehicle controls were identical to untreated in all experiments. ATP, ADP, UTP, UDP, ATP γ S, methyl-S-ATP, $\alpha\beta$ -methyl-ATP were obtained from Sigma (St. Louis, MO).

Results

Otopetrin 2 (Otop2) null allele was successfully generated.

The *Otop2* gene covers over 25 kb of genomic DNA on mouse chromosome 11 and is divided into seven exons. The coding sequence begins in exon 2 (exon 1 is in the 5' untranslated region) and only one coding (and two non-coding) splice form of *Otop2* has been identified (Hurle et al., 2003) (Figure 1A). To generate a null allele for *Otop2* and to create a histochemical tag to identify *Otop2*-expressing cells, the *Otop2* gene was targeted by insertion of a β -galactosidase gene in-frame with exon 2 after the first two amino acids (Figure 1A). A nuclear transport signal (Lanford et al., 1988) was added at the N-terminus of the β -galactosidase gene to target the fusion protein (n β GAL) to the nucleus. This design expressed *Otop2*^{n β gal} transcript under the control of *Otop2* transcriptional regulatory elements.

There are two genes located in the immediate vicinity of *Otop2*: *Ush1g* and *Otop3* (Figure 1B). The first intron of the *Otop2* gene contains the *Ush1g* gene, which is thought to be responsible for Usher syndrome type 1G (USH1G) in humans and in mice, the Jackson shaker (js) congenital sensorineural deafness, constant vestibular dysfunction, and retinitis pigmentosa with prepubertal onset syndrome. Given the close association with these neighboring genes, targeting *Otop2* could affect the expression of these genes. Therefore, the *Otop2* targeting vector was designed to remove a minimum amount of intron sequence while still ensuring a complete inactivation of *Otop2*. Importantly, genomic sequence analysis of the intronic regions deleted in *Otop2* showed no conserved sequence in the rat, human, dog, and chicken orthologous regions. Because the inserted PKG-Neo gene (Figure 1A) could also affect expression of neighboring genes, it was

removed by mating with germ-line expressed Cre recombinase before analyzing the phenotype.

The germ-line transmitted targeted allele was confirmed by Southern blotting (Figure 1C) and genomic PCR (Figure. 1D). Heterozygous (*Otop2*^{nβgal/+}) and homozygous (*Otop2*^{nβgal/nβgal}) mice were phenotypically normal. The otoconia and the underlying sensory epithelium were also intact, suggesting that OTOP2 has a less important role in the formation of otoconia compared to OTOP1 and/or the redundancy with other paralogues could be masking the function of OTOP2. This observation led us to generate double knockout mice for *Otop1* and *Otop2*. Unfortunately, there has been no apparent phenotype in the double knockout mice either, other than otoconial agenesis, which is most likely resulting from knocking out *Otop1*. X-gal staining was not positive in E16.5 or P0 inner ear, including the utricle and saccule, suggesting that endogenous OTOP2 may not be expressed in the inner ear. Future studies will involve investigating sites of *Otop2* expression and potential associated phenotypes.

EGFPOtop2 and EGFPOtop3 expressing COS7 cells respond to different purinergic agonists.

Previously, OTOP1 was shown to have the ability to modulate $[Ca^{2+}]_i$ *in vitro* (Hughes et al., 2007). Since OTOP2 and OTOP3 also contain the conserved Otopetrin Domains (Hughes et al., 2008), which are proposed to encode putative functional domains of the Otopetrin gene family, we hypothesized that expression of OTOP2 and OTOP3 would also modulate $[Ca^{2+}]_i$ in a similar manner to OTOP1.

The localization of EGFP-tagged proteins shows interesting characteristics. EGFPOTOP2 was prominently localized to the plasma membrane (PM) (arrow) (Figure 2A), while most EGFPOTOP3 was found in the endoplasmic reticulum (ER) (arrowhead) (Figure 2B), reminiscent of EGFPOTOP1. This suggested that OTOP2 may be trafficked differently from the other paralogues.

Wildtype COS7 cells show a biphasic response to 200 μM ATP, where a sharp initial peak is followed by a plateau phase, which lasts until removal of the agonist (wash) (Hughes et al., 2007). *Otop1*-expressing cells no longer show the initial peak but still have an increase in $[\text{Ca}^{2+}]_i$ characterized by a similar plateau phase. Previous studies have shown that the initial peak and plateau phase depicts the release of intracellular Ca^{2+} and influx of extracellular Ca^{2+} , respectively (Hughes et al., 2007). In terms of agonist sensitivity, EGFPOTop1 expressing cells responded to 200 μM ATP, ADP, and UDP (only half amount of the response compared to ATP and ADP) with increases in $[\text{Ca}^{2+}]_i$, but responded minimally to 200 μM ATP γ S, 50 μM $\alpha\beta\text{MeATP}$ and 50 μM 2MeSATP (methyl-S-ATP).

When EGFPOTop2 was expressed in COS7 cells a similar modulation of purinergic response was observed (Figure 2C). In EGFPOTop2-positive cells, the initial peak was absent, and the plateau phase persisted in response to 200 μM ATP. The agonist sensitivity of EGFPOTop2-expressing cells was similar to that of EGFPOTop1, except for the response to 2MeSATP. Stimulation with 2MeSATP showed a positive increase in $[\text{Ca}^{2+}]_i$, where the level of the plateau phase was lower than when stimulated with 200 μM UDP. The response profile of EGFPOTop3 expressing cells to purinergic ligands was exactly the same as that of EGFPOTop1 (Figure 2D), suggesting a more functional

redundancy between OTOPI and OTOPI3, at least in terms of modulating Ca^{2+} homeostasis in response to purinergic stimuli.

Future directions

Otopetrin 2 (Otop2) and *3 (Otop3)* are paralogous genes of mouse *Otop1*. They express highly conserved Otopetrin Domains (Hughes et al., 2008), and their expression patterns show extensive overlap (Hurle et al., 2003). *Otop1* is thought to be expressed in many major organs, but the fact that the apparent phenotype in the *Otop1* mutants (Hurle et al., 2003; Sollner et al., 2004) and the knockout is otoconial agenesis led us to hypothesize that there could be a considerable degree of redundancy between the three Otopetrins in mouse. Since *Otop3* showed the most restricted expression pattern, we decided to generate a knockout allele of *Otop2* (*Otop2^{nβgal}*) and ultimately produce double knockout mice with the previously made *Otop1* null allele (*Otop1^{βgal}*).

No apparent phenotype in *Otop2^{nβgal/nβgal}* mice and no new phenotype in *Otop1^{βgal/βgal};Otop2^{nβgal/nβgal}* (other than otoconia agenesis) mice was observed, suggesting that OTOPI2 and OTOPI3 may have significant functional redundancy with OTOPI1. To study this possibility we would need to generate a null allele of *Otop3*. Alternatively, OTOPI2 may have a subtler physiological role that will need a more detailed analysis to elucidate. To explore this possibility, various expression and functional analyses with *Otop2^{nβgal/nβgal}* and *Otop1^{βgal/βgal}; Otop2^{nβgal/nβgal}* mice would need to be followed.

Before pursuing detailed expression analysis, the integrity of nβGAL in *Otop2* null allele needs to be checked. So far, we have not found any tissue that can serve as a

positive control for *Otop2* expression. Previously published microarray data (Hurle et al., 2003) suggested several tissues with high expression of *Otop2*, such as brown fat, small intestine, salivary gland, tongue epidermis, stomach, kidney, etc. After checking *Otop2* mRNA levels in these organs, those that give a positive result will be tested for X-gal activity. One of the top priorities would be to check *Otop2* expression in the inner ear, including cochlea.

Gross morphology of the inner ear is not affected by ablating *Otop2*, but the close proximity of *Otop2* and *Ush1g* suggest that further exploration of possible inner ear phenotypes is warranted. Since *Ush1g* lies within an intron of *Otop2*, the promoter and regulatory domains for *Ush1g* expression could be embedded in *Otop2* and these genes may be co-regulated. To ensure that *Otop2* targeting does not interfere with the normal expression of either neighboring genes, the expression level of *Ush1g* needs to be checked and compared in the wildtype and *Otop2*^{nβgal/nβgal} mice. Alterations in *Ush1g* expression might cause a Ush1G syndrome, with ocular and cochlear malformations. Taking this into account, hearing and eye function tests will also be pursued.

The observation that OTOF2 and OTOF3 can also modulate purinergic response in COS7 in a similar manner to OTOF1 suggests that Otopetrin family proteins could have a conserved role in regulating Ca²⁺ homeostasis. Notably, the possible expression of Otopetrins have been shown (Hurle et al., 2003) in organs that require critical regulation of Ca²⁺, such as kidney, intestine and skeletal tissues. Studying possible defects (functional and/or developmental) in these organs in *Otop2*^{nβgal/nβgal} and *Otop1*^{βgal/βgal}; *Otop2*^{nβgal/nβgal} mice should reveal more *in vivo* functions of the Otopetrin family proteins.

References

- Hughes, I., Binkley, J., Hurle, B., Green, E. D., NISC Comparative Sequencing Program, Sidow, A., and Ornitz, D. M. (2008). Identification of the Otopettrin Domain, a conserved domain in vertebrate otopettrins and invertebrate otopettrin-like family members. *BMC Evolutionary Biology* *8*:41.
- Hughes, I., Blasiolo, B., Huss, D., Warchol, M. E., Rath, N. P., Hurle, B., Ignatova, E., Dickman, J. D., Thalmann, R., Levenson, R., and Ornitz, D. M. (2004). Otopettrin 1 is required for otolith formation in the zebrafish *Danio rerio*. *Dev Biol* *276*, 391-402.
- Hughes, I., Saito, M., Schlesinger, P. H., and Ornitz, D. M. (2007). Otopettrin1 activation by purinergic nucleotides regulates intracellular calcium. *Proc Natl Acad Sci U S A* *104*, 12023-12028.
- Hurle, B., Ignatova, E., Massironi, S. M., Mashimo, T., Rios, X., Thalmann, I., Thalmann, R., and Ornitz, D. M. (2003). Non-syndromic vestibular disorder with otoconial agenesis in tilted/mergulhador mice caused by mutations in otopettrin 1. *Hum Mol Genet* *12*, 777-789.
- Lanford, R. E., White, R. G., Dunham, R. G., and Kanda, P. (1988). Effect of basic and nonbasic amino acid substitutions on transport induced by simian virus 40 T-antigen synthetic peptide nuclear transport signals. *Mol Cell Biol* *8*, 2722-2729.
- Liu, P., Jenkins, N. A., and Copeland, N. G. (2003). A highly efficient recombineering-based method for generating conditional knockout mutations. *Genome Res* *13*, 476-484.
- North, R. A., and Surprenant, A. (2000). Pharmacology of cloned P2X receptors. *Annu Rev Pharmacol Toxicol* *40*, 563-580.
- Ralevic, V., and Burnstock, G. (1998). Receptors for purines and pyrimidines. *Pharmacol Rev* *50*, 413-492.
- Sollner, C., Schwarz, H., Geisler, R., and Nicolson, T. (2004). Mutated otopettrin 1 affects the genesis of otoliths and the localization of Starmaker in zebrafish. *Dev Genes Evol* *214*, 582-590.

Figure 1. Targeting scheme of *Otop2*^{nβgal} allele. A) *Otop2* has one splice variant, and its transcription starts at exon2. A β-galactosidase gene and LoxP-neo cassette was inserted in-frame with the second amino acid in exon 2 by homologous recombination using 4.8 and 2.8 kb 5' and 3' homology arms, respectively. The 5' and 3' probes used for Southern Blotting were extrinsic to the targeting vector. B) *Otop2* gene has *Ush1g* and *Otop3* in close proximity. *Ush1g* lies within the first intron of *Otop2* (1.5 kb 5' to exon2), and is transcribed in the opposite direction as *Otop2*. *Otop3* is located 3 kb downstream of exon7 of *Otop2*, and is translated in the same orientation as *Otop2*. C) Southern Blotting result with wildtype (*Otop2*^{+/+}), het (*Otop2*^{nβgal/+}), hom (*Otop2*^{nβgal/nβgal}) mouse tails. For 5' and 3' probes, the band sizes for the wildtype and null allele are 13 and 9 kb, 16 and 12 kb, respectively. D) Multiplex genomic PCR result. The product sizes for the wildtype and null allele are 527 and 380 bp.

Figure 1

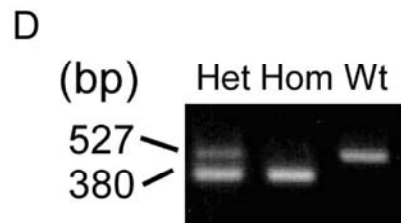
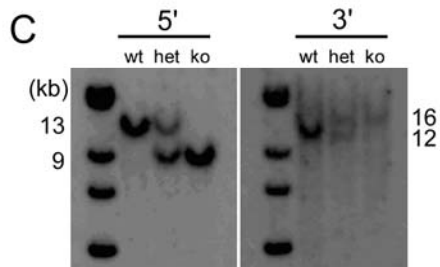
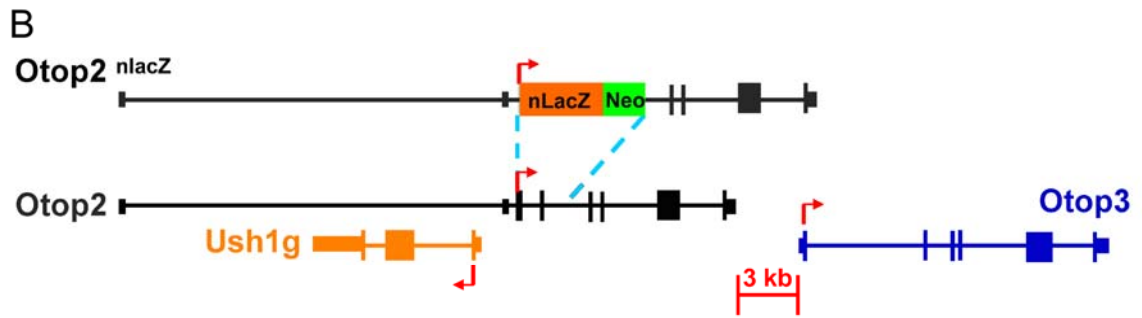
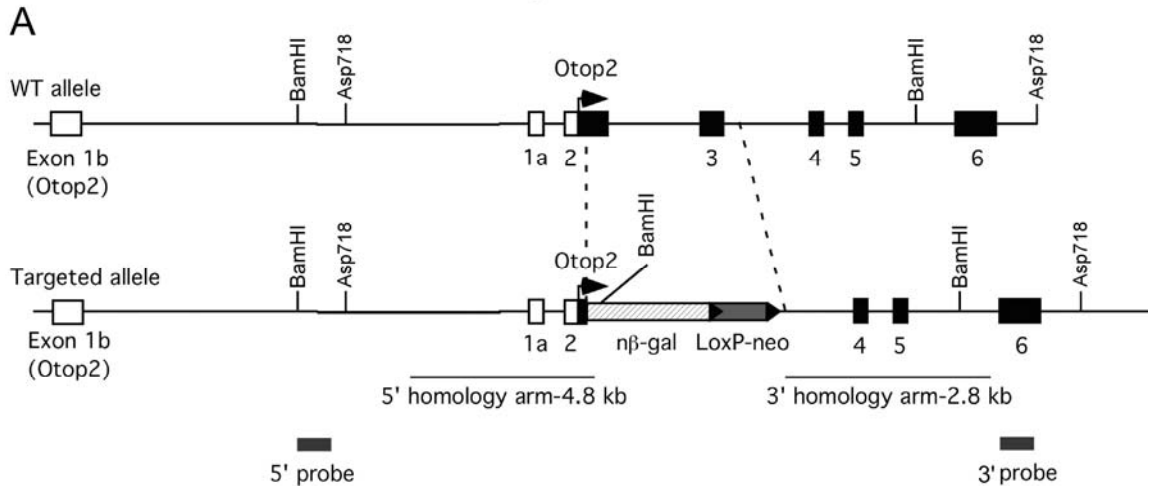
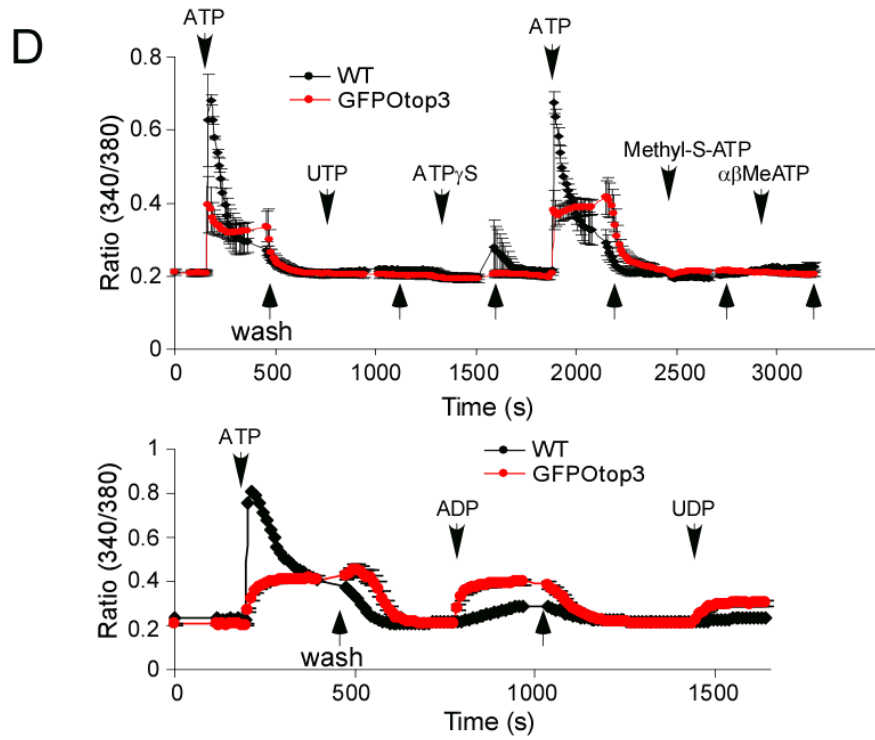
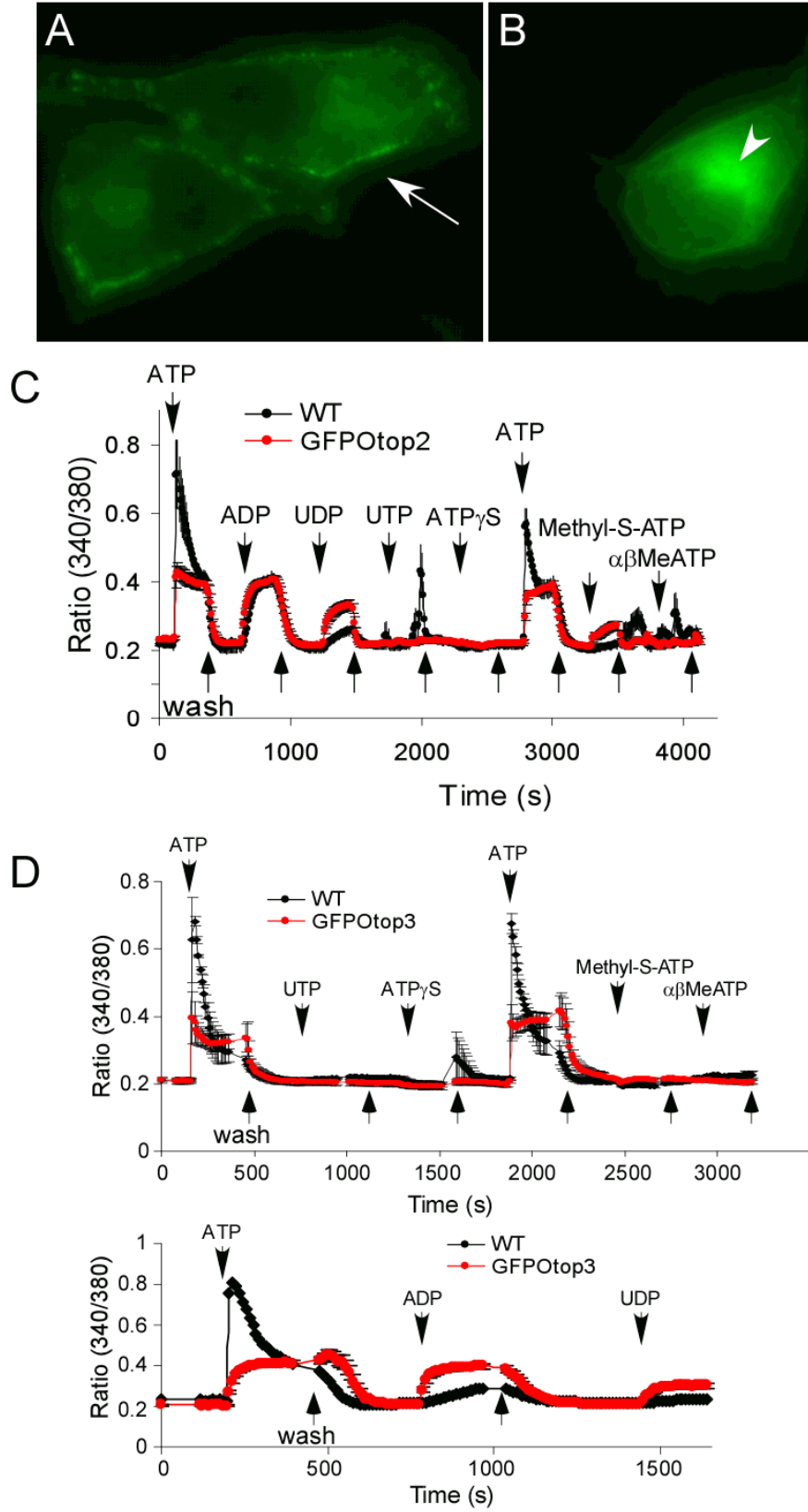


Figure 2. Response of GFPOtop2 and GFPOtop3-expressing COS7 cells to different purinergic agonists. A) COS7 cells expressing GFPOtop2. GFP signal is apparent in a punctate pattern at the plasma membrane (arrow). B) Cells expressing GFPOtop3 show GFP localization at the endoplasmic reticulum (arrowhead). C, D) GFPOtop2 (WT (n=7), GFPOtop2 (n=11)) and GFPOtop3-expressing cells (upper graph; WT(n=3), GFPOtop3 (n=4), lower graph; WT(n=1), GFPOtop3 (n=15)) show different agonist sensitivity to modulating purinergic response. GFPOtop2 and GFPOtop3-positive cells respond to ATP=ADP>UDP>Methyl-S-ATP and ATP=ADP>UDP, respectively,

Figure 2



Comparison of otoconia weight and expression of *Otopetrin 1* and *Otoconin 90* at normal and hypergravity in developing quail

Euysoo Kim¹, David Huss², Elena Ignatova², Ruediger Thalmann², Isolade E. Thalmann²,
David M. Ornitz¹, J. David Dickman²

Departments of Developmental Biology¹, Otolaryngology², Washington University
School of Medicine, St. Louis, MO USA

Corresponding author
J. David Dickman
Washington University School of Medicine
Department of Otolaryngology
Central Institute for the Deaf Research Building
4560 Clayton Ave., Room 2130
St. Louis, MO
Email: ddickman@wustl.edu
Phone: 314-747-7221
Fax: 314-747-7206

Introduction

In the vestibular system, the otolith organs contain mechanical inertial transducers, called otoconia, which are essential for detecting linear acceleration of the head with respect to gravity. In birds, the utricle, saccule, and lagena contain these tiny biominerals, embedded in a gelatinous membrane overlying the sensory epithelium. The fact that otoconia are approximately 3 times denser than the surrounding endolymph fluid (Carlstrom et al., 1953; Grant and Best, 1987) allows them to be effectively displaced and move the underlying stereocilia of the sensory cells, leading to initiation of a neuronal response. In the absence of otoconia, severe balance problems occur (Jones et al., 1999; Ornitz et al., 1998).

Each otoconium consists of a glycoprotein/proteoglycan core surrounded by the calcite polymorph of calcium carbonate. The core comprises Otoconin 90 (OC90), which accounts for 90% of the total protein in otoconia, and several minor proteins (Thalman et al., 2006) have been recently discovered. OC90 is homologous to secretory phospholipase A₂ (sPLA₂), and has been cloned from mouse and chicken (Wang et al., 1998; Wang et al., 1999). Production of *Oc90* is prominent in the nonsensory cell types of the semicircular canal, utricle, saccule and the cochlear duct (Verpy et al., 1999). Immunostaining of the OC90 protein in the nonsensory patches fades by post-natal day 0, whereas OC90 signal in the otoconia persists even after birth in mice.

Calcification of the proteinaceous otoconial precursor is rapid and ultimately results in mature otoconial shape, characterized by barrel shaped morphology with trihedral faceted ends (Ballarino and Howland, 1982; Ballarino et al., 1985; Lim, 1973; Ross and Peacor, 1975) (Figure 1A). In the quail (*Coturnix japonica*), the growth of

otoconia begins at E5 in the saccule and E6 in the utricle and fully developed by E12 in the saccule and and post-hatch day 7 (P7) in the utricle (Figure 1B, C). Otopetrin 1 (OTOP1) is essential for the nucleation and growth (calcification) of otoconia (Hughes et al., 2004). All the mutants of *Otop1* (*tilted* (*tlt*), *mergulhador* (*mlh*), and *backstroke* (*bsk*)) show nonsyndromic otoconial agenesis with no abnormal phenotypes in inner ear morphogenesis (Hurle et al., 2003; Ornitz et al., 1998; Sollner et al., 2004). Studies with these mutants suggested that OTOP1 has an essential and conserved role in the timing of formation and the size and shape of the developing otoconia/otolith (Hughes et al., 2004). Consistent with its proposed role, *Otop1* mRNA is expressed in the sensory epithelium (Hurle et al., 2003). Recently, three separate highly conserved regions of the murine *Otop1* cDNA have been identified in expressed sequence tag (EST) clones of chicks, strongly suggesting that similar mRNA and protein are also expressed in quails. As a multi-transmembrane protein, OTOP1 is postulated to be located in the calcium-enriched microvesicles called globular substance during initial stage of otoconial formation (Hurle et al., 2003). Coalesced OC90 would interact with these microvesicles and this interaction would initiate crystal nucleation and growth (Thalmann et al., 2001).

During manned spaceflight, 80-90% of the flight crews experienced space motion sickness, such as disorientation, nausea, and emetic attacks during the first 48-72 hours of weightlessness (Davis et al., 1988; Reschke et al., 1998; Thornton et al., 1987). It was apparent that the lack of gravity as a constant stimulus during spaceflight produced profound changes in vestibular system function, but the basic mechanisms that are affected by changes in gravity are poorly understood. The potential for gravity to

modulate vestibular mechanotransduction lead to the hypothesis that gravity could serve as a regulatory factor in the development of the otolith organs.

One possibility is that the otoconia structure and/or the afferent innervations are affected by altered gravity conditions. Several previous studies have shown that this may be true as changes in size of otoconia (Fermin et al., 1996; Ross and Donovan, 1986a; Wiederhold et al., 2000), in the receptor-afferent morphology (Gaboyard et al., 2002; Raymond et al., 2000; Ross, 1993), in vestibular afferent responsiveness (Boyle et al., 2001; Bracchi et al., 1975; Correia et al., 1992; Jones et al., 1993), and in vestibular related neuromotor responses (Dai et al., 1994; Sebastian et al., 1996; Takabayashi et al., 1993; von Baumgarten et al., 1975) were observed in animals exposed for brief periods in either microgravity or hypergravity.

Interestingly, exposure of mature animals to altered gravity environment (at least short term) appear to produce little detectable changes in otoconia at either the morphological or calcification level (Krasnov, 1991; Ross et al., 1985; Ross and Donovan, 1986b; Sondag et al., 1995). However, definite and systematic changes are observable when animals are exposed to altered gravitational states during embryonic development (Hara et al., 1995; Moorman et al., 1999; Pedrozo et al., 1997; Sondag et al., 1996; Wiederhold et al., 2000). To fully understand the effect of altered gravity on otoconia formation, it is necessary to analyze the molecular processes underlying biosynthesis of otoconia in embryos from various developmental time points after a chronic exposure to conditions of altered gravity throughout development.

In this study, we used Japanese quails developed under normal (1G) and hypergravity (2G) (Figure 2) to quantitatively determine how gravity affects the

expression of *Oc90* and *Otop1*. As OC90 and OTOP1 are indispensable for the two main mechanisms forming mature otoconia, protein core formation and the calcification process, respectively, we investigated effects of gravity on the expression of the genes involved in otoconia biosynthesis. In parallel, calcium weight of otoconia in these samples was measured to correlate with the results of the expression study. Quail is an ideal model to study the effect of altered gravity because of its small size, short development period, and their non-altricial nature.

Materials and Methods

Gravity experiment

Cooled fertilized eggs were exposed to normal (1G) or hypergravity (2G) for further development. The 1G eggs were kept in a standard lab incubator maintained at 37.5°C with a relative humidity of 55%. The hypergravity condition of 2G was provided by constant velocity rotation (365°/sec) using a 0.396m radius custom designed laboratory centrifuge housed inside an incubator (SHOT Inc.) (Figure 2).

Tissue dissection

In E2 through E7 embryos the region of the temporal bone containing the vestibular end organs and basilar papilla was dissected free and used for inner ear tissue. In E8 through E14 embryos the entire vestibular labyrinth, including the basilar papilla and lagena, was dissected free from the temporal bone and designated inner ear tissue. All tissues for qPCR were stored in RNA Later (Ambion) at -20C until use. Tissues from

3 embryos were collected in a single tube, and 3 tubes were prepared for each developmental time point (E2, 4, 6, 8, 10, 12, and 14).

Measurement of otoconial calcium weight

Temporal bones of E12 and E14 embryos were removed from the half head under sodium cacodylate buffer and fixed overnight. The endorgans (utricle and saccule) with the otoconia attached were then dissected free from the temporal bone, dried, and weighed. The calcium in the otoconia was then removed by EDTA. The remaining tissue was then dried and reweighed. Subtracting the second weighing from the first yielded the total weight of calcium removed from the otoconia.

Extraction of total RNA and cDNA synthesis

Total RNA was purified using RNeasy (Qiagen) spin columns. RNA was treated with RNase-free DNase (Qiagen) to avoid genomic DNA contamination. Total RNA was eluted in 40µl. 200ng of RNA was used for each reverse transcriptase reaction. SuperScript first strand synthesis system (Invitrogen) was used to generate cDNA, and samples without reverse transcriptase were processed in parallel to serve as negative controls. Prior to real-time quantitative RT-PCR, semi-quantitative RT-PCR with quail GAPDH primers was performed to check the efficiency of cDNA synthesis.

Real-time quantitative RT-PCR

The measurement was carried out in a 96-well plate in an iCycler machine. 23µl of mastermix (iQTM SYBR green supermix, forward and reverse primers and RNase-free

water) and 2µl of cDNA were added to each well. Each sample was loaded in triplicates. After PCR reaction, products were subjected to gel electrophoresis to confirm amplification of correct target. Relative expression was calculated by the following formula; $2^{-(\Delta Ct - \Delta Ct(\text{baseline}))}$, where $\Delta Ct = Ct(\text{Gene}) - Ct(\text{GAPDH})$ and $\Delta Ct(\text{baseline}) = \Delta Ct$ of E9 inner ear 1G tissue.

Gene	Primer sequence	Product size (base pair)
GAPDH	5'- GATGGGTGTCAACCATGAGAAA -3' 5'- ATCAAAGGTGGAAGAATGGCTG -3'	450 bp
Otopetrin 1	5'- TTAATTCTGGACTCCTTTAAAATTGGA -3' 5'- GAACACAGAATGGATAACCCCAAAC -3'	192 bp
Otoconin 90	5'- ACCTCTCCAGGCTCCTTCCA -3' 5'- TCCTGCAGGTCCATTGGGTC -3'	201 bp
Otogelin	5'- GAGGAATGTAATAATTGCACTTGCA -3' 5'- GGCAGGTTAATTTGTACTGGTCATATA -3'	332 bp

Oc90 in-situ hybridization

700bp digoxigenin labeled probes were produced by PCR using primers specific to chicken *Oc90*. 10 µm frozen sections were incubated with sense and anti-sense probes overnight at 55oC. Alkaline phosphatase conjugated anti-DIG antibody was used along with NBT/BCIP to localize the expression pattern of mRNA. Nuclear fast red was used as a counterstain.

OC90 immunohistochemistry

A rabbit anti-chicken OC90 antibody, which recognizes part of the linker region between the two PLA domains, was incubated at a 1:1000 dilution on 10 µm frozen sections overnight at 4oC. A Cy-3 conjugated horse anti-rabbit secondary antibody was used to localize the expression pattern of protein under epi fluorescence. Nuclei were

stained with bisbenzimidazole. Control sections were incubated with pre-immune serum or secondary antibody only.

Results

Expression pattern of Otoconin 90 (Oc90) mRNA and protein.

To determine whether the expression pattern of *Oc90* is conserved in quails, *in-situ* hybridization and immunohistochemical analysis was performed on developing quail tissues (Figure 3). *Oc90* mRNA expression was first detected at E6 in the restricted regions of the cochlear duct and otic vesicle. From E10, the localization of *Oc90* mRNA expression was apparent in the non-sensory epithelium of the vestibular labyrinth and in the tegmentum vasculosum (cochlea). A high level of *Oc90* expression continued through E12, and after this point *Oc90* mRNA subsequently declined and was not detected at E15. Sections incubated with the antisense probe did not show any positive *Oc90* signal (data not shown).

The onset of OC90 protein expression lagged behind that of its mRNA. OC90 was first faintly detected at E8, and stronger labeling was observed from E10 through P7. The apical regions of the non-sensory epithelium of the vestibular labyrinth showed the strongest signal. The presence of OC90 in otoconia was prominent starting at E12. Sections incubated with pre-immune serum or secondary antibody only, showed no labeling (data not shown). This pattern of expression was consistent with what had been previously observed in other species (Verpy et al., 1999).

Hypergravity does not significantly affect Oc90 expression.

To investigate the effect of gravity on the biosynthesis of otoconia during development we developed a system which can induce hypergravity (2G) through sustained centrifugation (Figure 2, materials & methods). Quail eggs were tightly held within each cylindrical slot and were maintained in the system throughout development until analysis. No change in body weight between embryos grown at 1G and 2G conditions (Figure 4) suggested that embryonic development was not delayed or significantly affected by hypergravity centrifugation. This supported the idea that any change in expression level of *Otop1* and *Oc90* was not a consequence of altered growth rates of the animals.

An important control experiment was to confirm the specificity of our tissues that were used for quantitative RT-PCR (qRT-PCR) analysis, as brain and inner ear temporal bones were too close to each other and therefore prone to contamination during the dissection process. *Otogelin* which is a component of the glycoproteins specific to the acellular membranes of the inner ear is not expressed in the brain, and therefore was a good positive control for inner ear tissue. cDNA from inner ear tissues was enriched with *Otogelin* message whereas brain tissue contained very little (Figure 5), confirming specificity of our tissue dissection.

qRT-PCR data showed that at 1G expression of *Oc90* was minimal until E6, reached a maximum at E9 and decreased toward hatching (Figure 6). This expression pattern was consistent with what was observed by *Oc90 in-situ* hybridization (Figure 3), confirming the integrity of our qRT-PCR analysis. Importantly, the expression of *Oc90* throughout development was not affected by hypergravity. This result suggested that

chronic hypergravity condition is unlikely to affect otoconia protein core formation or that some compensation has occurred in early development such that the effect of hypergravity could not be revealed at the later time points.

Hypergravity does not affect Otop1 expression or otoconia calcium weight.

To determine whether hypergravity can affect otoconia calcification, the expression level of *Otop1* was assayed. At 1G, *Otop1* showed a similar expression profile to that of *Oc90* (Figure 7). The rate of increase in expression level during early development increased greatly at E6 when immature, double fluted otoconial begin to form on the utricle (Figure 1C). Maximal levels of *Otop1* mRNA were observed at E9, and after E9, the level dropped dramatically. The low level of *Otop1* was maintained until hatching. Possible effects of hypergravity on *Otop1* expression was observed at E9 and E10, but the difference did not achieve statistical significance. This result suggested that the hypergravity condition did not interfere with calcification of otoconia. Accordingly, otoconial calcium weight did not show any significant difference between animals grown at normal and hypergravity (Figure 8). These results showed that the effect of gravity as an epigenetic determinant of formation of otoconia is relatively weak.

Conclusion

Gravity is sensed by receptors in the otolithic organs of the vestibular system. Otoconia, the dense biominerals that lie within the otolithic organs, are essential inertial transducers which move with respect to gravity and initiate a neuronal response (Hughes et al., 2006). Many previous studies reported changes in otoconia morphology and size in

animal models exposed to different gravity conditions (Hara et al., 1995; Moorman et al., 1999; Pedrozo et al., 1997; Sondag et al., 1996; Wiederhold et al., 2000), suggesting gravity as an epigenetic factor for regulating biosynthesis and maintenance of otoconia.

In this study, we investigated the effect of chronic hypergravity treatment on development of quail eggs by examining the expression of two important genes previously implicated for otoconia formation, *Otoconin90 (Oc90)* and *Otopetrin 1 (Otop1)*. Interestingly, the onset and decrease in expression of the two genes at normal gravity were tightly correlated, with maximum expression at E9, when mature otoconia are already localized over the sensory epithelia (Figure 1C). Higher levels of *Oc90* and *Otop1*, observed after initiation of otoconial calcification, suggest that relatively little amount of OC90 and OTOP1 are required to initiate otoconia formation. Alternatively, accumulated OC90 and OTOP1 may serve an additional role during growth and possibly maintenance of otoconia.

When the expression of *Oc90* and *Otop1* and calcium weight of the otoconia were compared in animals grown at normal (1G) and hypergravity (2G) no prominent difference was observed. This suggests that the effect of change in the force of gravity is unlikely to affect otoconia development through regulation of these genes. These data highlight the necessity to study the morphology and function of efferent and afferent innervations that innervate the sensory cells beneath the otoconia mechanotransduction structure. Importantly, our preliminary data show that calyx afferent formation is delayed in microgravity, with smaller axon diameters and smaller termination fields for all afferent types as compared to 1G controls. Animals raised to E12 in 2G appear to have the opposite result, with larger axonal diameters and increased terminal fields.

Comparison of expression of genes critical for formation of afferent structures in the otolithic organs, such as brain-derived neurotrophic factor (BDNF), may provide us additional clues to the effect of gravity on vestibular system development and function.

References

- Ballarino, J., and Howland, H. C. (1982). Otoconial morphology of the developing chick. *Anat Rec* 204, 83-87.
- Ballarino, J., Howland, H. C., Skinner, H. C., Brothers, E. B., and Bassett, W. (1985). Studies of otoconia in the developing chick by polarized light microscopy. *Am J Anat* 174, 131-144.
- Boyle, R., Mensinger, A. F., Yoshida, K., Usui, S., Intravaia, A., Tricas, T., and Highstein, S. M. (2001). Neural readaptation to Earth's gravity following return from space. *J Neurophysiol* 86, 2118-2122.
- Bracchi, F., Gualierotti, T., Morabito, A., and Rocca, E. (1975). Multiday recordings from the primary neurons of the statoreceptors of the labyrinth of the bull frog. The effect of an extended period of "weightlessness" on the rate of firing at rest and in response to stimulation by brief periods of centrifugation (OFO-A orbiting experiment). *Acta Otolaryngol Suppl* 334, 1-27.
- Carlstrom, D., Engstrom, H., and Hjorth, S. (1953). Electron microscopic and x-ray diffraction studies of statoconia. *Laryngoscope* 63, 1052-1057.
- Correia, M. J., Perachio, A. A., Dickman, J. D., Kozlovskaya, I. B., Sirota, M. G., Yakushin, S. B., and Beloozerova, I. N. (1992). Changes in monkey horizontal semicircular canal afferent responses after spaceflight. *J Appl Physiol* 73, 112S-120S.
- Dai, M., McGarvie, L., Kozlovskaya, I., Raphan, T., and Cohen, B. (1994). Effects of spaceflight on ocular counterrolling and the spatial orientation of the vestibular system. *Exp Brain Res* 102, 45-56.
- Davis, J. R., Vanderploeg, J. M., Santy, P. A., Jennings, R. T., and Stewart, D. F. (1988). Space motion sickness during 24 flights of the space shuttle. *Aviat Space Environ Med* 59, 1185-1189.
- Dickman, J. D., Huss, D., and Lowe, M. (2004). Morphometry of otoconia in the utricle and saccule of developing Japanese quail. *Hear Res* 188, 89-103.

- Fermin, C. D., Martin, D., Jones, T., Vellinger, J., Deuser, M., Hester, P., and Hullinger, R. (1996). MICROGRAVITY IN THE STS-29 SPACE SHUTTLE DISCOVERY AFFECTED THE VESTIBULAR SYSTEM OF CHICK EMBRYOS [Review]. *Histol Histopathol* 11, 407-426.
- Gaboyard, S., Blanchard, M. P., Travo, C., Viso, M., Sans, A., and Lehouelleur, J. (2002). Weightlessness affects cytoskeleton of rat utricular hair cells during maturation in vitro. *Neuroreport* 13, 2139-2142.
- Grant, W., and Best, W. (1987). Otolith-organ mechanics: lumped parameter model and dynamic response. *Aviat Space Environ Med* 58, 970-976.
- Hara, H., Sekitani, T., Kido, T., Endo, S., Ikeda, T., and Takahashi, M. (1995). Fine structures of utricle of developing chick embryo exposed to 2G gravity. *Acta Otolaryngol Suppl* 519, 257-261.
- Hughes, I., Blasiolo, B., Huss, D., Warchol, M. E., Rath, N. P., Hurle, B., Ignatova, E., Dickman, J. D., Thalmann, R., Levenson, R., and Ornitz, D. M. (2004). Otopetrin 1 is required for otolith formation in the zebrafish *Danio rerio*. *Dev Biol* 276, 391-402.
- Hughes, I., Thalmann, I., Thalmann, R., and Ornitz, D. M. (2006). Mixing model systems: Using zebrafish and mouse inner ear mutants and other organ systems to unravel the mystery of otoconial development. *Brain Res* 1091, 58-74.
- Hurle, B., Ignatova, E., Massironi, S. M., Mashimo, T., Rios, X., Thalmann, I., Thalmann, R., and Ornitz, D. M. (2003). Non-syndromic vestibular disorder with otoconial agenesis in tilted/mergulhador mice caused by mutations in otopetrin 1. *Hum Mol Genet* 12, 777-789.
- Jones, S. M., Erway, L. C., Bergstrom, R. A., Schimenti, J. C., and Jones, T. A. (1999). Vestibular responses to linear acceleration are absent in otoconia-deficient C57BL/6JEi-het mice. *Hear Res* 135, 56-60.
- Jones, T. A., Fermin, C., Hester, P. Y., and Vellinger, J. (1993). Effects of microgravity on vestibular ontogeny: direct physiological and anatomical measurements following space flight (STS-29). *Acta Vet Brno* 62, S35-42.
- Krasnov, I. B. (1991). The otolith apparatus and cerebellar nodulus in rats developed under 2-G gravity. *Physiologist* 34, S206-207.
- Lim, D. J. (1973). Formation and fate of the otoconia. Scanning and transmission electron microscopy. *Ann Otol Rhinol Laryngol* 82, 23-35.
- Moorman, S. J., Burrell, C., Cordova, R., and Slater, J. (1999). Stimulus dependence of the development of the zebrafish (*Danio rerio*) vestibular system. *J Neurobiol* 38, 247-258.

Ornitz, D. M., Bohne, B. A., Thalmann, I., Harding, G. W., and Thalmann, R. (1998). Otoconial agenesis in *tilted* mutant mice. *Hearing Res* 122, 60-70.

Pedrozo, H. A., Schwartz, Z., Dean, D. D., Harrison, J. L., Campbell, J. W., Wiederhold, M. L., and Boyan, B. D. (1997). Evidence for the involvement of carbonic anhydrase and urease in calcium carbonate formation in the gravity-sensing organ of *Aplysia californica*. *Calcif Tissue Int* 61, 247-255.

Raymond, J., Dememes, D., Blanc, E., Sans, N., Venteo, S., and Dechesne, C. J. (2000). Developmental study of rat vestibular neuronal circuits during a spaceflight of 17 days. *J Gravit Physiol* 7, P55-58.

Reschke, M. F., Bloomberg, J. J., Harm, D. L., Paloski, W. H., Layne, C., and McDonald, V. (1998). Posture, locomotion, spatial orientation, and motion sickness as a function of space flight. *Brain Res Brain Res Rev* 28, 102-117.

Ross, M., and Donovan, K. (1986a). Otoconia as test masses in biological accelerometers: What can we learn about their formation from evolutionary studies and work in microgravity? *Scan Elect Micro IV*, 1695-1704.

Ross, M. D. (1993). Morphological changes in rat vestibular system following weightlessness. *J Vestib Res* 3, 241-251.

Ross, M. D., Donovan, K., and Chee, O. (1985). Otoconial morphology in space-flown rats. *Physiologist* 28, S219-220.

Ross, M. D., and Donovan, K. M. (1986b). Otoconia as test masses in biological accelerometers: what can we learn about their formation from evolutionary studies and from work in microgravity? *Scan Electron Microsc*, 1695-1704.

Ross, M. D., and Peacor, D. R. (1975). The nature and crystal growth of otoconia in the rat. *Ann Otol Rhinol Laryngol* 84, 22-36.

Sebastian, C., Esseling, K., and Horn, E. (1996). Altered gravitational experience during early periods of life affects the static vestibulo-ocular reflex of tadpoles of the southern clawed toad, *Xenopus laevis* Daudin. *Exp Brain Res* 112, 213-222.

Sollner, C., Schwarz, H., Geisler, R., and Nicolson, T. (2004). Mutated otopetrin 1 affects the genesis of otoliths and the localization of Starmaker in zebrafish. *Dev Genes Evol* 214, 582-590.

Sondag, H. N., de Jong, H. A., van Marle, J., and Oosterveld, W. J. (1995). Effects of sustained acceleration on the morphological properties of otoconia in hamsters. *Acta Otolaryngol* 115, 227-230.

Sondag, H. N., De Jong, H. A., Van Marle, J., Willekens, B., and Oosterveld, W. J. (1996). Otoconial alterations after embryonic development in hypergravity. *Brain Res Bull* 40, 353-356; discussion 357.

Takabayashi, A., Watanabe, S., and Takagi, S. (1993). Postural control of fish related to gravity input. *Physiologist* 36, S81-82.

Thalmann, I., Hughes, I., Tong, B. D., Ornitz, D. M., and Thalmann, R. (2006). Microscale analysis of proteins in inner ear tissues and fluids with emphasis on endolymphatic sac, otoconia, and organ of Corti. *Electrophoresis* 27, 1598-1608.

Thalmann, R., Ignatova, E., Kachar, B., Ornitz, D. M., and Thalmann, I. (2001). Development and maintenance of otoconia: biochemical considerations. *Ann N Y Acad Sci* 942, 162-178.

Thornton, W. E., Moore, T. P., Pool, S. L., and Vanderploeg, J. (1987). Clinical characterization and etiology of space motion sickness. *Aviat Space Environ Med* 58, A1-8.

Verpy, E., Leibovici, M., and Petit, C. (1999). Characterization of otoconin-95, the major protein of murine otoconia, provides insights into the formation of these inner ear biominerals. *Proc Natl Acad Sci, U S A* 96, 529-534.

von Baumgarten, R. J., Simmonds, R. C., Boyd, J. F., and Garriott, O. K. (1975). Effects of prolonged weightlessness on the swimming pattern of fish aboard Skylab 3. *Aviat Space Environ Med* 46, 902-906.

Wang, Y., Kowalski, P. E., Thalmann, I., Ornitz, D. M., Mager, D. L., and Thalmann, R. (1998). Otoconin-90, the mammalian otoconial matrix protein contains two domains of homology to secretory phospholipase A2. *Proc Natl Acad Sci, USA* 95, 15345-15350.

Wang, Y., Thalmann, I., Thalmann, R., and Ornitz, D. M. (1999). Mapping the mouse otoconin-90 (Oc90) gene to chromosome 15. *Genomics* 58, 214-215.

Wiederhold, M. L., Harrison, J. L., Parker, K., and Nomura, H. (2000). Otoliths developed in microgravity. *J Gravit Physiol* 7, P39-42.

Figure 1. Development of otoconia in the embryonic quail. A) SEM pictures showing immature (double fluted) and mature (mature faceted) otoconia. Scale bar indicates 2.5 μm . B) Comparison of otoconia growth in the saccule and utricle during development and after hatching. Arrow indicates the hatching point. The utricular sensory epithelium (SE) acquires otoconia faster than the saccular SE after E10, and this faster increase in the utricle consequently results in larger otolith area compared to the saccule. After hatching, otoconia growth no longer occurs and mature otoconia are maintained in the adult. C) Characteristics of otoconia development before hatching. Time points in parenthesis indicates parallel developmental ages in the mouse. Figures A, B adapted from (Dickman et al., 2004).

Figure 1

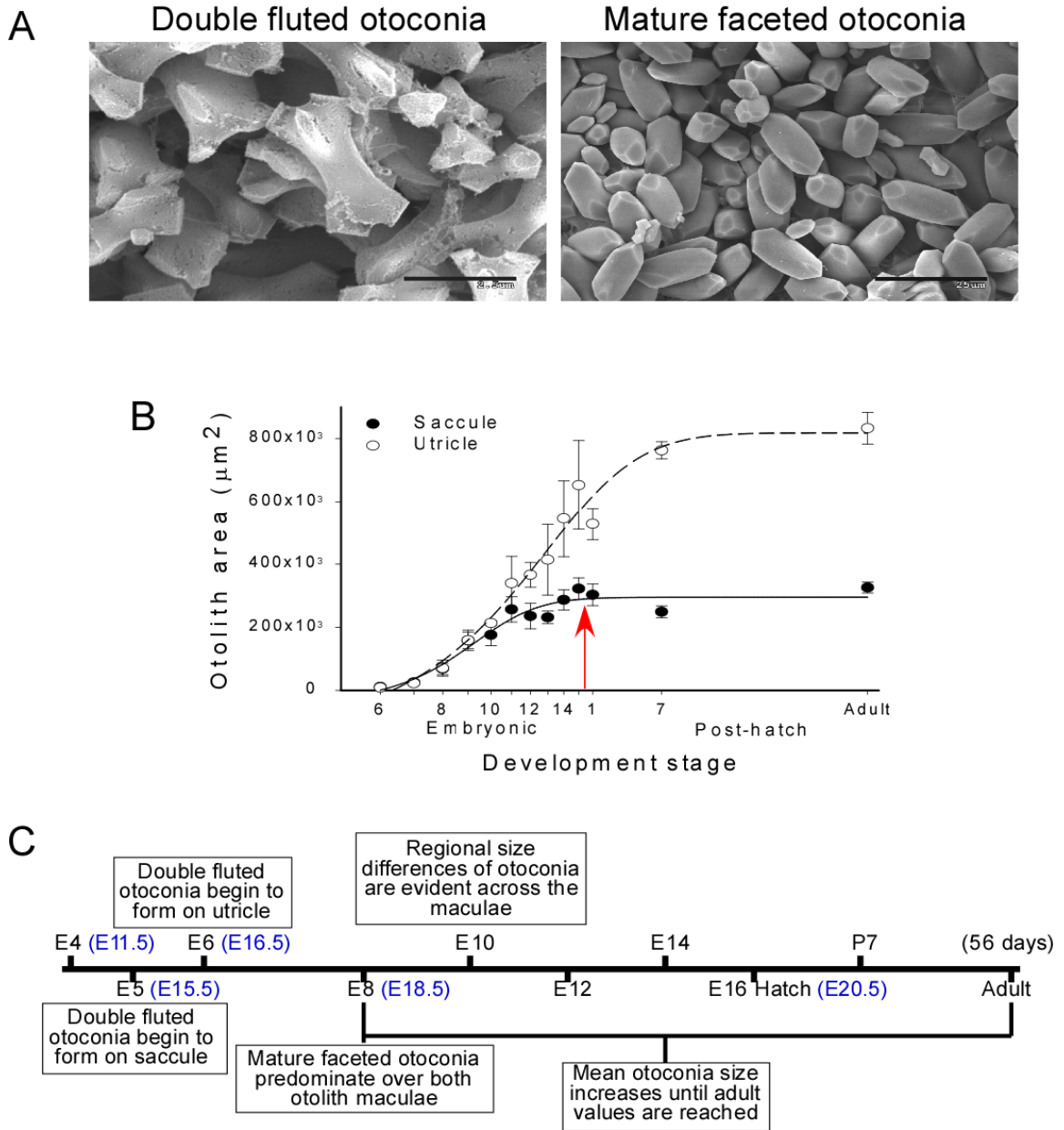


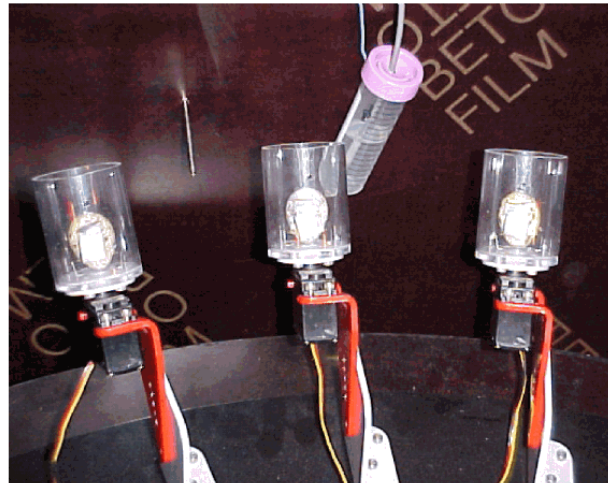
Figure 2. The equipment used to induce hypergravity during quail eggs development. A) Outside view of the equipment. B) Each quail egg was placed within a cylindrical chamber connected to the main rotor. Rotating these chambers created a centrifugation effect. C) A quail egg is securely restrained within the cylindrical chamber.

Figure 2

A



B



C

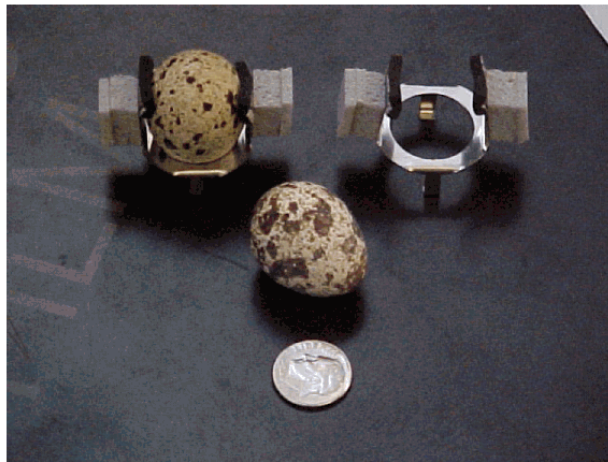


Figure 3. *Oc90 in-situ* hybridization and OC90 immunohistochemistry. *Oc90* mRNA expression was first detected at E6 in the nonsensory epithelia of the vestibular and cochlear labyrinth. Positive signals were detected until E12, and by E15, *Oc90* mRNA was no longer detectable. OC90 protein was first faintly detected at E8, and a stronger signal was observed in the apical regions of the nonsensory epithelia of the vestibular labyrinth from E10 through P7. Starting at E12, OC90 was detected within the otoconia. Sections incubated with antisense probe, pre-immune serum or secondary antibody only, showed no signal. M: medial, V: ventral, D: dorsal, L: lateral.

Figure 3

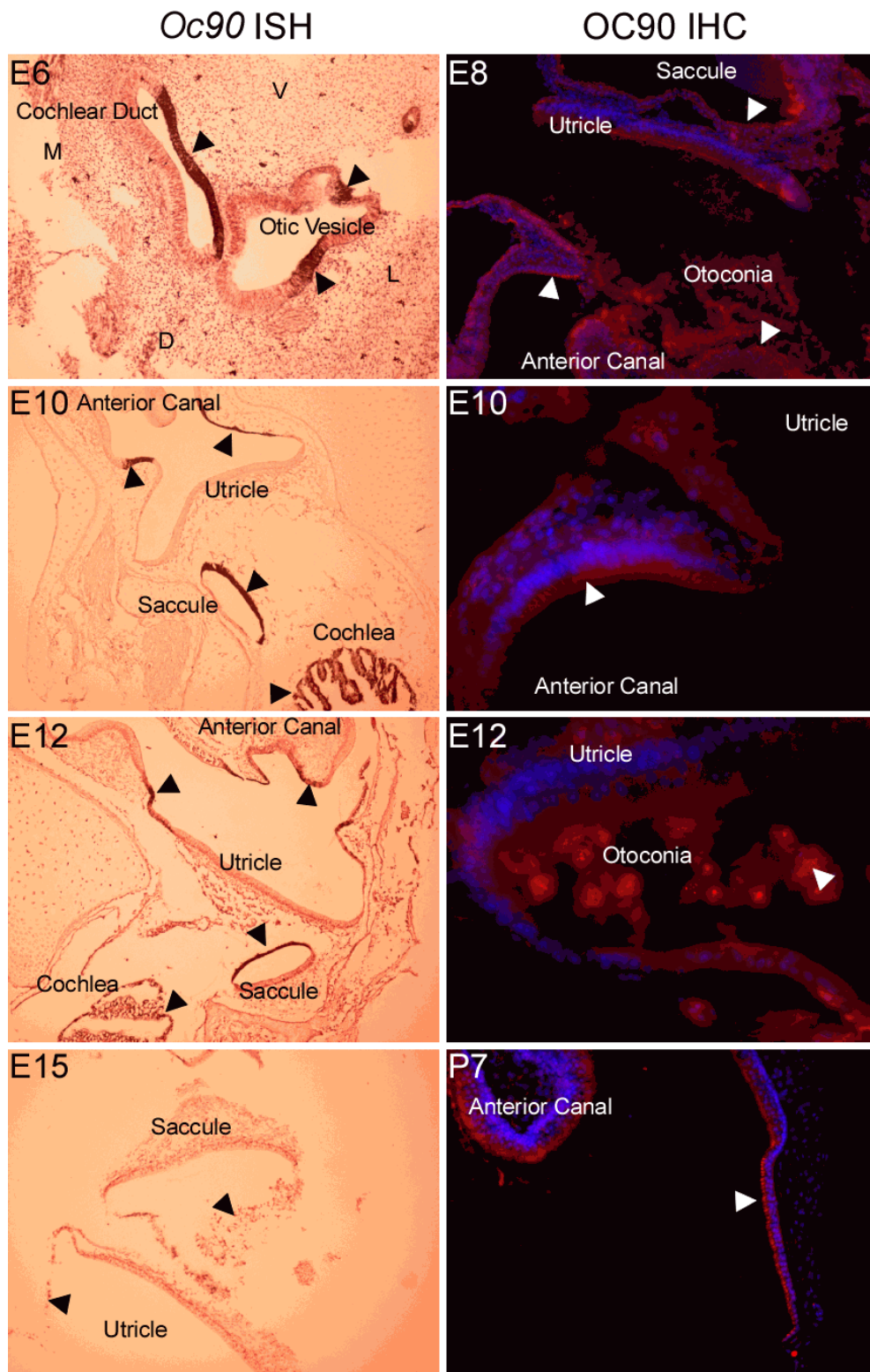


Figure 4. Comparison of body weight of embryos developed at normal (1G) and hypergravity (2G). Body weight of embryos grown at 1G and 2G showed no significant difference. Data points represent mean values with standard deviation.

Figure 4

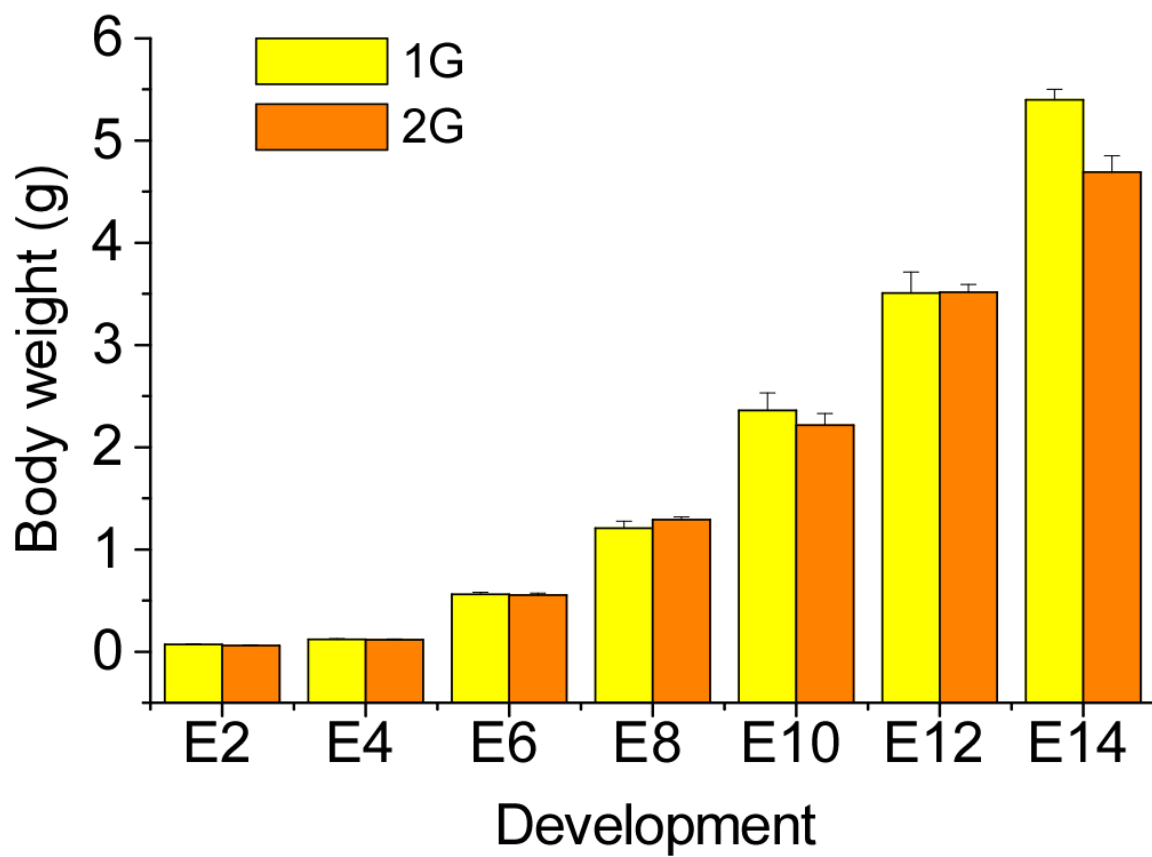


Figure 5. Relative quantification of *Otogelin* expression using qRT-PCR. Expression of *Otogelin* was first detected at E6. Inner ear tissues expressed much higher level of *Otogelin* compared to the brain, confirming the specificity of the tissues used for qRT-PCR analysis. Data points represent mean values with standard deviation.

Figure 5

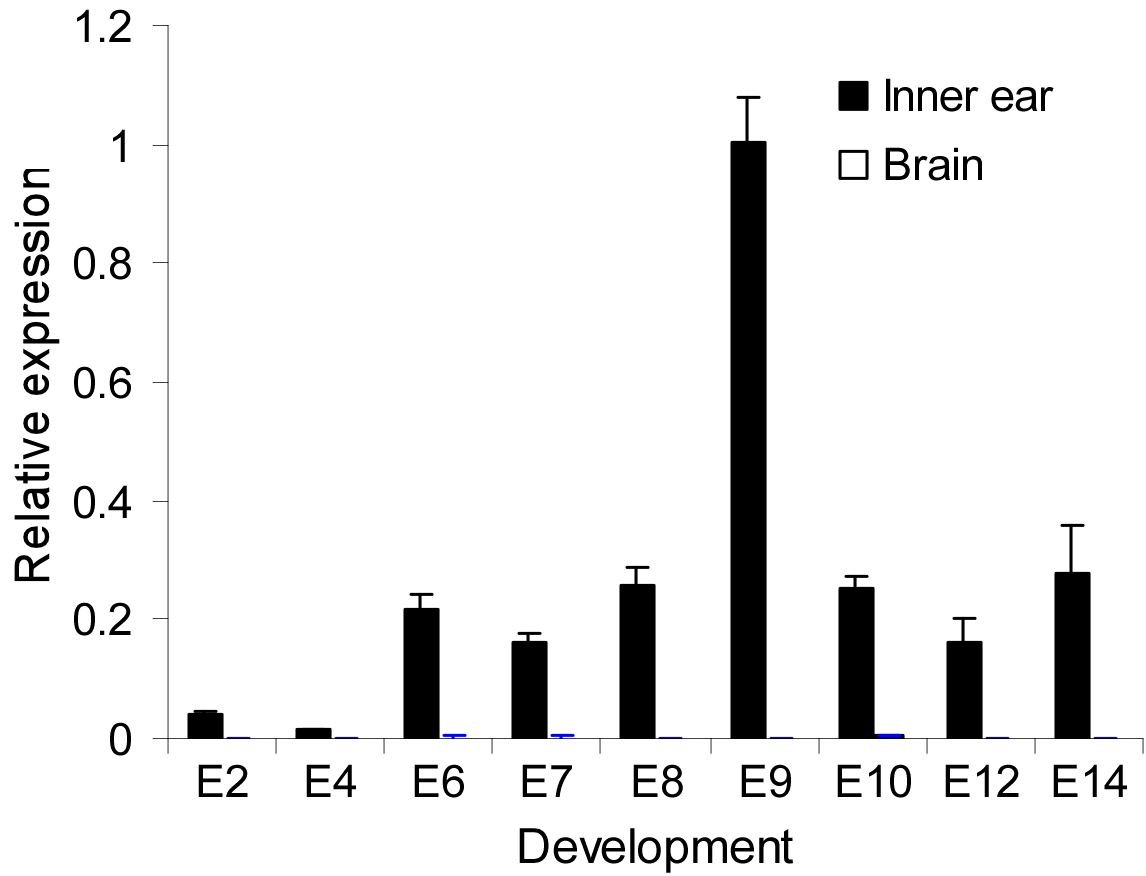


Figure 6. Relative quantification of *Oc90* gene expression at 1G vs 2G. Production of *Oc90* reached a maximum at E9 and decreased toward hatching. Hypergravity had no significant effect on *Oc90* expression. Data points represent mean values with standard deviation.

Figure 6

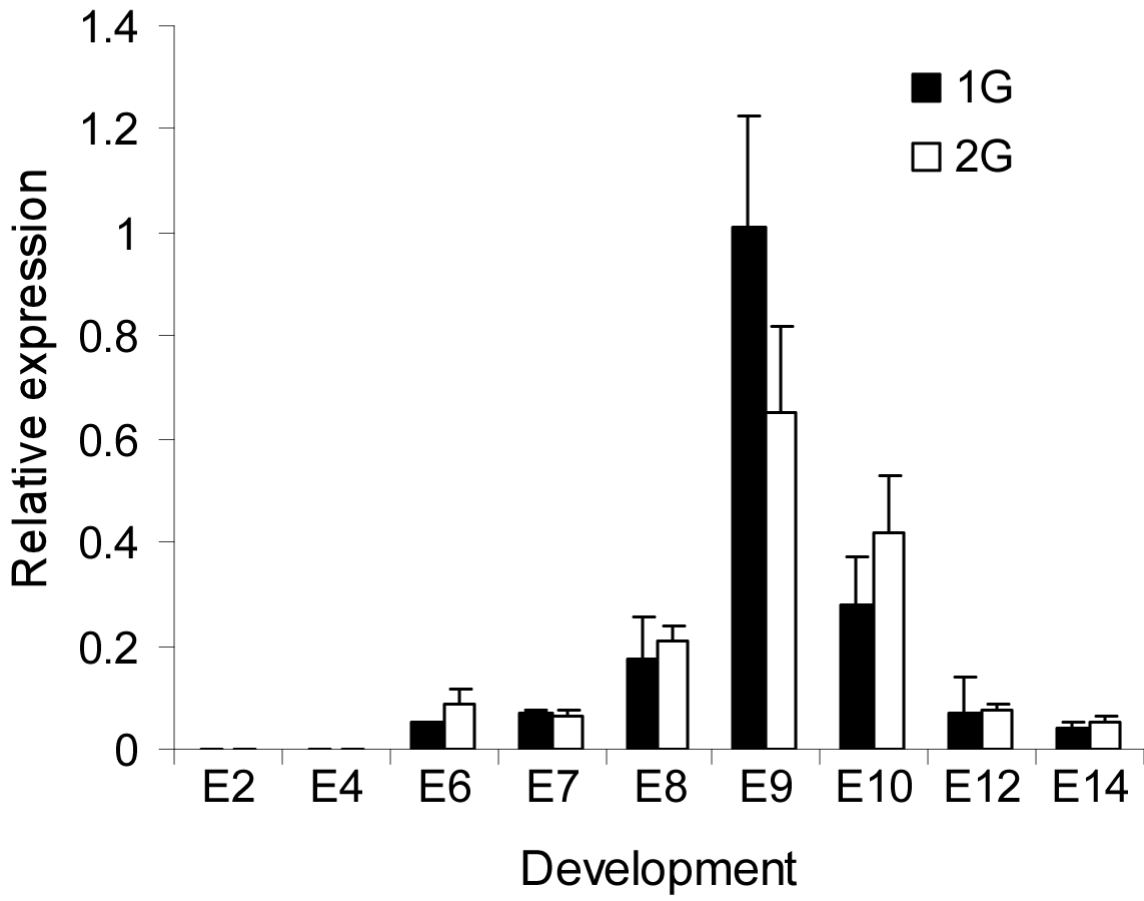


Figure 7. Relative quantification of *Otop1* expression at 1G vs 2G. The level of *Otop1* mRNA slowly increased during development, and showed regression after E9 toward hatching. Hypergravity conditions did not result in a significant change in *Otop1* expression levels. Data points represent mean values with standard deviation.

Figure 7

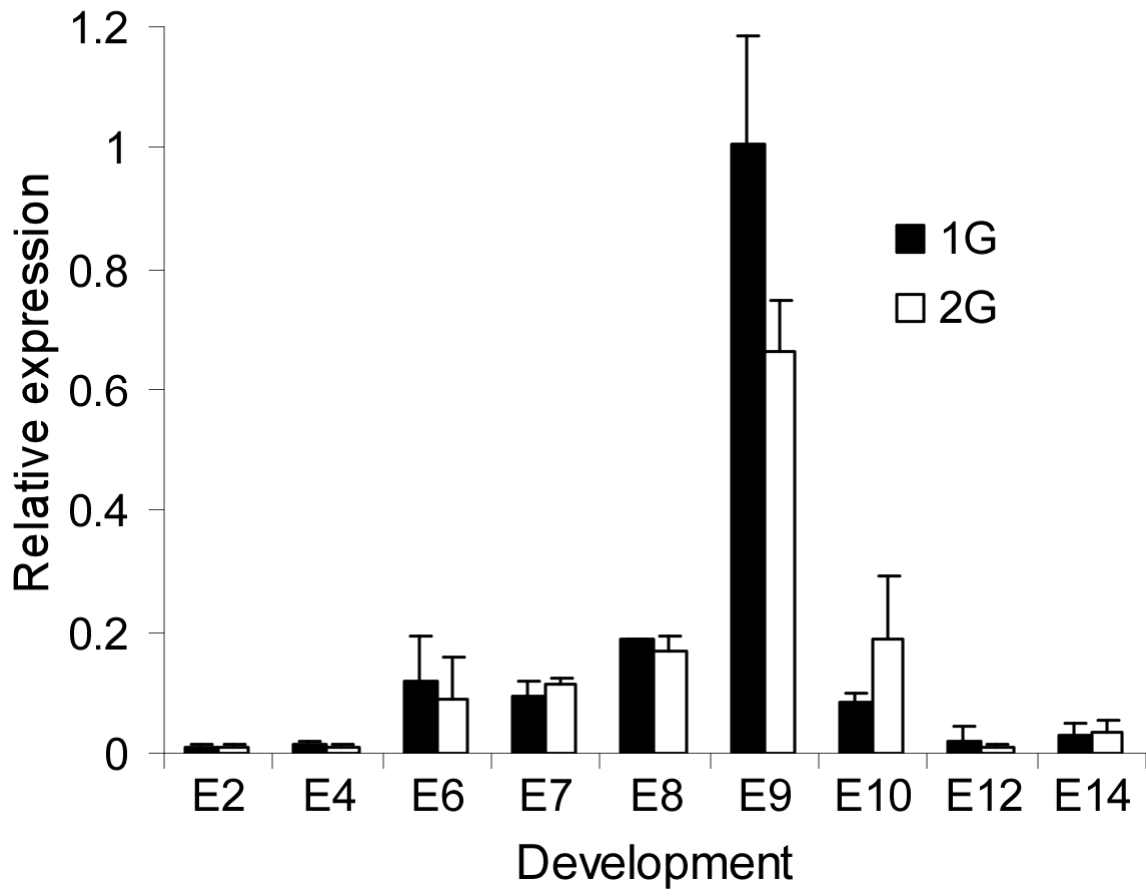
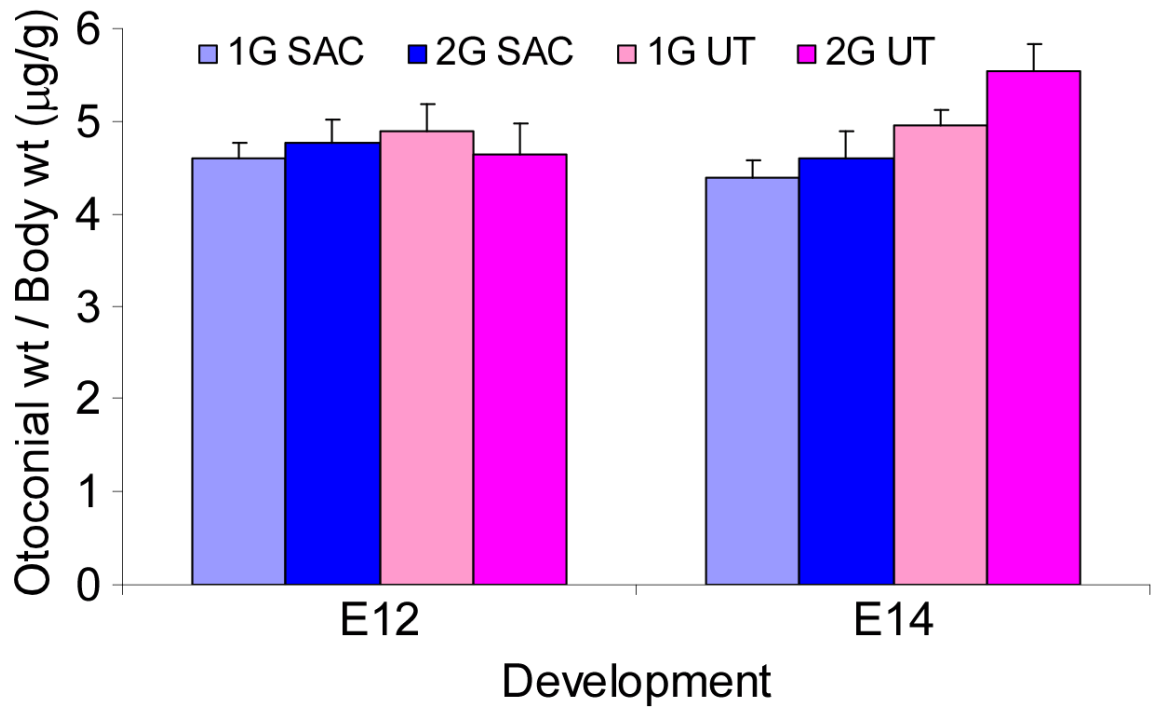


Figure 8. Comparison of otoconial calcium weight in 1G and 2G animal. At E12 and E14, otoconial calcium weight was measured by subtracting the weight of fused otoconia after EGTA treatment from the original weight. Otoconial calcium weight did not show any significant difference between animals grown at normal and hypergravity. Data points represent mean values with standard error. SAC: saccule, UT: utricle.

Figure 8



Conclusion and Future Directions

Conclusion

Otopetrins define a new gene family with highly conserved domains (Otopetrin Domains) (Hughes et al., 2008; Hurle et al., 2003). *Otopetrin 1 (Otop1)* was discovered by positional cloning of the *tilted* mice, which carry a missense mutation within the gene (Hurle et al., 2003). The mouse and zebrafish mutants of *Otop1* show a non-syndromic otoconial agenesis phenotype, indicating that the function of OTOP1 is essential for otoconia formation (Hughes et al., 2004; Hurle et al., 2003; Ornitz et al., 1998; Sollner et al., 2004).

Consistent with its proposed function, *Otop1* is expressed in the sensory epithelium of the utricle and saccule beneath the otoconia membrane (Hurle et al., 2003). As a multi-transmembrane protein, OTOP1 was predicted to be localized to the plasma membrane or vesicular structures. Previous results that the isolated globular substance vesicles, the otoconia precursors, can have local $[Ca^{2+}]$ increase in response to ATP (Suzuki et al., 1997) suggested a possible involvement of purinergic signaling during otoconia formation. This observation led us to hypothesize that OTOP1 may localize within globular substance vesicles and may induce calcification of otoconia in response to purinergic stimuli.

In vitro studies with *Otop1*-expressing COS7 cells showed that OTOP1 has the ability to modulate $[Ca^{2+}]_i$ by inhibiting P2Y receptor activity and allowing extracellular Ca^{2+} influx (Hughes et al., 2007). Because this activity was tested in heterologous cells we needed a system to more closely model the *in vivo* environment to test biochemical activity of OTOP1 during otoconia formation.

Possible expression of OTOPI in organs other than the inner ear (Hurle et al., 2003) suggested that OTOPI could have additional functions but that they have not been revealed in any of the mouse mutants. To decipher the additional *in vivo* functions of OTOPI, a null allele of *Otop1* (*Otop1^{βgal}*) was generated and analyzed. Homozygous *Otop1^{βgal/βgal}* mice were viable and the primary phenotype was non-syndromic otoconia agenesis. The presence of the *β-galactosidase* gene allowed us to efficiently mark its expression. *Otop1* was found in the non-striolar region of the utricle and saccule throughout development and this expression pattern persisted in the adult. OTOPI protein localized to the apical side of the supporting cells. Analysis of the purinergic response in primary macular epithelial cultures showed that *in vivo* OTOPI inhibits P2Y receptor-mediated release of intracellular Ca²⁺ stores and activates a P2X receptor-like influx of extracellular Ca²⁺. We also found that the P2Y inhibitory activity of OTOPI was dependent on the presence of extracellular Ca²⁺, suggesting a role for OTOPI in sensing extracellular or intravesicular Ca²⁺ concentrations. These data suggested that the identified *in vivo* biochemical activity of OTOPI may be important for otoconia formation and maintenance.

Because the same phenotype was exhibited in *Otop1^{βgal/βgal}*, *Otop1^{tlt/tlt}*, and *Otop1^{mlh/mlh}* mice it was likely that both *tlt* and *mlh* mutations resulted in inactivation of a common biochemical activity of OTOPI. Since *tlt* and *mlh* mutations lie within distinct Otopetrin Domains (Hughes et al., 2008) we hypothesized that the mechanism by which OTOPI function is altered or disrupted by these mutations could be different. Importantly, both endogenous mutant proteins showed altered subcellular localization compared to the wildtype OTOPI. As a multi-transmembrane protein OTOPI signals were in a punctate

pattern and were localized near the apical end of the sensory epithelium, whereas most mutant signals stayed between the mid and basal end. Interestingly, the *mlh* mutation seemed to affect more of the biochemical function of OTOP1 than *slt*, and further ratiometric imaging with primary utricular macular cultures will be pursued to confirm this effect *in vivo*. These data not only showed the effect of each mutation but also suggested putative functions of the Otopetrin Domains (OD-I and II) bearing each mutation.

The overlapping pattern of expression (Hurle et al., 2003) and the otoconial agenesis phenotype in *Otop1* ^{β gal/ β gal} mice suggested that OTOP2 and OTOP3, the paralogues of OTOP1, could have possible functional redundancy. *In vitro* experiments showed that OTOP2 and OTOP3 can mimic the biochemical function of OTOP1. However, when we generated the knockout for *Otop2* and double knockout for *Otop1* and *Otop2*, no additional phenotype besides otoconial agenesis was observed even though successful targeting of each gene was clearly confirmed. This result leads us to pursue a more careful analysis of the *Otop2* null allele and to pursue generating a null allele for *Otop3*.

Otoconia detects movement with respect to gravity and also can be disturbed by a change in the force of gravity. As the change in otoconia was observed when embryos were grown under altered gravity, we examined whether expression of *Otoconin90* (*Oc90*) and *Otop1*, which are essential for otoconia biosynthesis, could be affected in animals exposed to chronic hypergravity condition. Both genes showed an increase in expression during quail development, peaking at E9, and regressing afterwards until hatching. Hypergravity treatment did not seem to affect this expression pattern for either

gene, although a slight effect of hypergravity on *Otop1* expression observed with E9 and E10 tissues deserves further confirmation.

Future Directions

Otopetrin family knockout mice

To fully understand the biochemical activities of Otopetrin family proteins in otoconial formation and to identify their role in the development and function of other organ system, generation of a knockout allele for each Otopetrin gene and double or triple knockout alleles for different combinations of Otopetrin family genes will be necessary.

Homozygous knockout of *Otop1* (*Otop1* ^{β gal/ β gal}) is viable and shows otoconia agenesis. This phenotype confirmed that the otoconial agenesis found in *Otop1* mutants is due to loss of OTOP1 activity and not due to an alteration of native OTOP1 function. At this point, it is likely that the most important developmental role of OTOP1 is formation of otoconia. In addition to the utricle and saccule in the inner ear, positive β GAL staining was also observed in lactating mammary gland, kidney, and a faint staining in the brain. However, no apparent phenotype was observed in these organs. It is possible that OTOP1 may be expressed in these organs, but without any function, or there may be redundancy with other proteins that mask the function of OTOP1.

Redundancy between Otopetrin family proteins are suggested from their overlapping patterns of expression (Hurle et al., 2003). Importantly, ratiometric Ca^{2+} studies with COS7 cells expressing OTOP2 and OTOP3 showed that these proteins could also modulate $[\text{Ca}^{2+}]_i$ in a similar manner to OTOP1, with OTOP3 having an identical

purinergic against sensitivity to that of OTOP1. This conserved biochemical function further supports the likelihood that there is redundancy between Otopetrins, at least in terms of modulating $[Ca^{2+}]_i$. Therefore, if multiple Otopetrins are present in the same tissue, loss of activity of one Otopetrin could be compensated by other Otopetrins. This may explain why a single knockout allele of an Otopetrin may not fully reveal its *in vivo* function. Thus, future studies must emphasize the necessity of generating double and possibly triple knockouts of Otopetrin family genes.

Homozygous *Otop2* knockout mice (*Otop2*^{nβgal/nβgal}) are viable and so far a phenotype has not been identified. We think that the function of OTOP2 may be subtler than expected and/or the function of OTOP2 may be masked by redundancy with OTOP1 or 3. Identifying the tissues that express *Otop2* with nβGAL should help to focus experiments designed to identify phenotypes.

Considering that a novel phenotype has not been identified in homozygous *Otop1*^{βgal/βgal}; *Otop2*^{nβgal/nβgal} double knockout, and that there are more functional similarities between OTOP1 and OTOP3 in modulating Ca^{2+} , generation of an *Otop3* null allele and generation of double knockouts with the *Otop1* and 3 or *Otop2* and 3 seems indispensable to uncovering the redundancy between Otopetrin proteins. We found out that EUCOMM had already generated *Otop3* targeted ES cell line. OTOP3 was recently discovered as novel gene expressed in retina cone cells (Corbo and Cepko, 2005). Therefore, morphology of the retina and eye function will need be pursued when the null allele is generated.

Functional domains of Otopetrin proteins

Topological models generated through sequence comparison of multiple species identified three highly conserved domains within the Otopetrin family (Hughes et al., 2008). We have designated these domains as Otopetrin domains (OD-I, II, and III). The considerable conservation between vertebrate and invertebrate Otopetrin sequences suggests conservation of structure and function. To better understand the role of these sequences in the function of OTOPI, EGFP-tagged C-terminal deletion series and EGFP chimeric constructs containing isolated Otopetrin domains will need to be made and examined for the ability to modulate intracellular $[Ca^{2+}]$. Previous studies showed two major components of OTOPI activity in COS7 cells (Hughes et al., 2007): 1) *Otop1* expressing cells showed decreased release of intracellular Ca^{2+} stores in response to ATP, but could release stored Ca^{2+} in response to stimuli at other G-protein coupled receptors, suggesting that OTOPI specifically inhibited the activation of P2Y in response to ATP; 2) *Otop1* expressing cells exhibited a novel ATP-gated influx of extracellular Ca^{2+} , which had unique nucleotide sensitivity not observed in other P2X channels. We hypothesize that the two most highly conserved Otopetrin domains may be required for different components of these activities (binding purinergic agonists, suppressing P2Y activity, inducing influx of extracellular Ca^{2+}).

The set of biochemical functions of OTOPI suggest that Otop1 could constitute an ion channel on its own or alter the activity of an ion channel, transporter, or exchanger. Using P2X specific protocols, the correct conditions for measuring current induced calcium influx have not been identified. This suggests the need for continued attempts at electrophysiology of *Otop1* expressing cells using a variety of conditions. Alternatively,

lack of current in *Otop1* expressing cells could indicate that OTOPI acts as, or with, a transporter or exchanger, which do not always generate significant alterations in membrane current.

Examination of the primary amino acid sequence of the Otop family does not suggest the presence of an ATP-binding site, or any regions that could be consistent with hydrolysis of nucleotides. Since Otop constitutes its own, highly conserved family it may contain novel or cryptic nucleotide binding and hydrolysis domains, or may interact with other known or novel proteins to accomplish these activities.

Other biochemical roles of Otop1

So far, search for biochemical functions of OTOPI has been primarily related to the modulation of intravesicular Ca^{2+} observed in globular substance vesicles (Suzuki et al., 1997). Studies from our lab have shown *in vitro* and *in vivo* evidences (Hughes et al., 2007) which suggested that OTOPI may actually be the protein responsible for locally increasing Ca^{2+} and consequently allowing calcification of otoconia particles. We hypothesized that OTOPI modulates the activity of P2Y receptor-mediated regulation of $[\text{Ca}^{2+}]_i$.

Recently, purinergic signaling has been linked to the regulation of membrane trafficking in addition to regulation of Ca^{2+} signaling in brown adipose tissue (BAT) (Lee et al., 2005). They concluded that multiple P2 receptors mediate the ATP responses of BAT cells, and that membrane trafficking is regulated by a P2 receptor showing “unusual” properties. Since OTOPI has unique agonist specificity to purinergic stimuli, and data from microarray study (ref) and our qRT-PCR data (data not shown) show

expression of *Otop1* in BAT, it is possible that OTOPI may be involved in regulating membrane trafficking in BAT in response to purinergic stimuli.

Membrane trafficking can be studied with FM1-43 dye labeling (Betz et al., 1996). FM1-43 can partition into the outer leaflet of the plasma membrane but does not cross between membrane leaflets. Fluorescence increases many fold after partitioning into membrane, thus by examining the rate of change in fluorescence, the rate of membrane addition or loss can be deduced. Future studies will use *Otop1*^{+/+}, *Otop1*^{βgal/βgal}, *Otop1*^{tl/tl}, and *Otop1*^{mlh/mlh} utricular macular culture cells and brown adipocyte cells and compare the rate of change in FM1-43 fluorescence in response to different purinergic stimuli. This experiment will reveal a possible function of OTOPI in membrane trafficking in the maculae and in BAT. Because BAT is important for thermo-regulation *Otop1*^{βgal/βgal} mice will also be tested for cold stress tolerance.

OTOP1 topology

Analysis of the primary structure of OTOPI suggests a 12 span transmembrane domain structure with cytosolic localization of the N- and C-termini (Hughes et al., 2008). It will be important to experimentally examine this model, especially if OTOPI is predicted to behave as a novel channel. Knowledge of the domains of OTOPI that are intracellular will be essential information to have before we can begin studies to identify other proteins that interact with cytoplasmic domains of OTOPI.

To examine the topology of OTOPI, the method used by Lorenz et. al., called fluorescence protease protection (FPP) (Lorenz et al., 2006) can be applied. FPP makes use of EGFP tagged proteins transfected in heterologous cells and imaging the integrity

of the EGFP before and after adding trypsin with and without selective cell permeabilization process. Similar biochemical function of OTOPI with different epitope tags (Hughes 2007) suggests that the transmembrane topology of the tagged molecules would be similar to that of the wildtype OTOPI. For this analysis, a C-terminal deletion series for Otop1-EGFP, in which proposed TM domains are sequentially deleted will be generated. Deletion of an odd number of TM domains should alter the cytoplasmic or extracellular localization of the C-terminal EGFP tag. COS7 cells will be transfected with these series of deletion constructs and examined for the localization of EGFP. Cells transfected to express Otop1-EGFP chimeric proteins and a red fluorescent protein (RFP) tagged control will be exposed to trypsin either before or after plasma membrane permeabilization by digitonin. Digitonin (1-50 μ M) intercalates into cholesterol-rich membranes and causes the plasma membrane to become perforated. Cytosolic contents can then diffuse out of the cells, and small molecules, like trypsin, can diffuse into the cells. Notably, the permeabilizing effect of digitonin affects the cholesterol-rich plasma membrane but not intracellular organelles that have much lower concentrations of cholesterol and are unaffected. If the fluorescent protein moiety on the expressed protein faces the environment exposed to trypsin (the cytoplasm), then its fluorescence signal should be lost. Conversely, if the fluorescent protein moiety on the expressed protein faces the environment protected from trypsin (the lumen of a compartment such as the ER), then its fluorescence should persist.

Identifying OTOPI interacting proteins

The lack of obvious calcium binding or pore domains, or ATP binding or hydrolysis domains in the OTOPI primary sequence suggests that OTOPI may be part of a signaling complex. So far, the best candidates for OTOPI interacting proteins are P2Y receptors, NADPH Oxidase 3 (NOX3), and NOXA1.

Previous study has shown that overexpression of OTOPI in COS7 cells does not interfere with G-protein coupled signaling downstream of P2Y receptor, suggesting more direct interaction of OTOPI with the receptor itself. FLAG-Otop1 constructs are already made and can be used for immunoprecipitation in COS7 cells after transient transfection or in mouse utricles. Our anti-OTOPI antibody has been confirmed to work in Western Blots and the availability of all P2Y receptor antibodies allows us to apply the proposed technique. Ratiometric Ca^{2+} studies with mouse utricular cultures showed that OTOPI may most likely inhibit P2Y2 and/or P2Y4. This led us to collaborate with the laboratory of B. Robaye where the individual and double knockouts for P2Y2 and P2Y4 are generated. We will first look for any balance problems in these mice and examine whether intact otoconia are present in these mice.

The rationale for choosing NOX3 and NOXA1, which are required for generating reactive oxygen species (ROS) in the inner ear, as candidates for OTOPI interacting protein, comes from the observation that mutants with loss of function mutations in these genes, *headtilt* and *headslant*, respectively, show similar phenotypes to *tlt* and *mlh* mutants. All five mutant mice display non-syndromic otoconial agenesis, with normal formation and maintenance of the sensory maculae and non-sensory structures, which may suggest that OTOPI and NADPH family proteins interact in a single pathway.

Previous study showed that NOX3 is an inner ear specific NADPH Oxidase and that NOXA1 is required for the generation of ROS by NOX3 (Banfi et al., 2004). Co-transfection of OTOP1, NOX3, NOXA1, and NOXO1 (a second adaptor protein of the NOX3 complex) into COS7 cells and examination of both Ca²⁺ mobilization in response to ATP and ROS generation may help to elucidate interacting partners for OTOP1. In preparation for such experiments, we have obtained mammalian expression constructs for NOX3, NOXA1, and NOXO1 from the laboratory of B. Banfi (Banfi et al., 2004).

References

- Banfi, B., Malgrange, B., Knisz, J., Steger, K., Dubois-Dauphin, M., and Krause, K. H. (2004). NOX3, a superoxide-generating NADPH oxidase of the inner ear. *J Biol Chem* *279*, 46065-46072.
- Betz, W. J., Mao, F., and Smith, C. B. (1996). Imaging exocytosis and endocytosis. *Curr Opin Neurobiol* *6*, 365-371.
- Corbo, J. C., and Cepko, C. L. (2005). A hybrid photoreceptor expressing both rod and cone genes in a mouse model of enhanced S-cone syndrome. *PLoS Genet* *1*, e11.
- Hughes, I., Binkley, J., Hurle, B., Green, E. D., NISC Comparative Sequencing Program, Sidow, A., and Ornitz, D. M. (2008). Identification of the Otopetrin Domain, a conserved domain in vertebrate otopetrins and invertebrate otopetrin-like family members. *BMC Evolutionary Biology* *8*:41.
- Hughes, I., Blasiolo, B., Huss, D., Warchol, M. E., Rath, N. P., Hurle, B., Ignatova, E., Dickman, J. D., Thalmann, R., Levenson, R., and Ornitz, D. M. (2004). Otopetrin 1 is required for otolith formation in the zebrafish *Danio rerio*. *Dev Biol* *276*, 391-402.
- Hughes, I., Saito, M., Schlesinger, P. H., and Ornitz, D. M. (2007). Otopetrin1 activation by purinergic nucleotides regulates intracellular calcium. *Proc Natl Acad Sci U S A* *104*, 12023-12028.
- Hurle, B., Ignatova, E., Massironi, S. M., Mashimo, T., Rios, X., Thalmann, I., Thalmann, R., and Ornitz, D. M. (2003). Non-syndromic vestibular disorder with otoconial agenesis in tilted/mergulhador mice caused by mutations in otopetrin 1. *Hum Mol Genet* *12*, 777-789.

Lee, S. C., Vielhauer, N. S., Leaver, E. V., and Pappone, P. A. (2005). Differential regulation of Ca^{2+} signaling and membrane trafficking by multiple p2 receptors in brown adipocytes. *J Membr Biol* 207, 131-142.

Lorenz, H., Hailey, D. W., and Lippincott-Schwartz, J. (2006). Fluorescence protease protection of GFP chimeras to reveal protein topology and subcellular localization. *Nat Methods* 3, 205-210.

Ornitz, D. M., Bohne, B. A., Thalmann, I., Harding, G. W., and Thalmann, R. (1998). Otoconial agenesis in *tilted* mutant mice. *Hearing Res* 122, 60-70.

Sollner, C., Schwarz, H., Geisler, R., and Nicolson, T. (2004). Mutated otopetrin 1 affects the genesis of otoliths and the localization of Starmaker in zebrafish. *Dev Genes Evol* 214, 582-590.

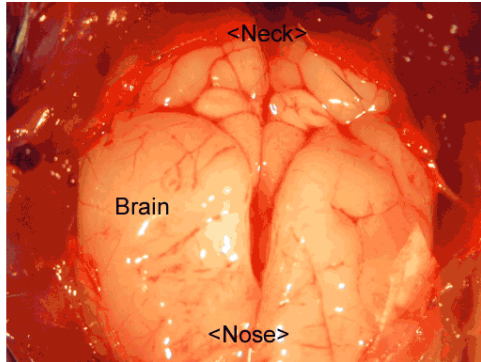
Suzuki, H., Ikeda, K., Furukawa, M., and Takasaka, T. (1997). P2 purinoceptor of the globular substance in the otoconial membrane of the guinea pig inner ear. *Am J Physiol* 273, C1533-1540.

Appendix

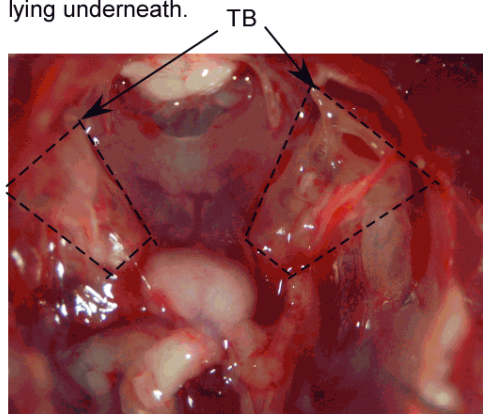
Technique for dissecting adult inner ear

Dissecting adult mouse temporal bone

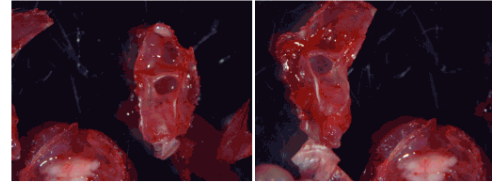
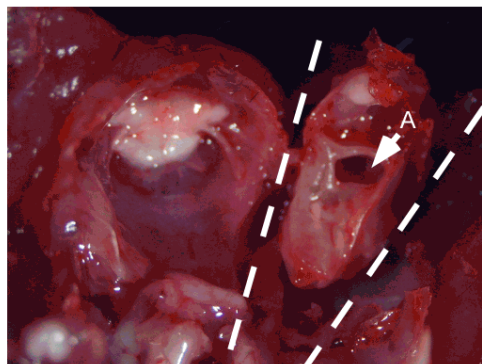
1. Sacrifice the mice with CO₂ inhalation or drugs.
2. Dissect the head by cutting at the neck area. Remove the skin.
3. Remove the calvarial bone by cutting through the midline and reflecting the calvaria laterally to expose the brain.



4. Remove the brain. You will see the two temporal bones (TB: bony structure surrounding inner ear) lying underneath.

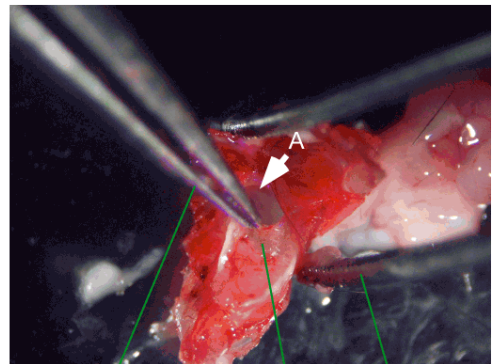


5. Isolate the temporal bones by making a cut at the two longer edges.



dissected temporal bones

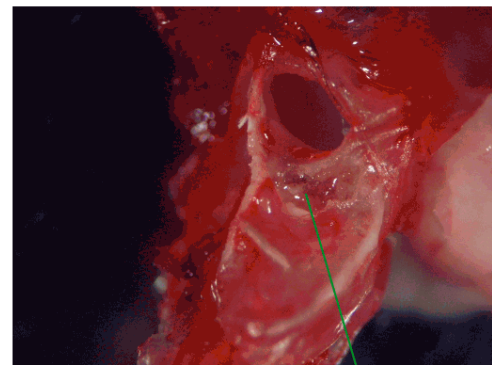
6. Make a small hole in the temporal bone just below the large hole (A) by scraping away at the bone with a sharp foreceps. This will allow the tissues inside to be efficiently fixed



sharp foreceps to make hole

Holding foreceps

make hole in this area



hole in temporal bone

CURRICULUM VITAE

Euysoo Kim

❖ **Education**

- 1998-2002 *Korea Advanced Institute for Science and Technology (KAIST),
Taejon, Korea: B.S. with Honors in Biological Sciences*
- 2003-present *Washington University School of Medicine, St. Louis, MO:
Candidate for the Ph.D. degree, Division of Biology and
Biomedical Sciences, Program in Molecular and Cellular
Biology*

❖ **Research Experience**

- Jun 2000-Jul 2002 *Undergraduate Research, with Jongkyeong Chung, Ph.D.,
KAIST*
- Sep 2002-Aug 2003 *Research Assistant, with Jongkyeong Chung, Ph.D., KAIST*
- Sep 2002-Dec 2003 *Laboratory Rotation, with Yi Rao, Ph.D., Washington
University*
- Jan 2004-present *Ph.D. Thesis Research, with David Ornitz, M.D., Ph.D.,
Washington University*

❖ **Honors**

- 1998-2002 *Korean Government Scholarship, KAIST*
- 1999-2002 *Full Merit-Based Scholarship, KAIST*
- 2002 *Honors in Biological Sciences, Magna cum Laude, KAIST*
- 2009 *Viktor Hamburger Award, Washington University School of
Medicine, Department of Developmental Biology*

❖ **Grant Support**

- July 2004-June 2007 *DC06974-01 "Otopetrin 1: a member of a novel family of
calcium regulating proteins"*
- July 2007-present *DC02236 "Biological functions of Otopetrin gene family"*

❖ Bibliography

Publications:

Lee SB, Cho KS, **Kim E**, Chung J. (2003) *blisterly* encodes Drosophila tensin protein and interacts with integrin and the JNK signaling pathway during wing development. *Development* 130:4001-4010.

Lee JH, Lee E, Park J, **Kim E**, Kim J, Chung J. (2003) In vivo p53 function is indispensable for DNA damage-induced apoptosis signaling in Drosophila. *FEBS Lett.* 550:5-10.

Cha GH, Cho KS, Lee JH, Kim M, **Kim E**, Park J, Lee SB, Chung J. (2003) Discrete functions of TRAF1 and TRAF2 in Drosophila mediated by JNK- and NF- κ B-dependent signaling pathways. *Mol. Cell. Biol.* 23:7982-7991.

Kim E, Hyrc KL, Speck J, Lundberg YW, Hughes I, Salles FT, Kachar B, Warchol ME, Ornitz DM. (2009) Regulation of cellular calcium in vestibular supporting cells by Otopetrin 1. *Submitted.*

Kim E, Hyrc KL, Speck J, Salles FT, Kachar B, Warchol ME, Ornitz DM. *Tilted* and *Mergulhador* mutations differentially disrupt Otopetrin 1 function. *In preparation.*

Kim E, Huss D, Ignatova E, Thalmann R, Thalmann IE, Ornitz DM, Dickman JD. Comparison of otoconia weight and expression of *Otopetrin 1* and *Otoconin 90* at normal and hypergravity in developing quail. *In preparation.*

Abstracts:

Kim E, Huss D, Ignatova E, Thalmann R, Thalmann IE, Warchol M, Ornitz DM, Dickman JD. Spatiotemporal expression profile of *Otopetrin 1* and *Otoconin 90* in developing quail at normal and hypergravity. Society for Neuroscience. Washington, DC: November 2005.

Kim E, Huss D, Ignatova E, Thalmann R, Thalmann IE, Warchol M, Ornitz DM, Dickman JD. Spatiotemporal expression patterns of *Otopetrin 1* and *Otoconin 90* in developing quail at normal and hypergravity. Association for Research in Otolaryngology Mid-Winter Meeting. Baltimore, MD: February 2006.

Kim E, Hughes I, Lundberg YW, Bohne BA, Salles FT, Kachar B, Warchol ME, Ornitz DM. Generation and characterization of *Otopetrin 1* knockout mice. Association for research in Otolaryndology Mid-Winter Meeting. Pheonix, AZ: February 2008

Kim E, Hughes I, Hyrc KL, Lundberg YW, Bohne BA, Salles FT, Kachar B, Warchol ME, Ornitz DM. *Otopetrin 1* regulates otoconia biomineralization in the vestibular sensory epithelium. Mouse Genetics & Genomics: Development & Disease Meeting. Cold Spring Harbor, NY: October 2008